UNIVERSITY OF OKLAHOMA

GRADUATE COLLEGE

ROLES OF UNIQUE MEMBRANE FUSION PROTEINS

A DISSERTATION

SUBMITTED TO THE GRADUATE FACULTY

in partial fulfillment of the requirements for the

Degree of

DOCTOR OF PHILOSOPHY

By

LOGAN MICHAEL NICKELS
Norman, Oklahoma
2015

ROLES OF UNIQUE MEMBRANE FUSION PROTEINS

A DISSERTATION APPROVED FOR THE
DEPARTMENT OF CHEMISTRY AND BIOCHEMISTRY

BY

_____
Dr. Helen Zgurskaya, Chair

_____
Dr. Valentin Rybenkov

_____
Dr. Wai Tak Yip

_____
Dr. Anthony Burgett

_____
Dr. Laura Bartley

Dedicated to my family, who has supported me, loved me, and given me the courage to find my own path.

Acknowledgements

I would like to give my thanks to all the people that have made this possible. I have grown as both a scientist and as a person during my time at OU, and it has everything to do with the amazing people surrounding me. In particular, I would like to thank the members of my lab, who have been fountains of friendship, knowledge and laughter. I will truly miss our time together. Also, I would like to thank my committee, who has given me thoughtful advice and pushed me to achieve as much as I can in graduate school.

However, there are some people that I would like to single out. I would like to thank my parents, who first taught me to ask questions and fostered my curiosity about how the world works. You have always supported me, pushed me to do the things that are difficult, and been there to catch me when I fall. I was never told there was something I wasn't capable of, and any new efforts were met only with encouragement and love. I am truly lucky to be born unto such wonderful people.

I would also like to thank my advisor, who taught me to ask the correct questions, and know when to believe the answer. You worked tirelessly to make me into a better scientist, and you did it with warmth and humor. Your passion for your work is evident every day, and thank you for showing me the door to that passion.

Finally, and most importantly, I would like to thank my wife Tara. She taught me that I will always find the answers I need within myself, and that no matter what, I have all I truly need within. I love you and cherish you every day.

Table of Contents

List of Tables

List of Figures

Abstract

One of the primary mechanisms of antibiotic resistance in bacteria stems from the expression of multicomponent efflux transporters, located in the membranes of both Gram-positive and Gram-negative bacteria. Although these transporters are divided into different families, many are dependent on membrane fusion proteins (MFPs). MFPs are thought to provide a functional linkage between the inner and outer membrane components of the complex in Gram-negative bacteria. However, these proteins have also been found in Gram-positive organisms, indicating a role beyond that of simply providing a link between transporter components. MFPs have since been shown to have diverse functions such as transporter stimulation and recruitment of outer membrane components. The extent to which MFPs participate in the transport reaction is still unclear. Also, the manner through which MFPs associate with their cognate inner membrane transporters (IMFs) and outer membrane channels (OMFs) is undefined. Furthermore, the details of MFP oligomerization and interaction with transporter components are unknown, leaving the picture of MFP-dependent transport incomplete.

This dissertation focuses on two unique MFP-dependent transporters. The first, TriABC-OpmH from *Pseudomonas aeruginosa*, is a paired-MFP transporter. TriABC relies on the two MFPs TriA and TriB in order for the resistance-nodulation division (RND) type transporter TriC to function with OpmH, an OMF. We constructed a functional, fused protein comprised of TriA and TriB. We also created deletion and point mutants of TriA and TriB, and analyzed the function and assembly of these mutants. Our functional genetic and biochemical studies

demonstrate that the functional unit of the MFP is a dimer, and that TriA and TriB occupy different binding sites on both the TriC transporter and OMF. These results suggest that TriA and TriB have non-equivalent roles in the transport process, and that one protomer in the MFP dimer may be responsible for interactions with the OMF such as recruitment and substrate export, and the other interacts primarily with the IMF and is responsible for functions such as transporter stimulation. We propose that these findings also apply to transporters utilizing a single MFP, which oligomerize to form homodimers, rather than heterodimers.

The second MFP-dependent transporter discussed is the four-component YknWXYZ from the Gram-positive bacterium *Bacillus subtilis.* Here, the MFP YknX functions in tandem with the ABC-type transporter YknYZ and a protein of unknown function, YknW. Gram-positive bacteria have no outer membrane, making the presence of an MFP puzzling. To determine the function of an MFP in a Gram-positive cell envelope, we created chimeric fusion proteins between YknYZ and the homologous *E. coli* transporter MacB, and we attempted to analyze the stimulatory activities of YknX. We also purified different components of the YknWXYZ transporter to determine ATPase activity of the complex. We conclude that YknWXYZ is a unique, four-component transporter that warrants further investigation into the functions of MFPs in Gram-positive bacteria.

I: Introduction

Bacterial antibiotic resistance has grown beyond being a rising concern to public health and positioned itself as an imminent threat. Currently, resistant species are pervasive within all nations. These resistant bacteria actively handicap effective treatment of infections that are commonplace in both daily life and clinical settings (WHO 2014). Humankind has known about the threat of antibiotic resistance since the inception of these drugs. The discoverer of penicillin, Alexander Fleming, warned of the possibility of resistance in his Nobel acceptance speech in 1945 (Rosenblatt-Farrell 2009). The population of drug resistant pathogens has increased significantly in the past decade, and the current situation demands that research be focused on antimicrobial resistance to ward off a "post-antibiotic era" in which common infections can kill simply because no effective antimicrobials exist. (WHO 2014) Bacterial resistance mechanisms have developed largely through the misuse of antibiotics in both human and animal populations. Exposure to sub-lethal levels of drug removes susceptible bacteria from the gene pool, but leaves resistant cells to grow and proliferate, thereby raising the basal level of resistance in a bacterial population. An increasing number of bacterial strains exhibit resistance towards many structurally unrelated drugs and are deemed to be multidrug resistant (MDR). (Nikaido 2009) MDR further reduces clinical treatment options for infections by restricting the effective set of antibiotic families. (Nikaido and Pages 2012)

Bacterial antibiotic resistance can either develop intrinsically, or be gained through exchange of genes with other bacteria. This exchange occurs through transduction, conjugation, and transformation of antibiotic-resistance genes. (Levy and

Marshall 2004) The specific mechanisms through which drug resistance is achieved include alteration of target proteins, drug inactivation, membrane permeability, and the expression of membrane-bound drug efflux pumps (Higgins 2007). Active efflux systems are recognized as some of the most clinically relevant mechanisms of antibiotic resistance, and expression of these pumps allows for the recognition and expulsion of drug from the cell before the concentration of drug reaches an effective level. Many of these pumps are promiscuous and able to expel structurally unrelated drugs, leading to MDR. (Zgurskaya and Nikaido 2000) As the pipeline of new antibiotics seems to be exhausted, targeting efflux pumps is a promising approach in efforts to combat drug resistance.

I.1 – Types of bacterial multidrug efflux transporters

Multidrug resistant transporters are present in all three kingdoms of life, but are very well represented in bacteria, making up 2-7% of total protein composition. (Saier and Paulsen 2001) Transporters are divided into a number of superfamiles based on characteristics such as the utilized energy source, substrate specificity, and accessory proteins (Piddock 2006). Efflux complexes are composed of individual protein subunits that together are able to utilize energy to bind and extrude substrate from the interior of the cell to the extracellular milieu. Currently identified MDR pumps fall into five major classes: the ATP-Binding Cassette (ABC) superfamily (Higgins and Linton 2004), the Small Multidrug Resistance (SMR) family, which is now a part of the DMT (Drug / Metabolite Transporter) superfamily (Chung and Saier 2001), the Major Facilitator Superfamily (MFS) (Saier, Paulsen et al. 1998), the Resistance Nodulation Division

(RND) family (Tseng, Gratwick et al. 1999), and the Multidrug and Toxic Compound Extrusion (MATE) family, which recently joined the MOP (Multidrug/Oligosaccharidyl-lipid/Polysaccharide) superfamily) (Jack, Yang et al. 2001, Hvorup, Winnen et al. 2003). The most relevant class of pumps with respect to antibiotic resistance in Gram-negative bacteria is the RND family (Yamaguchi, Nakashima et al. 2015). However, pumps of each class have been identified in both Gram-positive and Gram-negative bacteria. (Li and Nikaido 2004, Lorca, Barabote et al. 2007) **(Figure I.1)**

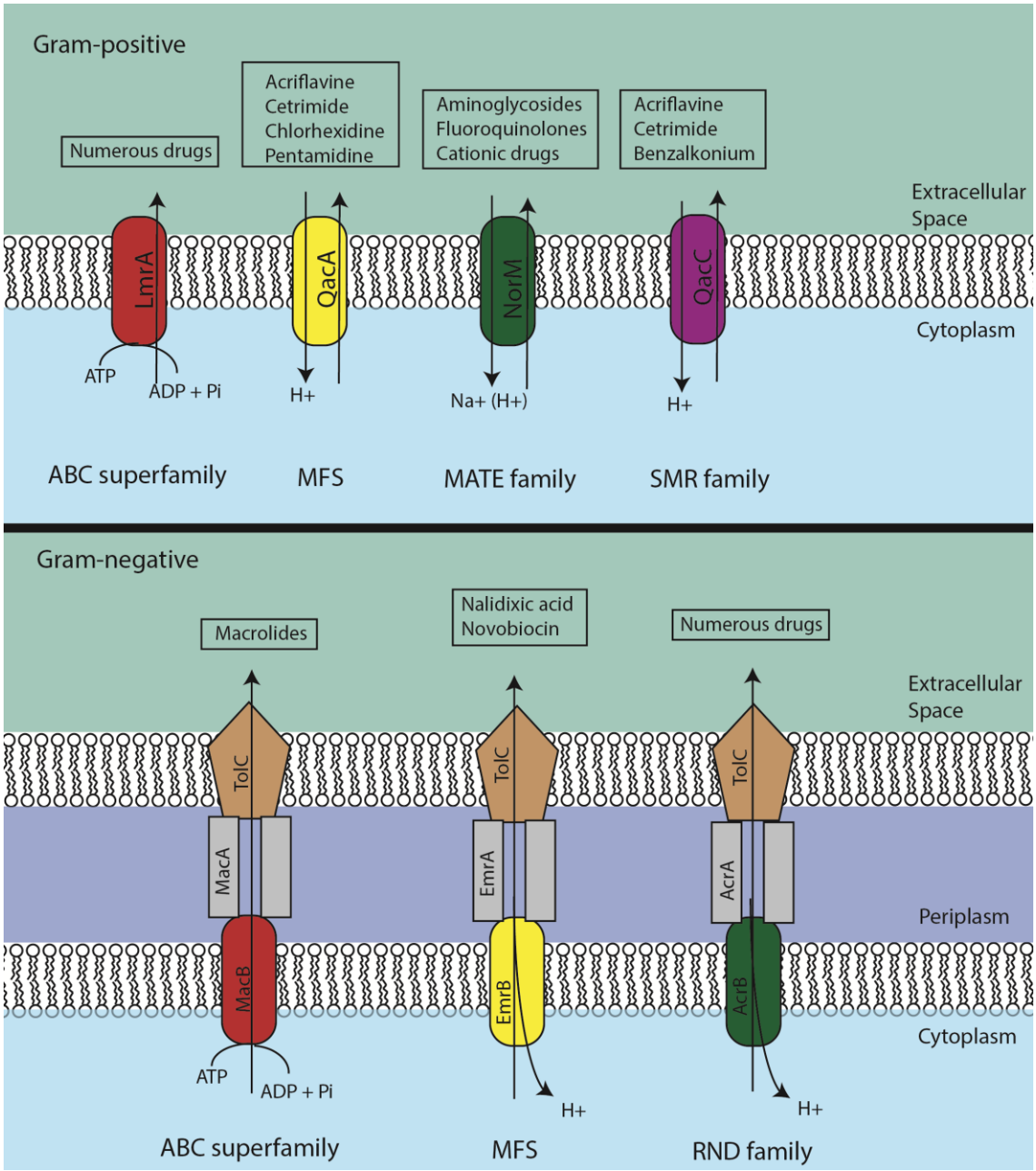

Figure I.1 – Efflux pump classes of Gram-positive and Gram-negative bacteria. Classes of efflux pumps are diagrammed along with typical substrates.

ABC-type MDRs are the only primary active transporters, whereas all other superfamilies utilize ion gradients to translocate substrate (Li and Nikaido 2004). These

ion gradients are normally protons, but occasionally found are sodium ions. Independent of classification and energy source, all transporters share at least three steps during the transport process. First, substrate must bind to the transport complex. Secondly, the substrate must be re-oriented to the opposite side of the membrane, and then thirdly, the substrate must be released through a conformational change in the binding site of the transporter (Zgurskaya, Weeks et al. 2015). Utilization of energy, either through ATP hydrolysis or proton / sodium motive force (PMF) occurs during the relaxation step of the transporter to re-orient the binding site to the original resting state (Davidson, Dassa et al. 2008, Eicher, Seeger et al. 2014).

I.2 – Mechanisms of ABC and RND-type efflux transporters

Transporters use a wide range of mechanisms in order to achieve efflux. AcrB, of the *E. coli* AcrAB-TolC complex is the most well-understood RND-type transporter, and has been crystallized in many forms, including in complex with substrate. Studies of this protein has shed light on the molecular mechanism of RND-type transporters (Murakami, Nakashima et al. 2002, Yu, McDermott et al. 2003, Murakami, Nakashima et al. 2006, Sennhauser, Amstutz et al. 2007, Du, Wang et al. 2014). AcrB functions as an asymmetric trimeric unit, in which each protomer moves through a three-conformation cycle, consisting of the open (O), loose (L), and tight (T) states. (Seeger, Schiefner et al. 2006) These three conformations differ in how the transporter interacts with substrate. The loose conformation is proposed to have an exposed binding pocket with a loose binding affinity for substrate. Upon binding, the conformation of the protomer switches to the T state, effectively capturing the substrate with a much higher

binding affinity in a hydrophobic pocket (Murakami, Nakashima et al. 2006). Finally, the conformation switches to the O state, releasing the substrate towards the periplasmic side of the membrane for eventual export through other complex components. Resetting the O state to the L state restarts the cyclic event, allowing the next substrate to bind. It is important to note that the individual monomers do not physically rotate, but rather have a conformational rotation. (Pos 2009).

The individual subunits of RND-type transporters are connected by interprotomer loops, and there is considerable flexibility within the trimeric structure, indicating an alternating site mechanism (Seeger, Schiefner et al. 2006). Symmetric structures of AcrB have also been solved and supported by crosslinking data (Murakami, Nakashima et al. 2002, Takatsuka and Nikaido 2007). These structures show all three protomers of the trimeric structure in the T or L conformations, indicating that the structure exists in a "resting state" in low substrate concentrations, and all protomers are available for substrate binding. The binding of substrate to one protomer causes a shift from the L to T state, and binding of substrate to an adjacent protomer is required for the shift from T to O, and release of the substrate (Yamaguchi, Nakashima et al. 2015). The functional rotation mechanism was verified through a covalently linked AcrB trimer, in which one monomer was inactivated through mutations in the proton relay network, and the complex was rendered nonfunctional (Takatsuka and Nikaido 2009).

Efflux in RND-type transporters is driven by PMF (Zgurskaya and Nikaido 1999). Specifically, four charged residues are thought to form a proton relay network that exists approximately 50 Å away from the drug binding pocket (Murakami,

Nakashima et al. 2002, Murakami, Nakashima et al. 2006). The distance between the relay network and the binding pocket indicates remote-conformational coupling of energy (Yamaguchi, Nakashima et al. 2015). The protonation of the transporter from PMF occurs in the periplasm, during the transition between the T and O states. Subsequent deprotonation of the transporter occurs during the transition from the O to L states, in which the proton is released into the cytoplasm, and the transporter is reset for the next transport cycle (Murakami, Nakashima et al. 2006).

In contrast to RND-type pumps, ABC-type efflux pumps utilize ATP as a primary energy source. Correspondingly, their overall structure greatly differs from RND-type transporters **(Figure I.2)**. Rather than forming a trimeric transporter, ABC-type transporters form a homodimer or heterodimer, in which each protomer of the dimer contains two domains required for efflux. The nucleotide-binding domain (NBD) is known to bind and hydrolyze ATP required for transport, and the transmembrane domain (TMD) is the membrane-spanning region of the protein that forms a tunnel through the lipid bilayer (Wilkens 2015). To satisfy the requirement of unidirectional transport, the TMDs alternate between inward and outward facing conformations, effectively forming a gate with different binding affinities for substrate on either side of the membrane (Senior, al-Shawi et al. 1995).

The NBD domains of the transporter each contain three conserved motifs, all involved in the binding and hydrolysis of ATP. Firstly, a Walker A motif which is involved in the binding of the phosphate groups of ATP. Secondly, the Walker B motif which contains a glutamate reside that is known to attack ATP and bind water. Finally, the last conserved structure is the ABC signature motif. This contains a signature

LSGGQ sequence that is known to contact ATP in the ATP-bound state of the NBD. Generally, ABC-type ATPases sandwich two ATP molecules between two ABC half-domains, in which the Walker A motif of one monomer works with the ABC signature motif from the other monomer in order to effectively hold both ATP molecules. (Locher 2009) The ABC-type MacAB-TolC transporter of *E. coli* is the most well-studied ABC-type bacterial drug efflux transporter to date. MacAB-TolC consists of the transporter MacB, the membrane fusion protein MacA, and the outer membrane factor TolC. Efflux transporters from different families have also been found in Gram-positive bacteria. (Freudl 2013) One such transporter, YknWXYZ of *B. subtilis,* is an ABC-type transporter known to provide resistance against an endogenously-produced toxin. (Yamada, Tikhonova et al. 2012)

There are multiple models describing the specific mechanism of ABC-type exporters. The common themes among these models are binding of both substrate and ATP to the NBD domains, dimerization of the NBD domains, a switch from the inward to outward-facing conformations, and ATP hydrolysis combined with a release of ATP, inorganic phosphate, and substrate. NBD dissociation also is thought to occur to reset the transporter for the next cycle. The differing characteristics of these models lie in the order and details of these individual steps. The "switch" model (Higgins and Linton 2004) shows that the NBD domains dissociate completely at the end of the cycle for product release and reset of the transporter. Other models such as the constant contact model speculate that the NBDs retain contact through one of the two ATP-binding sites and operate in a "seeswing" fashion, so that one nucleotide remains occluded at all times (Jones and George 2014, Wilkens 2015). While there are many specifics under

debate about how ABC-type transporters move substrate across the membrane (Senior, al-Shawi et al. 1995, Higgins and Linton 2004, Siarheyeva, Liu et al. 2010, Jones and George 2014) the prevailing theory is that the ATP hydrolysis and release results in resetting the transporter back to the pre-translocation state, similar to how the passage of protons in RND transporters drives the conformational change back to the L state.

The transport cycle of both ABC-type and RND-type transporters can be summarized in a three-step model, containing the steps consistent between transporters. Firstly, the transporter is in an open conformation, allowing binding of substrate. Second, substrate binding results in a conformational change that increases affinity of the transporter to the substrate. The third and final step of transport results in a re-orientation of the binding site to the opposite side of the membrane, and a decrease in affinity between the substrate and transporter, ultimately releasing the substrate (Zgurskaya, Weeks et al. 2015). In the case of Gram-negative organisms, the final step passes the substrate on to other complex components, such as the outer membrane factor (OMF).

I.3 – Roles of outer membrane factors in transport

The OMF forms a channel through the outer membrane that facilitates expulsion of substrate into the extracellular space, with an opening that can be triggered upon interaction with the other transporter components (Lobedanz, Bokma et al. 2007, Tikhonova, Dastidar et al. 2009). These channels are trimeric, and typically composed of three central domains. A β-barrel is imbedded into the outer membrane, providing transmembrane passage for substrate. The periplasmic portion of the channel forms a

large α-barrel, made up of bundles of α-helices, which extend into the periplasm from the outer membrane and are important for interaction with other transporter components. The equatorial domain lies in the central region of the α-barrel, and contains both the N- and C-terminus of the protein **(Figure I.2)** (Zgurskaya, Krishnamoorthy et al. 2011). The best-studied OMF, TolC of *E. coli*, is promiscuous, and known to interact with many efflux pumps from many different families, including AcrAB (RND), MacAB (ABC), and EmrAB (MF) (Koronakis, Sharff et al. 2000, Koronakis, Eswaran et al. 2004).

Crystal structures of TolC reveal a tight packing of the α-barrel domain, such that the periplasmic tip of the channel is tightly closed and unable to allow access to molecules as small as ions (Koronakis 2003). Due to this tight packing, the helices of the α-barrel are inclined with respect to the axis of the molecule, forming an aperture-like opening that models suggest undergoes a "twist" in order to open (Andersen, Koronakis et al. 2002, Bavro, Pietras et al. 2008, Pei, Hinchliffe et al. 2011). This conformational change rotates the helices, and allows an opening of the periplasmic tip, thereby allowing export of substrate.

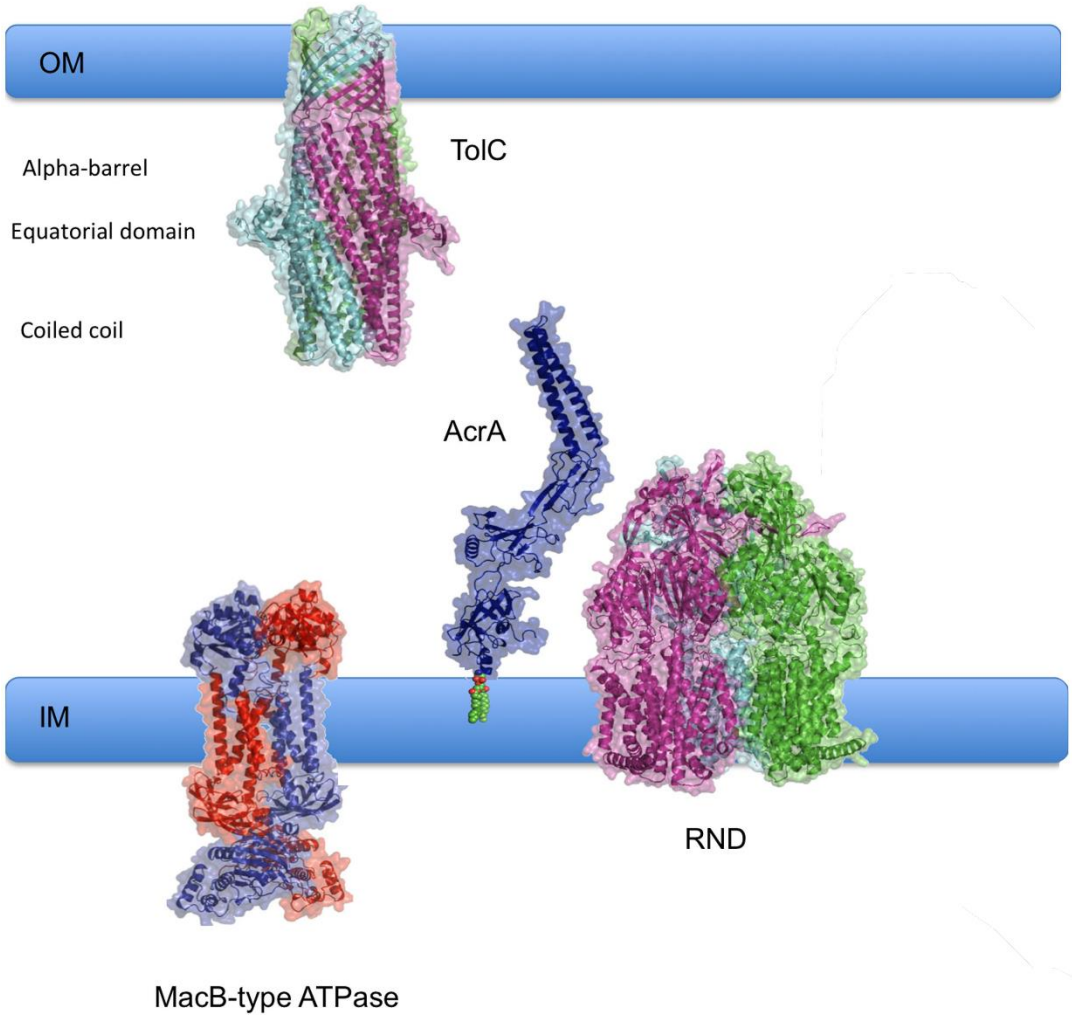

Figure I.2 – Typical Gram-negative efflux transporter components.

Components of a typical Gram-negative efflux transporter include an IMF, in this case either a MacB-type ATPase or a typical RND-type transporter that bridges the inner membrane, an OMF to bridge the outer membrane, in this case TolC, and an MFP, shown here as AcrA. Domains of the OMF are labeled. IM – Inner membrane. OM – Outer membrane. Figure modified from (Bavro, Marshall et al. 2015)

Studies have shown that OMFs and transporters can interact directly (Symmons, Bokma et al. 2009, Tikhonova, Yamada et al. 2011). However, an "open" mutant of TolC in which mutations in the aperture rendered the protein unable to close showed significantly lower affinity for the AcrB transporter than the wild-type TolC. (Tikhonova, Yamada et al. 2011) This suggests that opening of the channel leads to a destabilization of interactions between the transporter and OMF, ultimately resulting in disengagement of the channel and closing of the aperture. The interface between AcrB and TolC is proposed to form between β-hairpins extending from the TolC docking domain on the periplasmic side of AcrB and the periplasmic tip of TolC (Weeks, Bavro et al. 2014). This interface is considered limited, and while it could initiate opening of the channel, it is not sufficient to maintain interactions with the open OMF. Additionally, transporters from the ABC and MF superfamilies of transporters lack the same large periplasmic domains of RND-type transporters, indicating that the interface between the transporter and the OMF is not required for a functional efflux complex (Lu and Zgurskaya 2013). Opening and subsequent stabilization of the OMF is thought to be induced by the third and final component of Gram-negative tripartite complexes, the membrane fusion protein (Zgurskaya, Weeks et al. 2015).

I.4 – Roles of membrane fusion proteins in transport

In Gram-negative bacteria, MDR complexes typically consist of three components forming a large transporter capable of spanning both the inner and outer membranes of Gram-negative cell envelopes. Efflux occurs most effectively by transporting substrate through the outer membrane and into the medium. The inner membrane transporter (IMF) is responsible for binding of substrate and utilization of energy, and spans the inner membrane. Most IMFs extend into both the cytoplasmic and periplasmic space. To link the transporter to the OMF, periplasmic adaptor proteins, or membrane fusion proteins (MFPs) exist in the periplasmic space and provide a functional linkage of the transporter and OMF. MFPs pose an important, though not fully understood role in the overall transport process (Zgurskaya, Yamada et al. 2009, Zgurskaya, Weeks et al. 2015). Investigation of MFPs will provide important information about the mechanism of export in multidrug efflux systems.

MFPs are bacterial proteins known to associate with a wide diversity of transporters belonging to many protein families (Weeks, Nickels et al. 2015). A multitude of functions have been associated with MFPs, ranging from physical linkers between the inner and outer membrane components of the transporter, to actual binding of substrate in the case of some MFPs (Su, Yang et al. 2009, De Angelis, Lee et al. 2010, Delmar, Su et al. 2013, Lu and Zgurskaya 2013). AcrA and MacA have also been shown to stimulate the activities of their associated transporters (Zgurskaya and Nikaido 1999, Tikhonova, Devroy et al. 2007). MFPs function as a hexameric unit, and multiple MFPs from different families of transporters have been crystallized. Some MFPs such as CusB have been crystallized in complex with other transporter components, yielding

insight into how MFPs interact with their cognate transporters and OMFs (Akama, Kanemaki et al. 2004, Su, Yang et al. 2009, Yum, Xu et al. 2009, Greene, Hinchliffe et al. 2013, Du, Wang et al. 2014, Hinchliffe, Greene et al. 2014). The MFP is thought to have a resting state in complex with the transporter, upon response to stimuli, possibly binding of substrate, the MFP recruits the OMF to the complex. Binding of the OMF then triggers a conformational change in the MFP required for the stimulation of the cognate transporter. This dual role of the membrane fusion protein raises questions as to how the molecule interacts with and translates conformational energy to the rest of the complex. As a tripartite complex, all proteins work together to expel substrate into the extracellular space (Ge, Yamada et al. 2009, Modali and Zgurskaya 2011). While primary sequences among MFPs are not well conserved, their structures are generally conserved. MFPs are elongated molecules composed of four domains in a linear conformation that is proposed to extend from the inner membrane surface up through the periplasm to meet the OMF. **(Figure I.3)**

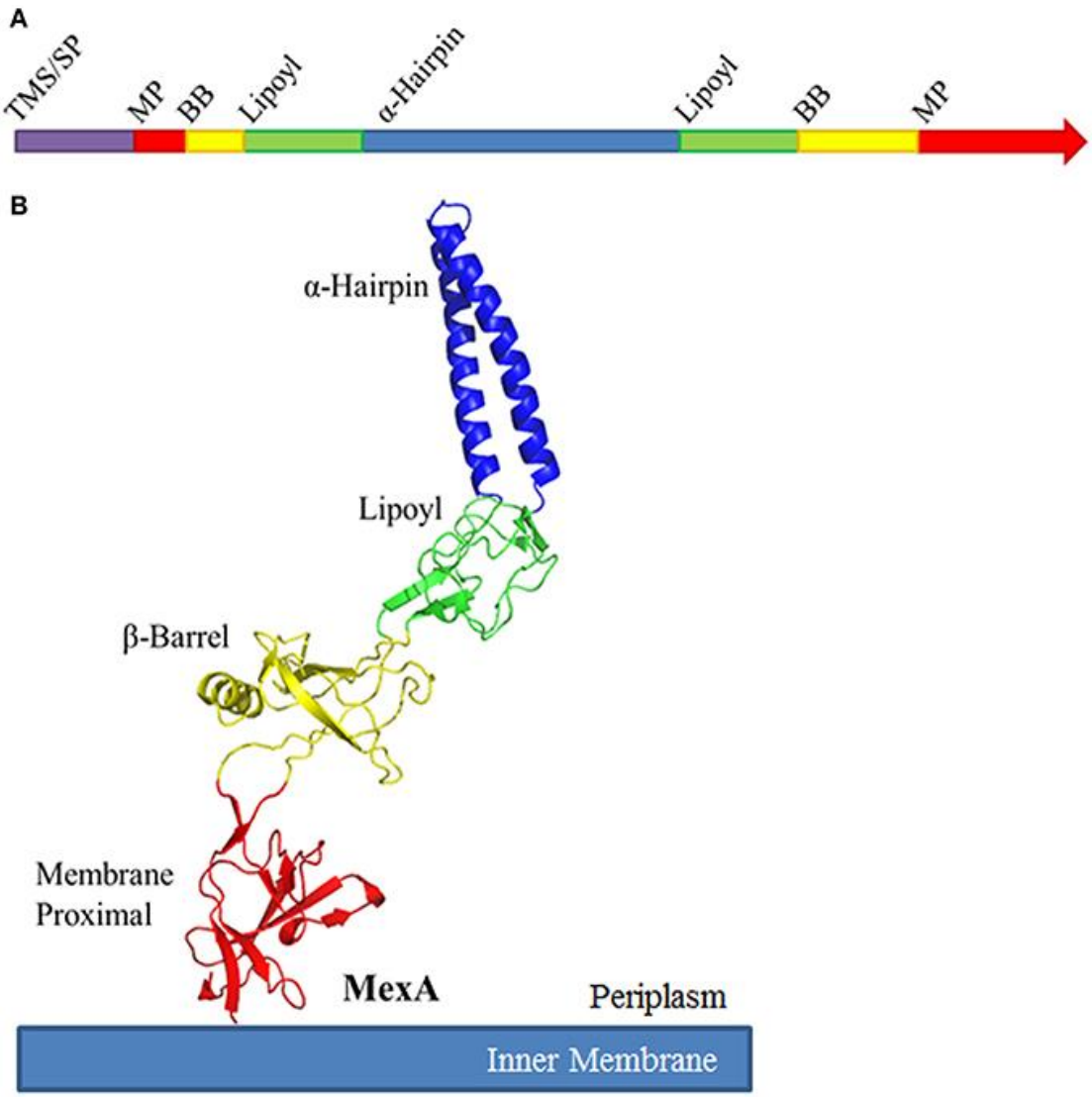

Figure I.3 – Diagram of typical MFP structure.

A. Linear representation of domain arrangement in MFPs from N-terminus to C-terminus. TMS / SP – Transmembrane segment / signal peptide. MP – Membrane proximal. BB – β-barrel. B. Crystal structure of the MFP MexA. (PDB ID: 2V4D) Domain organization is colored similarly in both primary sequence and in structure. Figure adopted from (Zgurskaya 2015)

The conserved 4-domain structure of MFPs begins with membrane proximal (MP) domain that lies near the inner membrane, containing both the N- and C-terminus of the MFP. Some MP domains contain a transmembrane segment that anchors the MFP to the inner membrane (Zgurskaya and Nikaido 1999, Zgurskaya, Weeks et al. 2015). Directly above the MP domain lies the β-barrel domain. This domain is comprised of a number of β sheets forming a tight barrel conformation. The lipoyl domain is above the β-barrel domain and the domain furthest from the membrane region of the MFP is the α-helical hairpin domain. The α-helical hairpin is composed of two large antiparallel α-helices connected by a short loop region. Each of these domains are connected via short unstructured regions which are thought to impart a large range of interdomain flexibility to the protein. This flexibility is believed to be important for functional interactions with both transporters and OMFs (Mikolosko, Bobyk et al. 2006).

MFPs oligomerize and assemble a structure in which the α-helical hairpins interact and form a funnel that interacts with the OMF. The cognate transporter interacts with the MP, β-barrel, and possibly the lipoyl domain (Zgurskaya, Weeks et al. 2015). Variations in the domains are seen in MFPs corresponding to unique transporters such as EmrB of *E. coli* (Hinchliffe, Greene et al. 2014). Crystal structures of the MF transporter EmrB reveals little to no periplasmic extension, and in accord, the MFP EmrA lacks a MP domain (Hinchliffe, Greene et al. 2014). Additionally, the α-hairpin of EmrA is very long in order to extend through the periplasmic space and interact with

the OMF. Contrarily, the MFP BesA of the BesABC complex of *Borrelia burgdorferi* lacks an α-hairpin domain entirely **(Figure I.4)** (Greene, Hinchliffe et al. 2013).

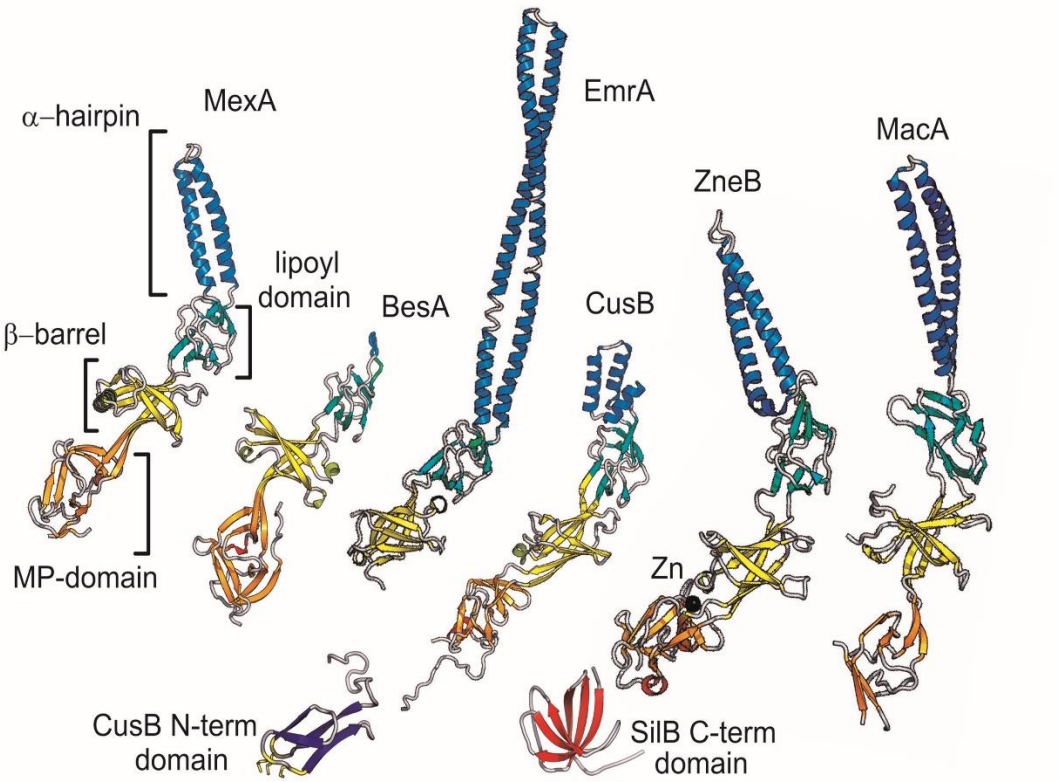

Figure I.4 – Comparison of some crystallized MFPs.

Comparison of the domains of a representative subset of MFPs, highlighting the structural diversity of the protein family. Figures adopted from (Bavro, Marshall et al. 2015)

The interactions of MFPs with OMFs and transporters have not been fully revealed, and much debate exists about placement of the MFP on either component of the complex. MFPs have also been identified in Gram-positive bacteria, which poses an

intriguing question as to the role of a membrane fusion protein in an organism containing only a single membrane (Harley, Djordjevic et al. 2000).

Some MFPs have been crystallized in complex with their cognate transporters, and components of the complex exist in a monomer ratio of 3 IMF : 6 MFP : 3 OMF (Symmons, Bokma et al. 2009, Su, Long et al. 2011, Du, Wang et al. 2014). When crystallized alone, MFPs repeatedly form dimer pairs, indicating the dimer is the functional unit for the MFP (Akama, Matsuura et al. 2004, Mikolosko, Bobyk et al. 2006, Yum, Xu et al. 2009). The affinity for oligomerization and stability of dimers varies between MFPs, and some studies have shown that interaction with the periplasmic domain of the transporter stabilizes the MFP oligomer (Tikhonova, Dastidar et al. 2009). However, due to the flexibility of the interdomain linker regions of the protein, different monomers of the dimer unit are believed to have different conformations (Akama, Matsuura et al. 2004). In addition, when crystallized with the transporter, the individual MFPs make different contact interfaces with both the transporter as well as the OMF (Su, Long et al. 2011). This suggests that one protomer may have a different role than the other when functioning together with the transporter. Possibly the strongest evidence for the inequivalence of MFP dimers comes from the *Pseudomonas aeruginosa* triclosan transporter TriABC-OpmH. This complex consists of two separate MFPs, TriA and TriB, that are both required for functionality of the complex (Mima, Joshi et al. 2007).

Previous studies have converged on a three-step model of MFP-dependent transport. Firstly, the MFP and transporter are proposed to exist in complex, located to the inner membrane (Lu and Zgurskaya 2012). Upon response to stimuli, possibly

binding of drug, a conformational change in the MFP occurs that recruits the OMF to the MFP-transporter complex (Janganan, Bavro et al. 2013). The channel is then opened through a conformational change (Lobedanz, Bokma et al. 2007, Tikhonova, Dastidar et al. 2009, Zgurskaya, Weeks et al. 2015). After formation of the fully assembled transporter, the MFP then stimulates the activity of the transporter (Ge, Yamada et al. 2009, Modali and Zgurskaya 2011) so that drug is expelled through the outer membrane channel and into the extracellular space. Interactions between the OMF and the rest of the complex are thought to be transient (Tikhonova, Dastidar et al. 2009), and upon dissociation of the OMF, the complex resets back to the resting state.

It has become recently clear that MFPs play a very active role in the efflux process (Zgurskaya, Weeks et al. 2015). They are shown to be involved with substrate binding, recruitment of OMFs, and stimulation of transporters. Although their role is becoming less vague, the exact interactions of this required transporter component with the other complex proteins are unclear. Specifically, it is still not understood how the MFP accomplishes the two roles of OMF recruitment and transporter stimulation. It is possible that homomultimeric MFPs assume different roles for each protomer, but we have not yet had the tools to investigate the differences between these protomers. Through the investigation of unique MFP-containing complexes such as YknWXYZ and TriABC, the specific roles of the MFP can be elucidated, providing insight into the mechanism of these transporters and paving the way for investigation of inhibitors of MDR complexes.

I.5 – TriABC contains two unique membrane fusion proteins

TriABC is an RND-type transporter found in *P. aeruginosa*. TriABC was identified by Mima *et. al* 2007 by subjecting an efflux-deficient *P. aeruginosa* strain PAO509 to increasing triclosan concentrations. The resulting triclosan-resistant strain PAO509.5 contained an overexpressed protein complex, TriABC (Mima, Joshi et al. 2007). TriABC functions with the outer membrane pump OpmH in *P. aeruginosa*. TriABC consists of the inner membrane RND transporter TriC, and the two MFPs TriA and TriB. The complex resembles a standard RND-type efflux complex, except that it contains two MFPs present in the same operon. Both membrane fusion proteins are required for function and are quite distinct (Mima, Joshi et al. 2007). TriA only has 36% identity and 51% similarity when compared to TriB. To envision how this dual-MFP system could function, Mima *et al.* suggested that TriA and TriB could oligomerize in a heteromultimer, in which the MFPs could exist in a ratio of 3:3:3:3 TriC:TriA:TriB:OpmH (Mima, Joshi et al. 2007). This fits with the model where the MFP exists as a stable dimer that then further trimerizes to form the fully functional MFP unit. While other efflux complexes are able to go through the efflux process utilizing a single MFP, TriABC requires both TriA and TriB individually. The inequal MFP dimer observed in previously mentioned crystal structures has led to speculation that the different conformations of MFPs observed retain unique functional aspects as well. However, it has been difficult to investigate this speculation, as most studies have focused on homomultimeric MFPs (Greene, Hinchliffe et al. 2013, Zgurskaya, Weeks et al. 2015). The heteromultimeric nature of TriABC provides a useful system in which to study the differential roles of MFPs. Investigation of TriABC can determine if the

individual protomers of the functional dimeric unit actually do assume different roles in the transport process.

I.6 – YknWXYZ is a unique Gram-positive MFP-dependent transporter

YknWXYZ is an ABC-type transporter from *Bacillus subtilis* that provides resistance to an endogenously-produced peptide, SdpC (Butcher and Helmann 2006). The unprocessed peptide, sporulation delaying protein (SDP) is produced by *B. subtliis* under starvation conditions and causes lysis of surrounding cells by collapse of proton-motive force. Lysis then frees nutrients to be absorbed by other cells in order to delay the costly process of sporulation (Lamsa, Liu et al. 2012, Yamada, Tikhonova et al. 2012). YknWXYZ is upregulated by the σ-W regulon, which is activated in response to antibiotic exposure in growing *B. subtilis* cells (Butcher and Helmann 2006). The first protein in the operon, YknW, is highly conserved among *Bacillus* species, but absent from the genomes of other bacteria (Yamada, Tikhonova et al. 2012). It contains a conserved Yip1 domain known to be involved with interaction of Rab GTPases in in eukaryotes, and in vesicular transport in yeasts (Yamada, Tikhonova et al. 2012).

The three other genes, YknXYZ, encode a membrane fusion protein, ATPase, and membrane permease respectively. The MFP YknX is predicted to contain a single N-terminal transmembrane segment, followed by the typical MFP structure. YknY and YknZ express components that are thought to assemble to form a complete ATPase and permease (Butcher and Helmann 2006). Other ABC-type transporters such as MacAB-TolC of *E. coli* contain the ATPase and permease components expressed as a single polypeptide (Kobayashi, Nishino et al. 2003), but YknWXYZ expresses these proteins

separately (Yamada, Tikhonova et al. 2012). The ATPase portion of YknY incorporates the three conserved motifs found in ABC-type transporters, the Walker A, Walker B, and ABC signature motif, while YknZ forms a permease thought to cross the membrane of *B. subtilis* (Butcher and Helmann 2006, Yamada, Tikhonova et al. 2012).

When overproduced from a plasmid, YknWXYZ was found to protect cells from both endogenous and exogenously produced SdpC. With the exception of YknW, the loss of any complex component resulted in a loss of functionality. However, YknW alone only provides a partial functionality to SdpC (Yamada, Tikhonova et al. 2012). The requirement of an MFP in a Gram-positive organism implies certain functions of the MFP that would be conserved between Gram-positive and Gram-negative organisms. This indicates that MFPs have a very active role in the transport process for them to be conserved in an organism only requiring transport across a single lipid bilayer, but their specific function in the context of a Gram-positive environment remains unknown.

I.7 – Specific aims and goals of this dissertation

Both TriABC and YknWXYZ are unique efflux systems that require nonstandard composition for function. They are also very different from one another, in that they are expressed in different native organisms and come from different efflux families. We currently do not know how MFPs interact with their complex components and how these interactions beget the dual role of OMF recruitment and transporter stimulation. Understanding how unique MFPs interact and work with their cognate transporters will give insight into the mechanism of MFP-mediated efflux. This

understanding will serve as a basis for updating the model of transport in both RND- and ABC-type transporters, and in the process shed light on the multiple roles of MFPs. In this dissertation, the goal is to characterize the unique MFPs TriA and TriB, and determine how two different MFPs interact with their cognate transporter and OMF. We will accomplish this using a combination of deletion and point mutations, combined with co-purification and functional studies. Understanding of the TriABC transporter serves to demonstrate how two unique MFPs interact differently with complex components, demonstrating the dual role of MFPs.

We also seek to characterize the Gram-positive MFP YknX, and investigate protein-protein interaction of the complex, as well as the conservation of known MFP functions in a Gram-positive system. We will accomplish this through the construction of fusion as well as chimeric proteins, combined with ATPase assays that allow us to quantify the activity of the complex. This understanding will demonstrate the function of the MFP in the absence of an OMF. The completion of these aims will provide an update to the model of MFP-mediated efflux transporters in bacteria, and lay the foundation for inhibitor and drug design in future studies.

II. Methods

Table 1. List of strains and plasmids

Strain or plasmid name	Relevant genotype or description	Source or reference
DH5α	*supE44* D*lacU169 hsdR17 recA1 endA1 gyrA96 thi-1 relA1*	Novagen
BL21 (DE3)	F- *ompT hsdS$_b$*(r_B^- m_B^-) *gal dcm*	Novagen
BW25113	Δ(*araD-araB*)*567* Δ(*rhaD-rhaB*)*568* Δ*lacZ4787* (::rrnB-3) *hsdR514 rph-1*	(Datsenko and Wanner 2000)
ET103	BW25113 Δ*ompT*::Km^r	(Tikhonova, Devroy et al. 2007)
JWW1	BW25113 Δ*ompT*-scar	This Study
JWW2	JWW1 Δ*acrAB*::Km^r	This Study
JWW3	JWW2 *tolC*::Tn*10-48*	This Study
C43	F- *ompT hsdS$_b$*(r_B^- m_B^-) *gal dcm lon* λDE3 pLys-S and two uncharacterized mutations as described in (Miroux and Walker 1996)	
HB6127	CU1065 yknWXYZ::Kan	(Butcher and Helmann 2006)
PAO1	Wild type	(Lomovskaya and *al.* 1999)
PAO509.5	PAO1 Δ*mexAB-oprM* Δ*mexCD-oprJ* Δ*mexEF-oprN* Δ*mexJK* Δ*mexXY* overexpressing *triABC*	(Mima, Joshi et al. 2007)
PAO1116	PAO1 Δ*mexAB-oprM* Δ*mexCD-oprJ* Δ*mexEF-oprN* Δ*mexJK* Δ*mexXY* Δ*triABC*	(Mima, Joshi et al. 2007)
JWW4	PAO509.5 Δ*opmH*::Gm^r	This Study
JWW5	JWW4 *att*Tn*7*::mini-Tn*7*T -Tp^r -*araC*-P$_{araBAD}$-MCS	This Study
JWW6	JWW4 *att*Tn*7*::mini-Tn*7*T-Tp^r -*araC*-P$_{araBAD}$-*opmH* (OpmH$_{His}$)	This Study
JWW7	JWW4 *att*Tn*7*:: mini-Tn*7*T-Tp^r -*araC*-P$_{araBAD}$-*tolC* (TolC$_{His}$)	This Study
p151AcrAB	pUC18 vector carrying acrAB; 6-His tagged AcrA	(Ma, Cook et al. 1993)
p151AcrA*B	pUC18 vector carrying acrAB; 6-His tagged AcrA with amber codon mutation at R225	This Study
pEVOL-Az	Cm^r; expresses aaRS/tRNA pairs for incorporation of UAA	(Young, Ahmad et al. 2010)

pEVOL-Bz	Cm^r; expresses aaRS/tRNA pairs for incorporation of UAA	(Young, Ahmad et al. 2010)
pPS1283	Ap^r; Gm^r; pEX18ap-*opmH*-Gm	(Chuanchuen, Murata et al. 2005)
pTJ1	Ap^r; Tp^r; pUC18T-mini-Tn7T-Tp-*araC*-P_{BAD}-MCS	(Damron, McKenney et al. 2013)
pTJ1-opmH	Ap^r; Tp^r; expresses *opmH* ($OpmH_{His}$)	This Study
pTJ1-tolC	Ap^r; Tp^r; expresses *tolC* ($TolC_{His}$)	This Study
pTNS2	Ap^r; Helper plasmid expressing Tn*7* transposase proteins TnsABCD	(Choi, Gaynor et al. 2005)
pBSPII (KS-/SK-)	Cb^r; broad-host-range cloning vector	(Schweizer, Hoang et al. 2001)
pPS1824	Cb^r; pBSPII P_{lac}-*triABC*; Bla^r	(Mima, Joshi et al. 2007)
pPS1947	Cb^r; pBSPII P_{lac}-*triA*; Bla^r	(Mima, Joshi et al. 2007)
pPS1950	Cb^r; pBSPII P_{lac}-*triB*; Bla^r	(Mima, Joshi et al. 2007)
pPS2071	Cb^r; pBSPII P_{lac}-*triC*; Bla^r	(Mima, Joshi et al. 2007)
pPS1948	Cb^r; pBSPII P_{lac}-*triAB*; Bla^r	(Mima, Joshi et al. 2007)
pPS2140	Cb^r; pBSPII P_{lac}-*triAC*; Bla^r	(Mima, Joshi et al. 2007)
pPS1954	Cb^r; pBSPII P_{lac}-*triBC*; Bla^r	(Mima, Joshi et al. 2007)
pBSP-AxBC	Cb^r; pPS1824 expressing *triAxBC;*TriA and TriB are expressed as a fusion protein	This Study
pBSP-A_{R130D}BC	Cm^r; expresses *triAxBC*; mutant *triA* ($TriA_{R130D}$)	Abigail Ntreh, unpublished
pBSP-AB_{R118D}C	Cm^r; expresses *triABC*; mutant *triB* ($TriB_{R118D}$)	Abigail Ntreh, unpublished
pBSP-A_{R130D}xBC	Cm^r; expresses *triAxBC*; mutant *triA* ($TriA_{R130D}$)	Abigail Ntreh, unpublished
pBSP-AxB_{R118D}C	Cm^r; expresses *triAxBC*; mutant *triB* ($TriB_{R118D}$)	Abigail Ntreh, unpublished
pBSP-$A_{\Delta CC}$BC	Cm^r; expresses *triABC*; mutant *triA* ($TriA_{\Delta coiled\ coils}$)	Abigail Ntreh, unpublished
pBSP-$AB_{\Delta CC}$C	Cm^r; expresses *triABC*; mutant *triB* ($TriB_{\Delta coiled\ coils}$)	Abigail Ntreh, unpublished
pBSP-$A_{\Delta CC}$xBC	Cm^r; expresses *triAxBC*; mutant *triA* ($TriA_{\Delta coiled\ coils}$)	Abigail Ntreh, unpublished

pBSP-$AxB_{\Delta CC}C$	Cm^r; expresses *triAxBC*; mutant *triB* ($TriB_{\Delta coiled\ coils}$)	Abigail Ntreh, unpublished
pBAD33	Cm^r; expression vector; arabinose inducible promoter	(Guzman, Belin et al. 1995)
pBAD33-ABC	Cm^r; expresses *triABC*; expresses Strep-tagged TriC	This Study
pBAD33-$A_{R130D}BC$	Cm^r; expresses triABC; mutant *triA* ($TriA_{R130D}$)	This Study
pBAD33-$A_{G350C}BC$	Cm^r; expresses *triABC*; mutant *triA* ($TriA_{G350C}$)	This Study
pBAD33-$AB_{R118D}C$	Cm^r; expresses *triABC*; mutant *triB* ($TriB_{R118D}$)	This Study
pBAD33-$AB_{G339C}C$	Cm^r; expresses *triABC*; mutant *triB* ($TriB_{G339C}$)	This Study
pBAD33-$A_{\Delta CC}BC$	Cm^r; expresses *triABC*; mutant *triA* ($TriA_{\Delta coiled\ coils}$)	This Study
pBAD33-$AB_{\Delta CC}C$	Cm^r; expresses *triABC*; mutant *triB* ($TriB_{\Delta coiled\ coils}$)	This Study
pBAD33-$A_{\Delta 26}BC$	Cm^r; expresses *triABC*; mutant *triA* ($TriA_{\Delta C\text{-terminal }26\text{ amino acids}}$)	This Study
pBAD33-$A_{\Delta 47}BC$	Cm^r; expresses *triABC*; mutant *triA* ($TriA_{\Delta C\text{-terminal }47\text{ amino acids}}$)	This Study
pBAD33-$AB_{\Delta 9}C$	Cm^r; expresses *triABC*; mutant *triA* ($TriA_{\Delta C\text{-terminal }9\text{ amino acids}}$)	This Study
pBAD33-$AB_{\Delta 30}C$	Cm^r; expresses *triABC*; mutant *triA* ($TriA_{\Delta C\text{-terminal }30\text{ amino acids}}$)	This Study
pBAD33-AxBC	Cm^r; expresses *triAxBC;*TriA and TriB are expressed as a fusion protein; expresses Strep-tagged TriC	This Study
pBAD33-$A_{R130D}xBC$	Cm^r; expresses *triAxBC*; mutant *triA* ($TriA_{R130D}$)	This Study
pBAD33-$A_{G350C}xBC$	Cm^r; expresses *triAxBC*; mutant *triA* ($TriA_{G350C}$)	This Study
pBAD33-$AxB_{R118D}C$	Cm^r; expresses *triAxBC*; mutant *triB* ($TriB_{R118D}$)	This Study
pBAD33-$AxB_{G339C}C$	Cm^r; expresses *triAxBC*; mutant *triB* ($TriB_{G339C}$)	This Study
pBAD33-$A_{\Delta CC}xBC$	Cm^r; expresses *triAxBC*; mutant *triA* ($TriA_{\Delta coiled\ coils}$)	This Study
pBAD33-$AxB_{\Delta CC}C$	Cm^r; expresses *triAxBC*; mutant *triB* ($TriB_{\Delta coiled\ coils}$)	This Study
pBAD33-$A_{\Delta 26}xBC$	Cm^r; expresses *triAxBC*; mutant *triA* ($TriA_{\Delta C\text{-terminal }26\text{ amino acids}}$)	This Study
pBAD33-$A_{\Delta 47}xBC$	Cm^r; expresses *triAxBC*; mutant *triA* ($TriA_{\Delta C\text{-terminal }47\text{ amino acids}}$)	This Study

pBAD33-AxB$_{\Delta 9}$C	Cm^r; expresses *triAxBC*; mutant *triA* (TriA$_{\Delta C\text{-terminal 9 amino acids}}$)	This Study
pBAD33-AxB$_{\Delta 30}$C	Cm^r; expresses *triAxBC*; mutant *triA* (TriA$_{\Delta C\text{-terminal 30 amino acids}}$)	This Study
pBAD-myc His, C	Ap^r; expression vector; arabinose inducible promoter	Invitrogen
pBAD-A	Ap^r; express *triA*; 6-His tagged TriA	This Study
pBAD-B	Ap^r; express *triB*; 6-His tagged TriB	This Study
pBAD-AB	Ap^r; express *triAB*; 6-His tagged TriB	This Study
pBAD-AxB	Ap^r; express *triAxB*; TriA and TriB are expressed as a fusion protein; 6-His tagged TriB	This Study
pBAD-C$_{His}$	Ap^r; express *triC*; 6-His tagged TriC	This Study
pUC-MZ	pUC18 expressing MacB ATPase and YknZ fusion protein	This Study
pUC-MLZ	pUC18 expressing MacB ATPase and YknZ fusion protein, with MacB linking region	This Study
pUC-YM	pUC18 expressing YknY and MacB permease fusion protein	This Study
pUC-YLM	pUC18 expressing YknY and MacB permease fusion protein, with MacB linking region	This Study
pET-MLZ	pET21a expressing MacB ATPase and YknZ fusion protein, with MacB linking region	This Study
pET-YLM	pET21a expressing YknY and MacB permease fusion protein, with MacB linking region	This Study
pET-YLZ	pET21d expressing YknYZ fusion protein	This Study
pET21D	Cloning vector, Ap	Novagen
pET-X	pET21d expressing YknX	(Yamada, Tikhonova et al. 2012)
pET-MacB	pET21d expressing MacB	(Lin, Bavro et al. 2009)
pET-Y	pET21d expressing YknY	(Yamada, Tikhonova et al. 2012)
pHC-WXYZ	pHCMC04 expressing YknWXYZ; 6-His tagged YknZ	(Yamada, Tikhonova et al. 2012)
pHC-YZ	pHCMC04 expressing YknYZ; 6-His tagged YknZ	(Yamada, Tikhonova et al. 2012)
pHC-sYZ	pHCMC04 expressing YknYZ; Strep-tagged YknY, 6-His tagged YknZ	This study

Plasmid construction

The amber codon was introduced to AcrA position R225 using a QuikChange Lightning site-directed mutagenesis kit (Agilent) using p151AcrAB as a template with AcrA*fwd and AcrA*rev primers (Ma, Cook et al. 1993) The resulting plasmid was sequenced at Oklahoma Medical Research Foundation to confirm the substitutions.

Genes encoding $TriA_{His}$, $TriB_{His}$, and $TriAB_{His}$ were cloned into pBAD/*Myc*-His C using PCR product from PAO1 genomic DNA as a template in combination with TriA *Nco*I FWD, TriB *Nco*I FWD, TriA-His *Xho*I REV and TriB-His *Xho*I REV primers where appropriate. PCR produce and vector were cut with *Nco*I and *Xho*I before ligation using T4 DNA ligase (New England Biolabs). A C-terminal tag composed of 6 histidine residues was introduced prior to the native stop codon of the *triA* or *triB* genes during PCR. Primers used for PCR are listed in appendix A. Additionally a construct encoding a TriA-TriB fusion protein (TriAxB) was also constructed in which the native stop codon of *triA* was removed, a flexible five amino acid linker region was added, and the N-terminal signal peptide of *triB* was removed including the proposed modified cysteine residue using the primers TriAxB *Xba*I Fusion FWD and TriAxB *Xba*I Fusion REV. This pBAD-AxB plasmid was constructed from the pBAD-AB plasmid using a QuikChange Lightning site-directed mutagenesis kit (Agilent). Primers used are listed in Appendix A. For ease of screening potential positives, an *Xba*I site was engineered into the linker region.

To construct pBSP-AxBC, pBAD-AxB was digested with *Age*I/*Bpu*10I, which created a fragment of DNA encoding the C-terminus of TriA, TriAxB fusion segment, and the N-terminus of TriB. This fragment was then cloned into pPS1824 digested with

*Age*I/*Bpu*10I, resulting in pBSP-AxBC. Positive clones were confirmed by *Xba*I digestion and sequencing at Oklahoma Medical Research Foundation. Additionally, genes encoding $TriABC_{Strep}$ and $TriAxBC_{Strep}$ were cloned into pBAD33 by using either pPS1824 or pBSP-AxBC as template for PCR with *Sac*I TriA FWD and TriC-Strep *Hind*III REV primers for amplification. PCR products, as well as pBAD33, were digested with *Sac*I-HF and *Hind*III-HF. Additionally, $TriC_{His}$ was cloned into pBAD/*Myc*-His C by first amplifying the *triC* gene with a primer TriC-His *Hind*III REV encoding a 6His-tag. The PCR product was then digested with *Pci*I and *Hind*III, while pBAD/*Myc*-His was digested with *Nco*I and *Hind*III. Ligation reactions were performed per the manufacturer's protocol (New England Biolabs).

Point mutations were introduced using a QuikChange Lightning Site-Directed Mutagenesis kit and primers designed according to manufacturer's guidelines (Agilent Technologies). Primers are listed in appendix A. Plasmids were purified using a Qiagen Mini-Prep Kit and the coding sequences of TriABC were sequenced at the Oklahoma Medical Research Foundation Sequencing Facility to confirm the introduction of the desired substitutions.

C-terminal deletions of TriA and TriB were constructed in pBAD33-ABC using PCR. Briefly, forward and reverse primers were designed to amplify in the forward direction from stop codon, and in the reverse direction from the beginning of the deleted area, creating a PCR product consisting of the entire pBAD33-TriABC plasmid, excepting the area to be deleted. A26rev and A47rev primers were designed to create PCR products missing the indicated number of 3-letter codons, resulting in deletions of the indicated number of amino acids from the final protein product. Actermfwd was

designed to amplify the region before the stop codon of TriA, replacing the native overlapping stop / start codon with an *NdeI* site, which would preserve the overlapping stop / start codon with an isoleucine residue inserted at the end of TriA. *Nde*I-digested PCR products and pBAD33 were ligated using T4 DNA ligase according to the manufacturers protocol (New England Biolabs). TriB deletions were constructed in the same way, but using primers B9rev, B30rev, and Bctermfwd. Primer sequences are listed in appendix A. TriAxBC TriA-deletion mutants were made using the same method, but instead of an *Nde*I site, an *Spe*I site was utilized, which encodes for serine and threonine before the AxB linker. Specific primers were Ax26rev, Ax47rev, and Axctermfwd. TriAxBC TriB mutations were made using the same primers as TriABC TriB-mutations.

pBSP-TriA$_{R130D}$BC, pBSP-TriB$_{R118D}$BC, pBSP-TriA$_{\Delta CC}$BC, and pBSP-TriB$_{\Delta CC}$BC along with their equivalent TriAxB variants were created by amplifying the entire coding gene from the corresponding pBAD33-based plasmid using the primers TriA-SacIfwd and TriC-HindIIIrev. PCR product and pBSPII(-SK) were digested using *Sac*I and *Hind*III before ligation according to the manufacturer's protocol.

To construct pET21d(+) YknYLZ, *yknY* and *yknZ* were amplified separately using PCR with *B. subtilis 168* genomic DNA as a template. The primers yknY-f and yknY-r were flanked by NcoI and XhoI sites, respectively, and the primers yknZ-f and yknZ-r were flanked by SalI and XhoI sites, respectively. The linking region, taken from pET-MacB was amplified using primers L-fwd and L-rev containing SalI and XhoI sites, respectively. DNA cut by either XhoI or SalI have an overhang of 5'-

TCGAC-3’ and are compatible for ligation, but upon ligation will form a site incapable of being cut by XhoI or SalI.

Strain construction

E. coli JWW1, JWW2, and JWW3 strains were derived from ET103 (BW25113 Δ*ompT*::Km^r) (Tikhonova, Devroy et al. 2007). The kanamycin resistance marker was scarred out using pCP20 as described in (Datsenko and Wanner 2000) in order to create JWW1. JWW1 was then transduced with P1 phage carrying the Δ*acrAB*::Km^r allele from RAM1419 (Weeks, Celaya-Kolb et al. 2010) using standard laboratory procedures to produce JWW2. JWW2 was then transduced with P1 phage carrying the *tolC*::Tn*10-48* allele from RAM958 (Vakharia, German et al. 2001) to construct JWW3. LB broth and Terrific Broth (TB) (12 g of Bacto tryptone, 24 g of yeast extract, 4 ml of glycerol per 900 ml of water supplemented with 100 ml of 0.17 M KH_2PO_4, 0.72 M K_2HPO_4) were used for bacterial growth and supplemented with ampicillin (100 µg ml^{-1}), chloramphenicol (12.5 µg ml^{-1}), kanamycin (25 µg ml^{-1}), carbenicillin (200 µg ml^{-1}), tetracycline (10 µg ml^{-1}), gentamicin (30 µg ml^{-1}), or trimethoprim (45 µg ml^{-1}) when necessary. All chemicals used were of Molecular Biology grade.

P. aeruginosa strains JWW4, JWW5, JWW6, and JWW7 were created by first deleting the *opmH* gene from *P. aeruginosa* PAO509.5 (Mima, Joshi et al. 2007) by mating with *E. coli* SM10 containing pPS1283 (pEX18-AP-*opmH*-Gm) leading to JWW4. For mating, PAO509.5 and SM10 freshly transformed with pPS1283 were grown to OD_{600} ~0.2. Donor and recipient cells (2 x 10^8 cells) were collected and mixed in 50 µl of LB and plated on LB agar plates overnight at 37°C. The next day, mated

cells were collected and resuspended in 5 ml of 10 mM $MgSO_4$. 100 µl of resuspended mated cells were plated on Vogel-Bonner (VB) minimal medium agar plates (0.2 g of magnesium sulfate, 2 g of citric acid, 10 g of anhydrous dibasic potassium phosphate, 3.5 g of sodium ammonium phosphate, 15 g of agar per liter (Vogel and Bonner 1956) supplemented with 30 µg ml^{-1} gentamicin and 5% sucrose for 24 – 48 hr at 37°C (de Lorenzo and Timmis 1994). Colonies were screened for carbenicillin sensitivity on LB agar containing carbenicillin (200 µg ml^{-1}) to confirm proper integration of the pPS1283 plasmid and removal of the wild type *opmH* gene. Gentamicin resistant, carbenicillin sensitive colonies were analyzed by PCR of genomic DNA to confirm the deletion of *opmH.* Insertion of genes encoding 6x histidine-tagged $OpmH^{His}$, $TolC^{His}$, or MCS onto the chromosome of JWW4 was performed by transforming PTJ1 carrying either $OpmH^{His}$, $TolC^{His}$, or an empty MCS by previously described protocols (Damron, McKenney et al. 2013).

Photocrosslinking of AcrAB

pUC151 plasmid containing AcrAB and variants were transformed into JWW2 cells either with or without pEVOL-AzF or pEVOL-BzF and grown on LB agar containing ampicillin (100 µg ml^{-1}) and chloramphenicol (12.5 µg ml^{-1}) where appropriate. Colonies were inoculated from plates into LB broth containing ampicillin (100 µg ml^{-1}) and chloramphenicol (12.5 µg ml^{-1}) where appropriate and allowed to grow overnight, and the next day, a fresh culture was inoculated at a 1/50 dilution and grown for 5 hours in either Luria-Bertani (LB) broth (10 g of Bacto tryptone, 5 g of yeast extract, and 5 g of NaCl per liter, pH 7.0), media or 2x YT (16 g tryptone, 10 g of

yeast extract, and 5 g of NaCl per liter, pH 7.0). *p*-azido-*L*-phenylalanine (AzF) (BACHEM) or *p*-benzoyl-*L*-phenylalanine (BzF) (BACHEM) were added where appropriate to a final concentration of 1 mM. Cells were collected via centrifugation at 3,220 g for 20 minutes, washed in 10 mM Tris-Cl, pH 7.5, and protected from UV exposure before any following experiments.

Cells containing AcrA* were resuspended in buffer containing 20 mM Tris-HCl (pH 7.5) and 100 mM NaCl. Resuspended cells were then placed in a 24-well sterile cell culture plate (Falcon) and the plate packed in ice. With the lid removed, cells were exposed to UV light for 0-60 minutes using a handheld lamp set to 365 nm. After exposure, cells were collected via centrifugation at 3,220 x g for 20 minutes and either frozen or lysed for membrane isolation. Lysis was performed by resuspending AcrA*-containing cells in buffer containing 1 mL of 20 mM Tris-HCl, 500 mM NaCl, 1 mM ethylenediaminetetraacetic acid (EDTA), and 100 μg / mL lysozyme. Resuspended cells were incubated on ice for one hour, and broken by sonication. Unbroken cells were then removed by centrifugation at 3,220 x g for 20 minutes, and membrane fractions were collected by centrifugation of the supernatant at 100,000 x g for 1 hour.

Purification of AcrA from *E. coli*

Cells containing AcrA were grown and lysed as previously described. Membranes were resuspended in 20 mM Tris-HCl (pH 7.5), 500 mM NaCl, 5% Triton X-100, and 1 mM phenylmethanesulfonylfluoride (PMSF), and allowed to solubilize on a rotator (Thermo) overnight at 4° Celsius. The next day, the solubilization suspension was centrifuged at 100,000 x g for 1 hour to pellet insoluble material, and the

supernatant was loaded onto a 1 mL Ni-NTA column charged with Cu^{2+}. The column was washed with a buffer containing 20 mM Tris-HCl (pH 7.5), 500 mM NaCl, 0.2% Triton X-100, 1 mM PMSF, and 5 mM imidazole. The column was washed using the same buffer containing increasing imidazole concentrations of 10 column volumes of 20 mM imidazole, 10 column volumes of 50 mM imidazole, and then protein elution utilized 2x 1 column volume of 100 mM imidazole and 3x 1 column volume of 500 mM imidazole.

Minimal inhibitory concentrations (MICs)

Overnight cultures of *P. aeruginosa* or *E.coli* carrying indicated constructs were diluted 1 to 100 in LB broth supplemented with a selective marker grown at 37°C with shaking at 200 RPM for 5 hours. MICs of antimicrobial agents were measured using the two-fold dilution technique in 96-well microtitre plates (Tikhonova, Wang et al. 2002). At an optical density at 600 nm (OD_{600}) of ~1.0, cells were inoculated at a density of $5x10^4$ cells per ml in LB in the presence of two-fold increasing concentrations of antibiotics under investigation. The cultures were incubated for 24 h, and the lowest concentration that completely inhibited bacterial growth was designated the MIC. When required, protein expression was induced by adding 1.0 mM IPTG, 0.2% L-arabinose, 1% L-arabinose, or 1% xylose to cell cultures at OD_{600} of ~0.3-0.5, and cells were further incubated at 37°C for 3 more hours till OD_{600} ~1.0-1.2.

Purification of TriABC components from *E. coli*

E. coli JWW2 competent cells were co-transformed with pBAD33-TriABC constructs and / or pBAD-TriC where appropriate, plated on LB agar supplemented with ampicillin (100 µg ml^{-1}) and chloramphenicol (12.5 µg ml^{-1}) where appropriate, and grown overnight at 37°C. Cells were then cultured in 5 ml LB containing ampicillin (100 µg ml^{-1}) and chloramphenicol (12.5 µg ml^{-1}) where appropriate overnight at 37°C with shaking, and sub-cultured 1/50 into 250 ml TB supplemented with ampicillin (100 µg ml^{-1}) and chloramphenicol (12.5 µg ml^{-1}) where appropriate. Cultures were grown at 37°C with shaking for 3 hours before induction with 0.2% L-arabinose for 5 hours. Membrane fractions were collected by lysing cells in 35 mL of 20 mM Tris-HCl pH 8.0, 500 mM NaCl, 1 mM EDTA, and 100 µg / mL lysozyme. Resuspended cells were incubated on ice for one hour, and broken by sonication. Unbroken cells were then removed by centrifugation at 3,220 x g for 20 minutes, and membrane fractions were collected by centrifugation of the supernatant at 100,000 x g for 1 hour. Membrane pellets were then re-suspended in 3 ml solubilization buffer (20 mM Tris-HCl pH 7.5, 500 mM NaCl, 1 mM PMSF, 5 mM imidazole, 5% Triton X-100) and incubated overnight on a rotator. Insoluble fractions were collected via centrifugation at 100,000 x g for 1 hour, and the solubilized membrane fractions were loaded onto a 100 µl Cu^{2+} charged HisBind Resin (EMD Millipore) column equilibrated with Buffer A (50 mM Tris-HCl pH 7.5, 500 mM NaCl, 1 mM PMSF, 5 mM imidazole) supplemented with 0.2% Triton X-100. Flow-through was re-applied to the column to ensure complete binding, and the column subsequently washed with 10 column volumes of Buffer A containing 5 mM imidazole followed by 20 column volumes of Buffer A containing 40

mM imidazole. Protein was eluted using 3.5 column volumes of Buffer A containing 400 mM imidazole. Fractions were then analyzed for protein amount using sodium dodecyl sulfate polyacrylamide gel electrophoresis (SDS-PAGE), and combined for normalization and immunoblotting.

Purification of OpmH^{His} from *P. aeruginosa*

To purify OpmH^{His}, *P. aeruginosa* JWW6 cells were grown overnight in LB, cells were subcultured 1:100 into fresh LB and incubated until OD_{600} ~0.3. At OD_{600} ~0.3, cultures were induced with 1% L-arabinose for an additional 4.5 hours. Cells were collected by centrifugation at 3220 x g for 20 min. Membranes were prepared as described above. Membranes were resuspended in Buffer A (50 mM Tris-HCl pH 7.5, 150 mM NaCl, 1 mM PMSF, 5 mM imidazole pH 7.5) supplemented with 2% n-Dodecyl β-D-Maltoside (DDM) overnight at 4°C. Solubilized membranes were centrifuged for 1 hour at 100,000 x g. Soluble proteins were applied to a 100 µl Cu^{2+}-charged His-Bind Resin column equilibrated with Buffer A containing 5 mM imidazole and 0.03% DDM. Columns were washed with 10 column volumes of Buffer A containing 5 mM imidazole and 0.03% DDM, followed by 20 column volumes of Buffer A containing 75 mM imidazole and 0.03% DDM. OpmH^{His} was eluted in 4 column volumes of Buffer A containing 400 mM imidazole and 0.03% DDM. Fractions were then analyzed for protein concentration using SDS-PAGE as described below, and peak fractions were combined for immunoblotting.

Purification of YknYLZ

pET-21d(+) plasmid containing YknYLZ was transformed into *E. coli* C43 cells and plated on LB agar plates containing ampicillin (100 μg ml^{-1}) and incubated at 37° Celsius overnight. After incubation, cells were inoculated from plates into LB broth containing ampicillin (100 μg ml^{-1}) and grown overnight at 37°C with shaking. The next day, a fresh culture was inoculated at a 1/100 dilution and grown for 2-3 hours until O.D. 600 reached 0.3-0.5. Protein expression was induced using a final concentration of 1 mM IPTG for 3-4 hours. Cells were then collected via centrifugation at 3,220 x g for 20 minutes, washed with 10 mM Tris-HCl (pH 8.0), and either frozen for later use or resuspended in lysis buffer containing 20 mM Tris-HCl (pH 8.0), 5 mM EDTA, 1 mM PMSF, and 100 μg / mL lysozyme. Resuspended cells were incubated on ice for one hour, and then broken by sonication. Unbroken cells were then removed by centrifugation at 3,220 x g for 20 minutes, and membrane fractions were collected by centrifugation at 100,000 x g for 1 hour. Membranes were resuspended in 40 mM Tris-HCl (pH 8.0), 2 mM PMSF, and solubilized by addition of lysophosphatidylglycerol (LPG) to a final concentration of 20 mg/mL and incubation on a rotator at 4° Celsius overnight. The next day, the solubilization mixture was centrifuged at 100,000 x g for 1 hour to pellet insoluble material, and the supernatant was loaded onto a 1 mL Ni-NTA column charged with Ni^{2+}. Protein was washed and eluted with a buffer containing 20 mM Tris-HCl (pH 8.0), 100 mM NaCl, 1 mM PMSF, and 1 mg/mL LPG and increasing imidazole concentrations of 5 mM, 30 mM, 50 mM, 100 mM, 250 mM and 500 mM.

For detergent exchange, protein was purified in the same manner, except solubilized in 5% Triton X-100 rather than LPG. After elution, purified protein was dialyzed twice over in 1 L of 20 mM Tris-HCl (pH 8.0), 100 mM NaCl, 1 mM PMSF

and 1 mg/mL LPG. Dialyzed fractions were then re-loaded onto the Ni-NTA column, and detergents were exchanged by running 20 column volumes of binding buffer containing 2 mM LPG, then eluting the protein and dialyzing as previously done in Triton X-100. To quantify, protein was then run on an SDS-PAGE gel using known BSA amounts as a standard. Amount of protein was quantified using ImageQuant, and protein concentrations were normalized to 1 mg/mL.

Purification of proteins from B. subtilis

Transformed *B. subtilis* HB6127 cells were scraped from solid media and inoculated into 5 mL of LB and grown overnight at 37° C with shaking. Cells were then re-inoculated into 20 mL of LB, grown for 2-3 hours, and then re-inoculated into 2 liters of LB and grown until the OD_{600} reached 0.4-0.5. Protein production was induced via addition of L-xylose to a final concentration of 0.5% for 3 hours. Cells were collected via centrifugation at 3,220 x g for 20 minutes and washed with 20 mM Tris-HCl (pH 8.0). Cells were then resuspended in lysis buffer containing 50 mM Tris-HCl (pH 8.0), 5 mM $MgCl_2$, 1 mM PMSF, 50 mM NaCl and 0.05 mg/mL DNAse I for 1 hour, and then passed through a French Press at 18,000 psi. Unbroken cells were collected by centrifugation at 3,220 x g for 20 minutes, and membrane fractions were collected via centrifugation at 100,000 x g for 1 hour. Membranes were resuspended in 10 mL of 2x binding buffer (100 mM Tris-HCl pH 8.0, 10 mM $MgCl_2$, 2 mM PMSF, and 100 mM NaCl) and then membranes were solubilized by addition of 10 mL of 2% DDM to a final concentration of 1% and incubation with rotation overnight at 4° C. Insoluble fractions were pelleted via centrifugation at 100,000 x g for 1 hour, and the soluble

portion was loaded onto a 1 mL Ni-NTA column charged with Ni^{2+} and equilibrated with 1x binding buffer (50 mM Tris-HCl pH 8.0, 5 mM $MgCl_2$, 1 mM PMSF, and 50 mM NaCl). The column was washed using imidazole concentrations of 5, 15, and 50 mM, and then proteins were eluted in 100 mM and 500 mM imidazole steps.

Transformation of B. subtilis

B. subtilis HB6127 cells were plated onto solid media and incubated overnight at 37° C. The next morning, colonies were scraped and inoculated into 5 mL of SpI medium (1.4% K_2HPO_4, 0.6% KH_2PO_4, 0.1% sodium citrate, 0.002% $MgSO_4 – 7H_2O$, 0.2% ammonium sulfate) + (0.002% casamino acids, 0.1% yeast extract, 50 μg/mL L-tryptophan, and 0.5% glucose) and incubated at 37° Celsius for 4 hours. The 5-mL mixture was then re-inoculated into 50 mL of SpII medium (1.4% K_2HPO_4, 0.6% KH_2PO_4, 0.1% sodium citrate, 0.002% $MgSO_4 – 7H_2O$, 0.2% ammonium sulfate) + (0.02% yeast extract, 5 mM $MgCl_2$, 50 μg/mL L-tryptophan, and 0.5% glucose) and incubated for 90 minutes at 37° Celsius. Cells were then collected via centrifugation and concentrated 20-fold by resuspension in SpII. 250 μL of concentrated cells were then mixed with 5 μL of plasmid DNA and incubated on ice for 30 minutes, then mixed with 1 mL of LB broth. This mixture was then allowed to grow for 1 hour at 37°C with shaking, and plated on selective media.

Antibody production

Anti-$TriA^{His}$, anti-$TriB^{His}$, and anti-$TriC^{His}$ antibodies were produced in rabbits by Covance. Briefly, proteins were purified from *E. coli* as described above.

Concentrations were determined and 250 µg of protein was used for initial immunization. Rabbits were boosted with 125 µg of protein at 21 day intervals for 3 boosters. Production bleeds were collected 10 days post boosters with a final collection after 77 days. Rabbits were euthanized antibody post collection.

SDS-PAGE and Western blotting

SDS-PAGE was performed according to standard protocols. After SDS-PAGE, immunoblots were performed by electro-transfer of proteins onto a polyvinylidene fluoride (PVDF) membrane via immersion in transfer buffer (25 mM Tris-Cl, unadjusted pH, 192 mM glycine, 20% v/v methanol) at 70 V for one hour. After transfer, membranes were blocked in 10% dry milk solution for at least one hour. Primary antibodies were used at a dilution of 1:30,000 and incubated with membranes for at least three hours. Anti-rabbit and anti-mouse IgG secondary antibodies conjugated to alkaline phosphatase (Sigma) were also used where appropriate at a 1:30,000 dilution for an incubation period of at least one hour. Color development solution was prepared by mixing 1% 5-bromo-4-chloro-3-indolyl phosphate (BCIP) and 1.5% nitro blue tetrazolium (NBT) to a final concentration of 0.02% BCIP and 0.03% NBT in AP buffer (100 mM Tris-Cl, pH 9.5, 100 mM NaCl, 5 mM $MgCl_2$). Membranes were developed by three subsequent washes in tris-buffered saline (TBST) solution (50 mM Tris-Cl, pH 7.6, 150 mM NaCl, 0.05% Tween 20) and then incubation in color development solution until bands appeared. The reaction was stopped by addition of 1 mL EDTA.

ATPase assays

ATP hydrolysis by YknYLZ, MacB, YknY, and YknYZ was measured to determine the effect of YknX on the ATPase activity of the transporter. Generally, a 20 μL reaction mixture containing 0.5 μg of protein, 20 mM HEPES-KOH (pH 7.0), 2 mM $MgCl_2$, 50 mM KCl, 40 mg/mL lysophosphatidyl glycerol (LPG), and 1 mM Mg-ATP was incubated at 37° Celsius. ATP was prepared by mixing 32-P γ-phosphate ATP (3000 Ci $mmol^{-1}$, Amersham) with 1 mM unlabeled Mg-ATP and added to a final reaction concentration of 1 mM. At designated time points, a 1 μL aliquot of the reaction was removed and added to 10 μL of stop buffer containing 50 mM Tris-HCl (pH 8.0), 20 mM EDTA (pH 8.0), 0.5% SDS, 200 mM NaCl, and 0.5 mg/mL proteinase K. The stopped reaction was then incubated at 55° Celsius for at least 20 minutes to completely denature ATP-hydrolyzing proteins. Afterwards, 1 μL of the stopped mixture was spotted on PEI-F cellulose plates, and reaction components were separated utilizing thin-layer chromatography (TLC). The mobile phase was composed 10% formic acid and 0.5 mM LiCl. Amounts of free Pi were quantified using a Storm Phosphoimager and ImageQuant software (Molecular Dynamics). ATPase rates were calculated using pre-established protein concentration values in combination with reaction times and ATP concentration.

Protein Concentration Determination

Protein concentrations were determined using the Bradford Protein Assay (Bio-Rad) with varying amounts of bovine serum albumin (BSA) as a protein standard. To determine the concentration of proteins solubilized in detergent solution, protein

samples and BSA were together separated on SDS-PAGE gels and stained with Coomassie Brilliant Blue (CBB). Gels were then scanned and protein band intensities quantified using either ImageQuant software (Molecular Dynamics) or ImageJ (NIH). Protein concentrations were then determined using intensities from known BSA concentrations as a standard curve.

Chapter 1. Interactions between TriC and the MFPs TriA and TriB

1.1 Abstract

MFPs function in tandem with an inner membrane transporter and an outer membrane factor. In Gram-negative bacteria, the MFP is proposed to provide a link between the two membrane-bound components of the transporter, and facilitate conformational changes in each component that are required for the efflux process. This study focuses on the paired-MFP transporter TriABC, in which the two MFPs TriA and TriB function with the RND-type transporter TriC in order to provide *P. aeruginosa* resistance against the antimicrobial compound triclosan. Through a mixture of co-purification and functional studies, I establish that TriA and TriB function as a heterodimer in a 1:1 ratio and that the fused polypeptide TriAxB is functional. I also found that deletions in the membrane proximal domain of TriA and TriB severely affect their ability to interact with TriC, and that analogous mutations in TriA and TriB affect each protein differently. Additionally, point mutations in the MP domain of each protein affect complex function and assembly as observed through MIC measurements and co-purification. Results show that TriA and TriB are not dependent on one another for interaction with TriC, and that their function and binding sites are unique, which suggests that TriA and TriB serve different roles in the transport process. This result implies that homomultimeric transporters also assume a dual role in transport, wherein each protomer of the dimer serves a distinct purpose. Additionally, I investigated using unnatural amino acids to photocrosslink membrane-bound transporter components using the well-studied RND transporter AcrAB as a model. I establish that unnatural amino acids can be used to photocrosslink AcrA to membrane-bound proteins.

1.2 Introduction

MFPs are known to stimulate their cognate transporters (Zgurskaya and Nikaido 1999, Tikhonova, Devroy et al. 2007), and a number of experiments have been performed to map the MFP-transporter interface (Tikhonova, Devroy et al. 2007, Weeks, Celaya-Kolb et al. 2010, Su, Long et al. 2011, Xu, Lee et al. 2011, Weeks, Bavro et al. 2014). These experiments focus mostly on the MP domain of MFPs, which is known to primarily interact with the transporter, and contains both the N- and C-terminus of the protein (Zgurskaya and Nikaido 1999, Mikolosko, Bobyk et al. 2006). In RND transporters, the stoichiometry of the MFP:transporter complex is 6:3, resulting in two MFPs contacting each subunit of the transporter. Thusly, RND-associated MFPs are able to bind the transporter in different positions. In the only crystallized MFP-transporter complex to date (Su, Long et al. 2011), the MFP CusA contacts the transporter CusB through two different interfaces. Additionally, the monomers forming the dimeric unit of the MFP retain two distinct conformations. Consistent with this result, when the MFP MexA is crystallized, the dimer unit shows two separate conformations independent of the presence of a transporter (Akama, Kanemaki et al. 2004). This indicates that MFPs may serve a dual role, and that the individual conformations held may serve a distinct functional purpose in transporters containing a single MFP.

The TriABC-OpmH efflux complex was identified in *P. aeruginosa* (Mima, Joshi et al. 2007). In this study, it was shown that overexpression of *triABC* as a result of a promoter-up mutation increased the resistance of *P. aeruginosa* cells to the antimicrobial compound triclosan. Triclosan is a commonly used biocide, appearing in

many hand soaps and other household items. TriABC is unique among MFP-dependent transporters due to the requirement of TriA and TriB, which have both been identified as MFPs, and are each required for complex function. Paired MFPs present the most natural evidence that the functional unit of MFPs is a dimer, and could provide a good model for studying how separate MFPs interact with their cognate transporter.

To characterize the interactions between MFPs and transporters, we first focused on the *P. aeruginosa* transporter TriABC. TriABC is known to have two required MFPs, TriA and TriB that together form a functional efflux complex with TriC. To study how TriA and TriB interact differently with TriC, we made truncated versions of the MFPs as well as site-specific mutations in conserved residues. Making changes in TriA and TriB separately allows validation of a model in which each MFP of a dimeric unit serves a specific role and interacts with transporter components in a unique way. We then attempted to use a new method to determine the positions of of the MFP on the transporter by crosslinking site-specific residues of a typical MFP and cognate transporter. For this purpose, we used the best-characterized MFP-dependent transporter complex to date, AcrAB (Pos 2009). While crosslinking techniques such as cysteine-cysteine and amine-based crosslinking have been utilized with membrane proteins previously (Elkins and Nikaido 2002, Symmons, Bokma et al. 2009, Yamada, Tikhonova et al. 2012), a relatively new technique of photocrosslinking (Chin, Santoro et al. 2002, Young, Ahmad et al. 2010) has not yet been tested in the realm of membrane-bound transporters. This approach would validate a new method for mapping site-specific interactions between MFPs and transporters, expanding the versatility of techniques available to those studying efflux transporters.

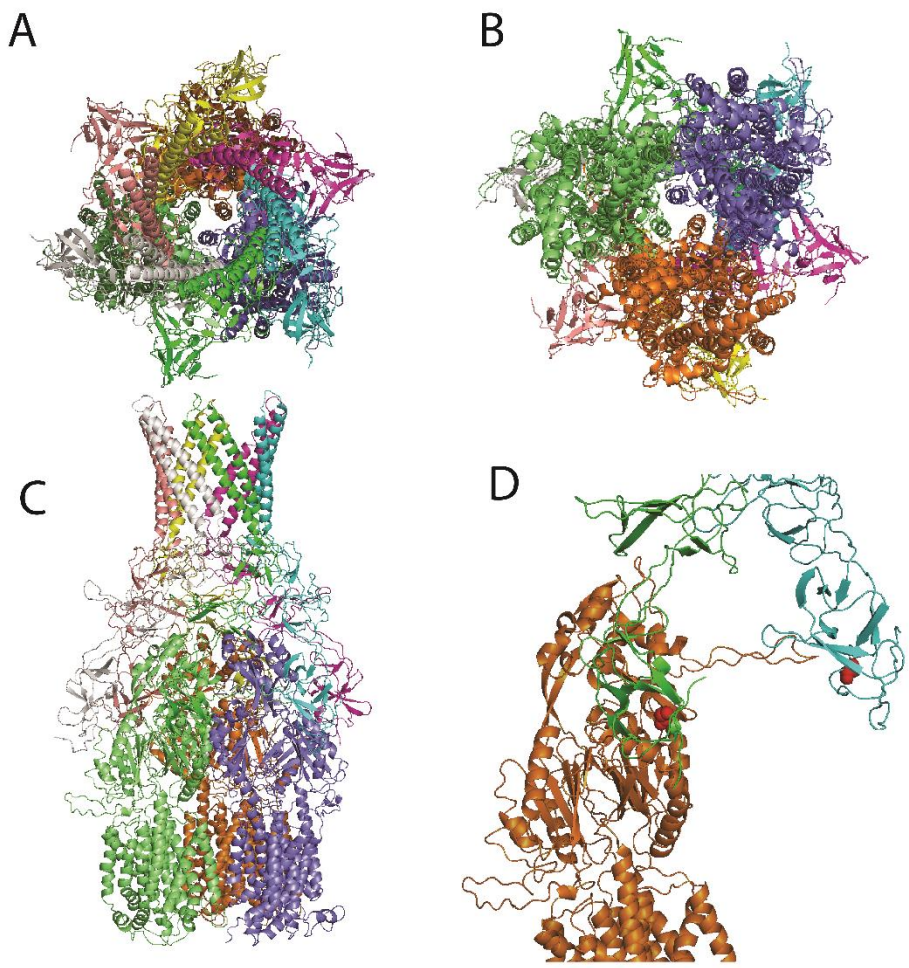

Figure 1.1 – Model of TriABC interactions.

A. Top-down view of the complex. Individual protomers are distinctly colored. B. Bottom-up view of the complex. C. Side view of the complex. D. Interactions between a single protomers of TriA, TriB, and TriC. TriA is colored in green, TriB is colored in cyan, and TriC is colored in orange. Residues selected for point mutations in TriA and TriB are highlighted in red.

1.3 Results

1.3.1 – TriABC-OpmH is a functional triclosan efflux complex in *P. aeruginosa* and *E. coli*

Mima et. al. in 2007 isloated the *P. aeruginosa* strain PAO509.5, which reportedly overexpresses TriABC as a result of a promoter-up mutation. To confirm the increase in TriABC expression, we grew and isolated membrane fractions from various *P. aeruginosa* strains, including wild-type PAO1, the TriABC-deficient PAO1116, and the TriABC-overexpressing PAO509.5 **(Table 1)**. Detection of TriA, TriB, and TriC using polyclonal antibodies specific for each protein showed that all three proteins are significantly upregulated in PAO509.5, likely leading to the increase in triclosan resistance observed in (Mima, Joshi et al. 2007). **(Figure 1.2, panel A)**

Mima et. al also identified OpmH as the native OMF associated with the TriABC transporter. To investigate the interactions between TriABC and different OMFs, wild-type OpmH was deleted from the PAO1 chromosome, and PTJ1 plasmid recombination was used as described in (Damron, McKenney et al. 2013) to insert a gene at the *att:*Tn*7* locus under an arabinose-inducible promoter. Empty vector, histidine-tagged OpmH, or histidine-tagged TolC was inserted create *P. aeruginosa* strains JWW5, JWW6, and JWW7, respectively **(Table 1)**. JWW5, containing empty vector, was used as a negative control. TolC, a promiscuous OMF from *E. coli* was selected because of its similarity with OpmH as well as ability to function with multiple MFPs in *E. coli* (Zgurskaya, Krishnamoorthy et al. 2011). Cells were grown and membrane fractions collected as described in Methods, except when solubilizing membrane fractions, the inner membrane was solubilized by mild detergent extraction

of 0.2% Triton X-100. This allowed inner membrane proteins to be detected in the soluble fraction whereas the outer membrane and associated proteins remained in the insoluble pellet. Results indicate histidine-tagged OpmH is expressed, and is localized to the outer membrane. However, TolC is not expressed when chromosomally integrated onto the *P. aeruginosa* chromosome. **(Figure 1.2, panel B)** To purify OpmH, JWW5 cells were grown to mid-log phase and OpmH expression induced via 1% *L*-arabinose for 4.5 hours. Cells were then lysed and membrane fractions collected as described in the Methods. Membrane fractions were solubilized in 2% DDM before isolating OpmH via a His-bind affinity chromatography column charged with Cu^{2+}. Upon probing purified fractions with anti-poly His antibody to visualize OpmH, bands appeared confirming purified protein. Additionally, upon probing the same fractions with anti-TriA, anti-TriB and anti-TriC antibodies, bands corresponding to all three proteins were identified. **(Figure 1.2, panel C)** These results show that all three components of the TriABC complex interact with OpmH in *P. aeruginosa*, and that the complex can be purified via affinity chromatography of a histidine-tagged OpmH.

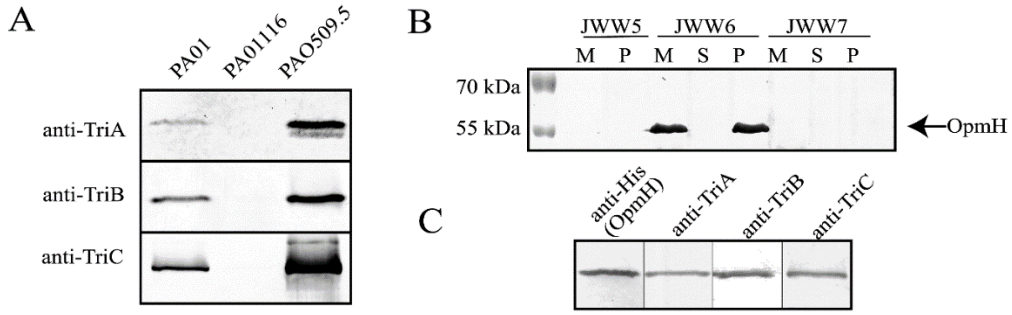

Figure 1.2 – TriABC-OpmH is overexpressed in PAO509.5 and assembles as a complex localized to the membrane.

A. Immunoblotting analysis of membrane fractions isolated from wild type PAO1 *P. aeruginosa,* the efflux-deficient PAO1116 strain, and the TriABC-overexpressing PAO509.5. Membranes were probed with anti-TriA, anti-TriB, or anti-TriC antibodies. **B.** OpmH localizes to the outer membrane of *P. aeruginosa* and co-purifies with TriABC. Immunoblotting of membrane fractions from *P. aeruginosa* strains containing either the integrated empty vector (JWW5), $OpmH_{His}$ (JWW6), or $TolC_{His}$ (JWW7). M – total membrane fraction. S – solubilized membrane fractions (inner membrane). P – insoluble membrane pellet (outer membrane). Membrane fractions were isolated from log phase cells after induction with 1% *L*-arabinose for 3 hours. Inner membrane proteins were solubilized by mild detergent (0.2% Triton X-100) extraction. Outer membrane proteins remained in the insoluble pellet. Membranes were probed with anti-poly His antibodies. **C.** Immunoblotting analysis of purified $OpmH_{His}$ and co-purified proteins. Membranes were probed with anti-poly His, anti-TriA, anti-TriB, or anti-TriC. In this figure and others, unless indicated otherwise, membrane fractions were isolated from log phase cells, resolved by 10% SDS-PAGE and electro-transferred onto PVDF membranes.

Having confirmed that TriA, TriB, TriC, and OpmH together make a complex when overexpressed together **(Figure 1.2)**, we set out to establish how TriA and TriB form a fully functional MFP unit. Current models of MFP-dependent transport place the MFPs in a side-to-side arrangement, forming a trimer of dimers that make connections to the IMF and OMF through the MP / β-barrel domains and the coiled-coil region, respectively (Zgurskaya, Weeks et al. 2015) **(Figure I.3)**. Traditional MFPs are proposed to form homodimers, as a single MFP is used. Since TriA and TriB are distinct MFPs, they could either form homo- or heterodimers depending on arrangement. To determine the arrangement of paired-MFPs around the transporter, we created a fused construct, in which TriA and TriB are covalently linked as a single polypeptide by a flexible linker region. **(Figure 1.3)** This fusion protein, AxB, fixes the arrangement of MFPs in a heterodimer, allowing the ability to distinguish the functional unit of the MFP. This heterodimeric, fused MFP was expressed in *P. aeruginosa* through the plasmid pBSP-TriAxBC which was created through site-directed mutagenesis of pPS1824. TriAxBC was also expressed in *E. coli* by subcloning pBSP-TriAxBC into pBAD33 using the restriction enzymes *Sac*I and *Hind*III **(Table 1)**.

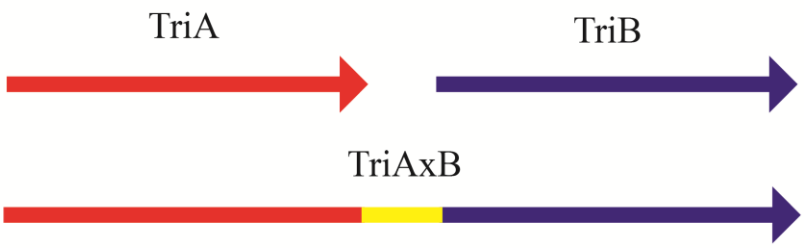


```
TriA    375  RDAVGGGQP*                          383
TriB    1              MKPFSLAGLFGFALLLSGCGDE   22
TriAxB  375  RDAVGGGQPGNSRGGDE                   391
```

Figure 1.3 – Schematic representation of the TriAxB fusion protein.

Illustration of the TriAxB fusion protein, in which the stop codon of TriA is removed and replaced with a flexible linker region, which is followed by TriB with the proposed signal peptide removed. Amino acid sequences of TriA and TriB show removed portions as underlined, and the linker region in TriAxB is underlined.

MIC measurements were performed to determine substrate specificity of the pump. Only triclosan and SDS were found to be substrates of the TriABC complex. (Data not shown) To determine the functionality of the TriAxBC complex in *P. aeruginosa*, various plasmid constructs were transformed into the *P. aeruginosa* TriABC-deficient PAO1116. Additionally, the functionality of the complex was investigated in the *E. coli* strain JWW2 (BW25113 Δ*ompT*-scar, Δ*acrAB*::Km^r). OpmH, the native outer membrane channel that functions with TriABC shares a high degree of similarity with the *E. coli* outer membrane channel TolC. If TriABC is functional in *E.*

coli, it would provide an ideal model system in which to study interactions between the well-known TolC and the comparatively little-studied TriABC.

pBAD33-based plasmids were co-transformed into *E. coli* with the plasmid pBAD-TriC due to low expression of TriC from the full-length operon contained in pBAD33-TriABC (Data not shown). Additionally, to confirm OpmH as the functional OMF for TriABC, *P. aeruginosa* strains JWW5 (JWW4 *att*Tn*7*::mini-Tn*7*T -Tp^r -*araC*-P$_{araBAD}$-MCS), JWW6 (JWW4 *att*Tn*7*::mini-Tn*7*T-Tp^r -*araC*-P$_{araBAD}$-*opmH*), and JWW7 (JWW4 *att*Tn*7*:: mini-Tn*7*T-Tp^r -*araC*-P$_{araBAD}$-*tolC*) were tested, expressing TriABC from the chromosome. After cell growth and induction via 1% arabinose for 5 hours, cells were plated in MIC experiments to test susceptibility to SDS and triclosan. Results show that the TriABC pump is functional in *E. coli* and *P. aeruginosa*, as is the fused TriAxBC construct. **(Table 2)** Thus, TriABC provides resistance against triclosan in *E. coli* and this organism can be used as a good host to study the TriABC complex. Additionally, the functionality of TriAxB indicates that TriA and TriB function side by side in a 1:1 stoichiometry.

Because *E. coli* does not natively express OpmH, the native OMF to TriABC, it seems reasonable that the complex is assembling with the promiscuous *E. coli* OMF TolC, which is known to interact with a number of different RND-type efflux transporters. To determine if TriABC functions with TolC, MICs were tested again in the *E. coli* strain JWW3, which is TolC-deficient. Results show that JWW3 susceptibility to SDS and triclosan is not rescued by TriABC or TriAxBC, indicating that indeed, TolC functions with the TriABC complex. (Data not shown) Finally, results in *P. aeruginosa* using strains with either chromosomally-integrated OpmH or TolC

show that deletion of OpmH from the chromosome eliminates complex functionality, as well as that TolC is unable to rescue the defect in efflux caused by OpmH absence **(Table 2)**. This data establishes a baseline of the resistance level provided by TriABC, and the functionality of TriAxBC indicates that the two membrane fusion proteins function together as a dimer in a 1:1 molar ratio.

	Strains	Tri complex	SDS ($\mu g\ ml^{-1}$)	Triclosan ($\mu g\ ml^{-1}$)
1	*Pae* JWW5 (*att*Tn*7*::P_{araBAD})	-	39	0.25-0.5
2	*Pae* JWW6 (*att*Tn*7*::P_{araBAD}-*opmH*)	TriABC-$OpmH_{His}$	>2500	>128
3	*Pae* JWW7 (*att*Tn*7*::P_{araBAD}-*tolC*)	TriABC-$TolC_{His}$	39	0.5
4	*Pae* PAO1116 (pBSPII)	-	156-312	16
5	*Pae* PAO1116 (pPS1824)	TriABC-OpmH	>2500	128
6	*Pae* PAO1116 (pBSP-AxBC)	TriAxBC-OpmH	>2500	128
7	*E. coli* JWW2 (pBSPII)	-	39	0.000125
8	*E. coli* JWW2 (pPS1824)	TriABC-TolC	>2500	0.008
9	*E. coli* JWW2 (pBSP-AxBC)	TriAxBC-TolC	>2500	0.008

* *Pae- P. aeruginosa*

Table 2 – TriABC and TriAxBC are functional in *P. aeruginosa* and *E. coli.*

Minimal inhibitory concentrations of SDS and triclosan are indicated for cells producing TriABC or TriAxBC in different *P. aeruginosa* and *E. coli* genetic backgrounds.

1.3.2 – Deletions in the MP domain of TriA and TriB drastically affect function

Having confirmed the identity of the TriABC-OpmH complex, as well as the functionality of TriABC-TolC in *E. coli*, we began investigating the differences between the MFPs TriA and TriB. Sequence alignment of TriABC with various paired MFPs showed alignment of conserved residues in both the MP domain as well as the CC domain of TriA and TriB, indicating that they share the same architecture and general design as other MFPs **(Figure 1.4)** (Zgurskaya, Weeks et al. 2015). In order to determine if the MFPs TriA and TriB share the same role in the transport process, we used this sequence alignment to select site-specific substitutions of conserved residues in the MP domains of each TriA and TriB, as well as C-terminal truncations to determine if they would affect the function of the complex differently.

It stands to reason that if TriA and TriB have different binding sites and interactions with TriC, then analogous mutations may affect the MFPs differently. Selections were made to mutate conserved glycine residues known to have an effect on interactions between the transporter and MFP in other transporters (Ge, Yamada et al. 2009, Modali and Zgurskaya 2011). Using sequence alignment to find the corresponding residues in TriA and TriB, these conserved residues correspond to G350 in TriA and G339 in TriB **(Figure 1.4)**. These glycine residues were mutated to cysteine using site-directed mutagenesis for the possibility of utilizing functional crosslinkers in future experiments.

To further characterize the role of the MP domain in MFP-transporter interactions, truncations were made, removing the C-terminal end of the MP domain up until a conserved proline-glycine motif, as well as past another conserved glycine in the

MP domain. Alterations in the MP domain could determine if TriA and TriB interact differently with the transporter. If disruptions between the MP domain and the transporter affect one protein, but not the other, it would stand to reason that interactions between MFPs and transporters can occur through different domains. Thus, the MFPs would likely have different functions in the fully assembled complex. After removal of the proposed signal peptide, TriA is longer than TriB by 17 residues **(Figure 1.4)**, and thusly when making deletions based on sequence alignment, would have a larger truncation than TriB. In TriA, deletions of both 26 and 47 amino acids were made, while in TriB, deletions of 9 and 30 residues were made. The rationale behind making both a small and a large deletion was to provide a range of truncations that may affect complex function in an intermediate manner. Deletions were constructed by PCR as described in Methods. Deletion mutants were created in plasmids carrying TriABC as well as the fused TriAxBC to further clarify interactions between the MFP dimer and the transporter.

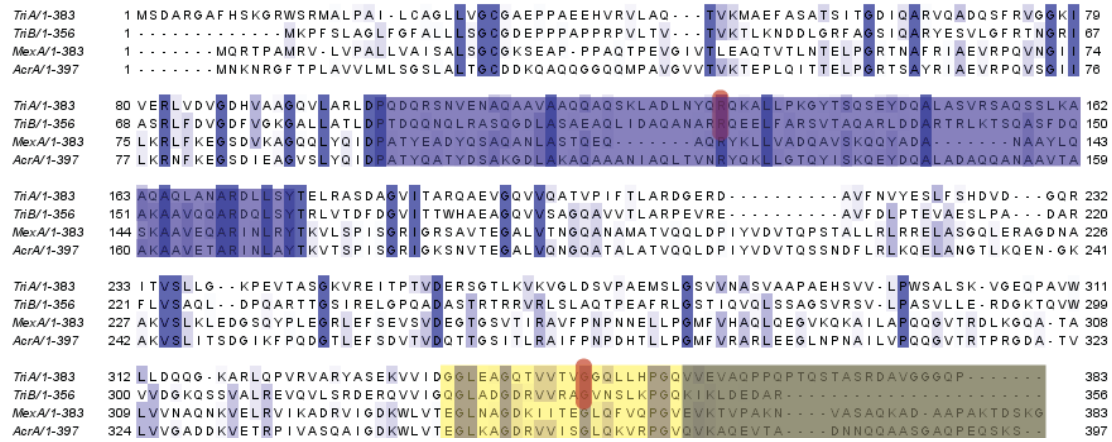

Figure 1.4 - Sequence alignment and deletions of TriA and TriB.

Primary sequence alignment of the MFPs TriA, TriB, MexA, and AcrA. Deletions made in the MP domain of TriA and TriB are marked with yellow and grey boxes for the large and small deletion, respectively. Point mutations are indicated with a red highlight. Conserved residues are highlighted individually, and the coiled-coil region is highlighted in blue.

Mutants of TriA and TriB were created through site-directed mutagenesis. C-terminal truncations were created using forward and reverse primers designed to amplify the entire pBAD33-TriABC or pBAD33-TriAxBC plasmid, excepting the area to be deleted. Both forward and reverse primers contained an *Nde*I site for cloning, which preserved the overlapping start stop / start stop codon, but inserts a single isoleucine residue before termination. TriAxBC TriA-deletion mutants were made through the same method, but using a *SpeI* site, due to the presence of an *Nde*I site in the portion of AxB coding for the linker region. This change of restriction site inserts a serine and threonine before the AxB linker. TriAxBC TriB mutations were made using the same primers as TriABC TriB-mutations. All plasmids were confirmed via sequencing at Oklahoma Medical Research Foundation.

The new plasmids, pBAD33-TriA$_{\Delta 26}$BC, pBAD33-TriA$_{\Delta 47}$BC, pBAD33-TriAB$_{\Delta 9}$C, and pBAD33-TriAB$_{\Delta 30}$C, as well as their pBAD33-TriAxBC equivalents, were transformed into *E. coli* JWW2. Cells were grown to mid-log phase before protein expression with 0.2% L-arabinose for 5 hours and subsequent cell lysis. Membrane fractions were collected and probed with anti-TriA and anti-TriB antibodies to determine expression of TriA and TriB in the newly constructed vectors. **(Figure 1.5)**

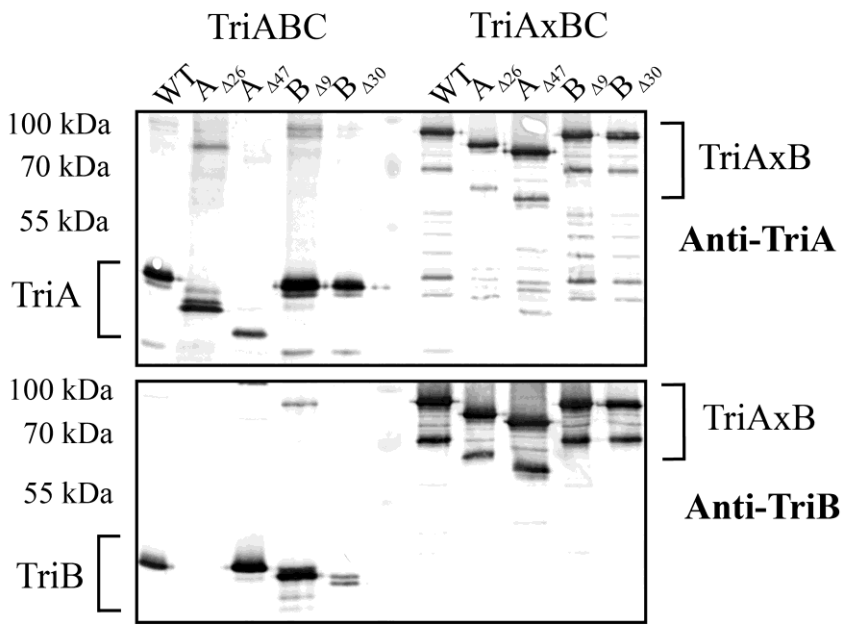

Figure 1.5 – Expression of MP deletion mutants.

Total membrane fractions of *E. coli* JWW2 cells carrying pBAD33-TriABC, pBAD33-TriAxBC and their derivatives producing the indicated C-terminal deletions for TriA and TriB were isolated, total protein quantified and analyzed via SDS-PAGE and immunoblotting with anti-TriA and anti-TriB antibodies. 100 ng of total membrane protein was loaded for each sample.

Results indicate that with the exception of TriB in the pBAD33-TriA$_{\Delta 26}$BC construct, both TriA and TriB are expressed at levels detectable by anti-TriA and anti-TriB antibodies in all unfused constructs. A corresponding mobility shift is seen as well, with deletion mutants appearing smaller compared to the wild-type TriA and TriB. The lack of TriB expression in the construct may result from the removal of an upstream Shine-Dalgarno sequence before the overlapping stop / start codon. In the pBAD33-

TriA$_{\Delta 47}$BC construct, a modified Shine-Dalgarno site exists just upstream of the stop / start codon, likely preserving the expression of TriB in this construct. All deletion mutants created in fused TriAxBC express at levels comparable to the parental TriAxBC, but TriAxB$_{\Delta 9}$C and TriAxB$_{\Delta 30}$C do not exhibit the same gel shift observed in all other deletions. This could be because deletions in the C-terminal end of the fused protein do not significantly affect the electrophoretic mobility of the protein, or result in different protein-protein and protein-detergent contacts than the corresponding fused TriA or unfused TriB deletions (Rath, Glibowicka et al. 2009).

To test functionality of the TriABC and TriAxBC deletion mutants, constructs were co-transformed with pBAD-TriC into *E. coli* JWW2 and cells were tested for their susceptibility to SDS and triclosan. SDS and triclosan are currently the only identified substrates for TriABC. MICs were performed using the 2-fold dilution technique in 96-well plates. **(Table 3)**

	Variant	JWW2	
		SDS (μg ml^{-1})	Triclosan (ng ml^{-1})
1	-	39	0.25
2	TriABC	>2500	8
3	TriAxBC	>2500	4
4	$TriA_{G350C}BC$	≥2500	16
5	$TriAB_{G339C}C$	39	1
6	$TriA_{G350C}xBC$	>2500	8
7	$TriAxB_{G339C}C$	78	1
8	$TriA_{\Delta 26}BC$	39	<0.125
9	$TriA_{\Delta 47}BC$	39	<0.125
10	$TriAB_{\Delta 9}C$	39	1
11	$TriAB_{\Delta 30}C$	39	0.125-0.25
12	$TriA_{\Delta 26}xBC$	20	1
13	$TriA_{\Delta 47}xBC$	20	0.25
14	$TriAxB_{\Delta 9}C$	39	1
15	$TriAxB_{\Delta 30}C$	20	0.125-0.25

Table 3 – C-terminal deletions in TriA and TriB impair complex function. Minimal inhibitory concentrations of SDS and triclosan were measured for calls producing various TriABC complexes expressed from pBAD33-based plasmids.

MIC measurements indicate that cells expressing protein containing any deletion made from the C-terminal end of either TriA or TriB have a severe defect in triclosan and SDS resistance, and this effect is seen regardless of if TriAB or TriAxB is used. However, the deficiency does not seem to be equal when making comparisons between TriA and TriB. Deletions made in the unfused TriA seem to completely abolish functionality of the complex, however the hypersusceptibility phenotype of cells

expressing TriA$_{\Delta 26}$BC is likely due to the lack of expression of TriB. Examination of the unfused TriB mutants show that cells expressing TriAB$_{\Delta 9}$C retain a low, but partial resistance to triclosan in contrast to cells expressing TriAB$_{\Delta 30}$C, which do not show any resistance to triclosan or SDS. The fused constructs follow this same pattern in which the cells expressing the small deletions retain some low level of functionality, but cells expressing large deletions of either TriA or TriB completely eliminate functionality of the complex.

1.3.3 – C-terminal deletions affect interaction of TriA and TriB with TriC

Having established the functionality of TriA and TriB containing truncations in the MP domain, we then set out to determine which complex interactions were retained or abolished by these deletions. Since previous experiments showed that TriABC-OpmH readily co-purifies together, we chose to express the various mutant constructs in tandem with histidine-tagged TriC and purify the transporter to establish complex interactions. This would allow us to determine if the MP domains are important for interaction with the transporter, as well as shed light on if TriA and TriB can independently bind TriC. Co-purifications were performed as described in the Methods **(Figure 1.6).**

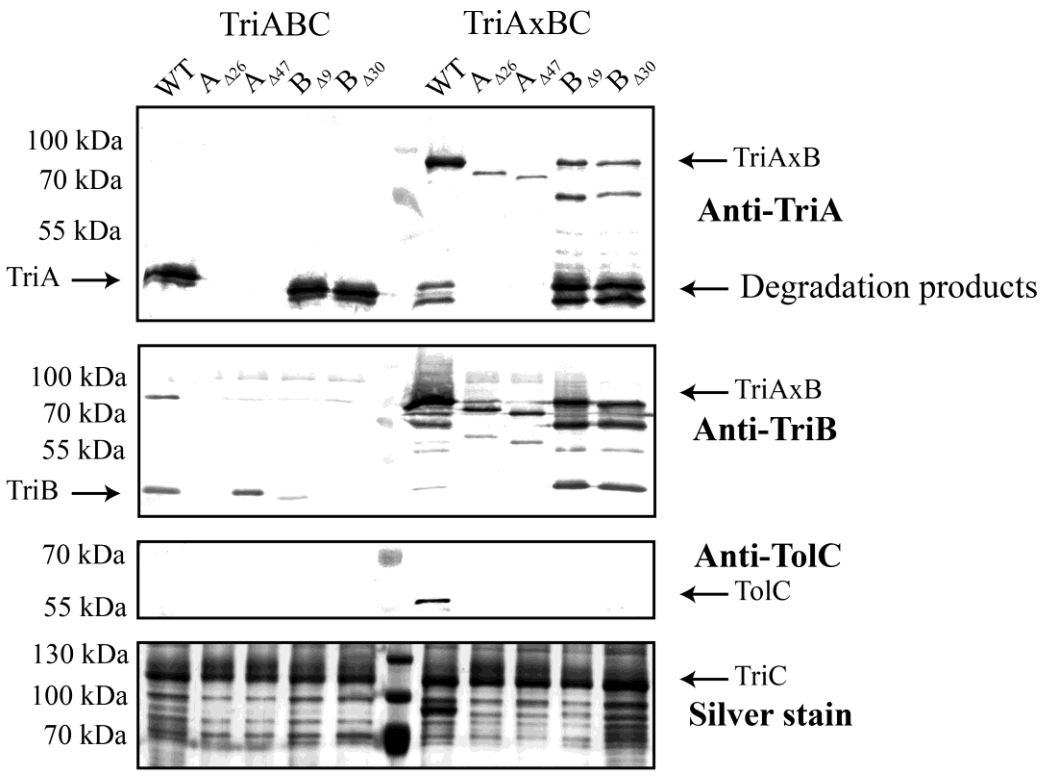

Figure 1.6 – Co-purification of C-terminal TriA and TriB deletions.

Membrane fractions containing the indicated plasmid-expressed TriA, TriB, or TriAxB mutants with $TriC^{his}$ were solubilized and purified using affinity chromatography. Proteins were quantified and 0.5 μg of purified $TriC^{his}$ was loaded onto SDS-PAGE gels and analyzed via immunoblotting and silver staining.

Co-purification experiments showed that TriA and TriB co-purify with TriC when expressed as full-length, unfused proteins. When expressed as separate polypeptides, deletions made in TriA do not affect the co-purification of TriB and vice versa. This indicates that binding of TriA and TriB to the transporter are independent events and are not dependent of the partner MFP. However, any deletions made in the MP domain of either TriA or TriB severely inhibit the ability of the truncated protein to

maintain interactions with TriC during the purification process. Only co-purified $TriB_{\Delta 9}$ could to be detected with immunoblotting, indicating that it may interact with TriC, albeit to a lesser degree than wild-type.

The fused TriAxB constructs provided new insight, as deletions made in TriA seem to affect co-purification with TriC much more than deletions made in TriB. Relative amounts of co-purified AxB seemed to be lower in TriA mutants than in TriB mutants, indicating that TriA and TriC may interact more strongly through the MP domain of the MFP than TriB and TriC.

Finally, TolC could only be detected in purified fractions containing fused TriAxBC with no deletions made. This indicates that interaction between TriABC and TolC may be stabilized by the fused TriAxB, but unfused proteins do not stabilize interactions with a non-cognate OMF enough with that TolC can be detected by co-purification and immunoblotting. Additionally, this result suggests that even a small deletion of MP domain residues disrupts interaction of AxBC with TolC, possibly due to an inability to recruit the OMF. Since all TriAxB deletion mutants co-purify with TriC, this suggests that the full-length MFP stabilizes the partner MFP in the complex with transporter interactions, but activity of the transporter requires both intact domains.

1.3.4 – Analogous point mutations in the MP domain affect TriA and TriB differently

Results of co-purification experiments highlighted the importance of the MP domain in either MFP, but also suggested the idea that TriA and TriB do not share equal roles in the transport process. The disparate amounts of TriAxB co-purified when deletions were made in TriA versus TriB suggests that the strength of interactions, and

therefore binding sites, between TriA / TriB and TriC may be unique. Additionally, the very small amount of unfused $TriB_{\Delta 9}$ that was co-purified as compared to the undetectable $TriA_{\Delta 26}$ furthers the idea that TriB interactions with TriC are not as dependent on the MP domain as TriA interactions. To investigate further, we created TriA and TriB mutant proteins wherein a conserved glycine residue known to be important for MFP-transporter interactions in other efflux systems was mutated to cysteine. (Ge, Yamada et al. 2009) (Modali and Zgurskaya 2011).

Using site-directed mutagenesis, G350 in TriA and G339 in TriB were converted to cysteine residues. Mutagenesis was carried out in pBAD33-TriABC and pBAD33-TriAxBC constructs. As previously described for deletion mutants, these point mutants were tested for expression, functionality, and ability to co-purify with TriC and TolC. **(Figure 1.7)**

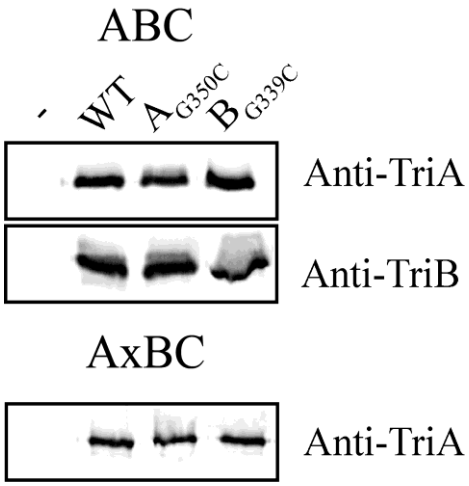

Figure 1.7 – TriA, TriB, and TriAxB carrying MP domain point mutations are expressed.

As previously described, point mutations were introduced into the MP domain of TriA and TriB encoded by their respective genes in pBAD33-TriABC and pBAD33-TriAxBC plasmids. Mutated proteins were expressed in *E. coli* JWW2, induced with 0.2% L-arabinose for 5 hours, membranes collected. 100 ng of total membrane extracts were analyzed via SDS-PAGE and immunoblotting with anti-TriA and anti-TriB antibodies.

Expression analysis shows that all proteins carrying mutations express at levels comparable to wild-type, and are readily visualized using antibodies specific for TriA and TriB. **(Figure 1.10)** Having established that point mutations in the MP domain do not affect expression of TriA and TriB in either the fused or unfused construct, MICs were determined as previously described in the Methods in order to establish functionality of the newly constructed proteins. **(Table 4)** Interestingly, MIC results

indicate that fused and unfused complexes containing $TriA_{G350C}$ are functional and protect the cell from both SDS and triclosan, whereas complexes containing $TriB_{G339C}$ yield MIC values comparable to empty vector, suggesting that $TriB_{G339C}$-containing complexes are nonfunctional. This is in contrast to results from deletion mutants wherein C-terminal deletions in TriA affect the complex more drastically than corresponding deletions in TriB **(Figure 1.9)**.

To compare the effects of point mutations and deletion mutants on complex assembly, we utilized co-purification as previously described to isolate TriC and any co-purifying components of the complex. **(Figure 1.11)**

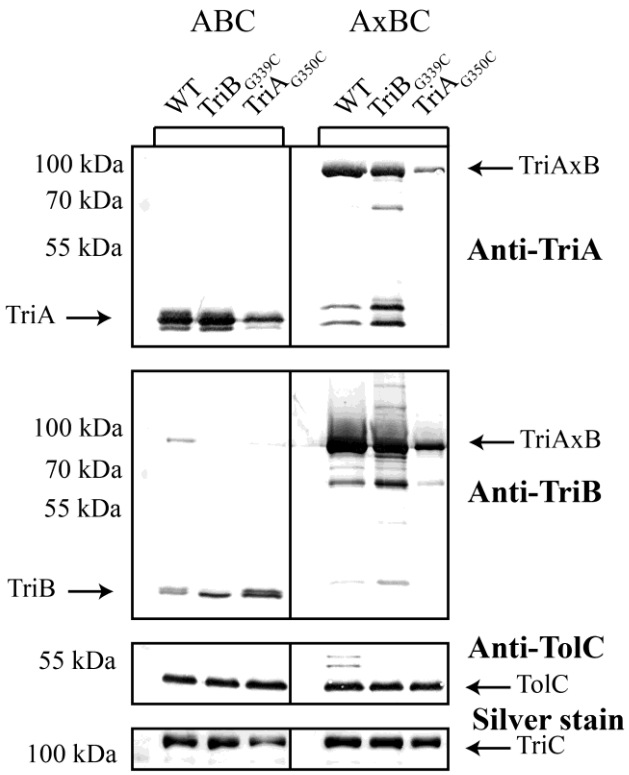

Figure 1.8 – Co-purification of TriA and TriB carrying MP domain point mutations.

Membrane fractions containing the indicated plasmid-expressed TriA, TriB, or TriAxB mutants with $TriC^{His}$ were solubilized and purified using affinity chromatography. Fractions were quantified and 100 ng of purified $TriC^{His}$ was loaded onto SDS-PAGE gels and analyzed via immunoblotting and silver staining.

Co-purification of TriA and TriB containing point mutants in the MP domain yielded interesting results when compared to MIC measurements. While $TriA_{G350C}$ seems to be functional in terms of efflux and $TriB_{G339C}$ is nonfunctional, the opposite

effect is seen in co-purification. The $TriA_{G350C}$ mutants in either fused or unfused constructs co-purify with TriC in limited amounts compared to the wild-type, and $TriB_{G339C}$ co-purifies at levels comparable to wild-type. As seen with deletion mutants **(Figure 1.6)**, co-purification of one MFP in unfused constructs is not dependent on the ability of the partner MFP to co-purify. Additionally, neither fused point mutant is able to co-purify with TolC. Taken together, these observations indicate that while $TriA_{G350C}$ is functional, this point mutation reduces the overall stability of the complex with TriC. In contrast, $TriB_{G339C}$ is nonfunctional, but this point mutation has no effect on the assembly and stability of the complex.

Having established that TriA and TriB are unequal MFPs, we set out to identify the specific MFP-transporter contact interface and position the MFPs on the TriC transporter.

1.3.5 Amber codon-incorporated AcrA is functional

To determine the interfaces formed between TriA, TriB, and TriC during complex assembly, we first sought to establish a method that would serve as a novel, convenient way of establishing direct contact interfaces. For this purpose, we used photocrosslinking of proteins containing modified amino acid residues. Site-directed photocrosslinking has been developed as a method utilizing unnatural amino acids (UAA) that are photoreactive, such as p-benzoyl-L-phenylalanine (BzF) or p-azido-L-phenylalanine (AzF) (Kauer, Erickson-Viitanen et al. 1986, Chin, Santoro et al. 2002). Utilizing various pEVOL plasmids, the necessary tRNA synthetase and suppressors are produced so that the amber codon UAG in mRNA is recognized to incorporate the UAA

into the produced protein (Young, Ahmad et al. 2010). Upon irradiation with UV light, a reactive form of the UAA is created that covalently binds with nearby C-H bonds, with different chemistries occurring depending on the utilized UAA. (Bayley and Staros 1984, Dorman and Prestwich 1994) Koronakis et al 2009 reported crosslinking of the well-studied *E. coli* RND-type MFP AcrA and its associated transporter AcrB utilizing specific cysteine point mutants in tandem with functional crosslinkers, identifying likely interaction points between the transporter and the MFP. In order to establish our method with membrane-bound efflux transporters, we chose to first test the method with AcrAB. Residue R225 of AcrA was previously identified as an interface between AcrA and AcrB, and we chose this residue as a test for the photocrosslinking method to determine if this method could be adapted for efflux transporters, including TriA and TriB.

The amber codon was introduced into the *acrA* gene encoded by the plasmid p151AcrAB **(Table 1)** utilizing site-directed mutagenesis (Quikchange Agilent). The result was then confirmed by sequencing (Oklahoma Medical Research Foundation). Then, the AcrAB-deficient *E. coli* strain JWW2 was transformed with the empty vector, wild-type p151AcrAB, and the mutated plasmid, p151AcrA*B containing the amber codon at position AcrA R225. To ensure the incorporation of an unnatural amino acid did not disrupt functionality of the complex, MICs of known AcrAB substrates were measured using the two-fold dilution method (Tikhonova, Wang et al. 2002).

	Strain	SDS (μg ml^{-1})	Ery (μg ml^{-1})	Nov (μg ml^{-1})	Nor (μg ml^{-1})
1	BW25113 WT	>10000	64	64	128
2	JWW2 (ΔAcrAB) + pUC18	40	8	4	8
3	JWW2 (ΔAcrAB) + pUC151AcrAB	>10000	32	32	64
4	JWW2 (ΔAcrAB) + pUC151AcrA*B	40	8	4	8
5	JWW2 (ΔAcrAB) + pUC151AcrA*B + pEVOL	>10000	64	64	128

Table 4 - Amber-codon mutated AcrA is functional.

MIC measurements of antibiotics in *E. coli* BW25113 and mutants carrying indicated plasmids. WT BW25113 contains chromosomally-encoded AcrAB and served as a positive control, while JWW2 contains no chromosomal AcrAB, and is transformed with either empty vector, plasmid-encoded AcrAB, or plasmid-encoded AcrAB with AcrA containing the amber codon at position R225. SDS – sodium dodecyl sulfate. Ery – Erythromycin. Nov – Novobiocin. Nor – Norfloxacin.

Results show that AcrA with an amber codon is functional at a level comparable to wild-type AcrA expressed either from the chromosome or plasmid only when expressed in tandem from the pEVOL plasmid **(Table 4)**. This is expected, as without pEVOL, the amber codon, UAG, acts as a stop codon within AcrA*. This results in a truncated version of the protein that ends at residue 225, and is expected to be non-functional. Small 2-fold differences in MIC were observed between plasmid-encoded AcrA and chromosomal, but are not considered significant.

Having confirmed that an unnatural amino acid did not decrease functionality of the complex, we then grew *E. coli* JWW2 cells expressing pUC151AcrA*B, exposed whole cells to UV light and attempted to characterize crosslinked complexes.

1.3.6 – Usage of the UAA BzF results in significant background incorporation of non-specific amino acids.

As previously mentioned, JWW2 (pUC151AcrA*B + pEVOL) cells were grown in LB media containing the unnatural amino acid, p-benzoyl-l-phenylalanine (BzF) (BACHEM) at a concentration of 1 mM (Chin, Santoro et al. 2002). After collection, cells were exposed to UV light for times ranging from 1 minute to 60 minutes in order to determine conditions most effective for crosslinking. Controls included cells carrying plasmid-borne wild-type AcrAB, AcrA*B with no pEVOL plasmid, and AcrA*B with pEVOL grown in medium without BzF. Theoretically, no full-length AcrA should be produced in AcrA*B expressing constructs that do not have both pEVOL as well as BzF, as the amber codon acts as a stop codon in the absence of pEVOL, and should only code for the UAA BzF in the presence of pEVOL. After UV exposure, cells were lysed and membrane fractions collected as described in the Methods before protein amounts were quantified and normalized using SDS-PAGE with a BSA standard. 2 μg of total membrane extracts were then separated on a 12% SDS-PAGE gel, and subjected to immunoblotting with anti-AcrA antibodies.

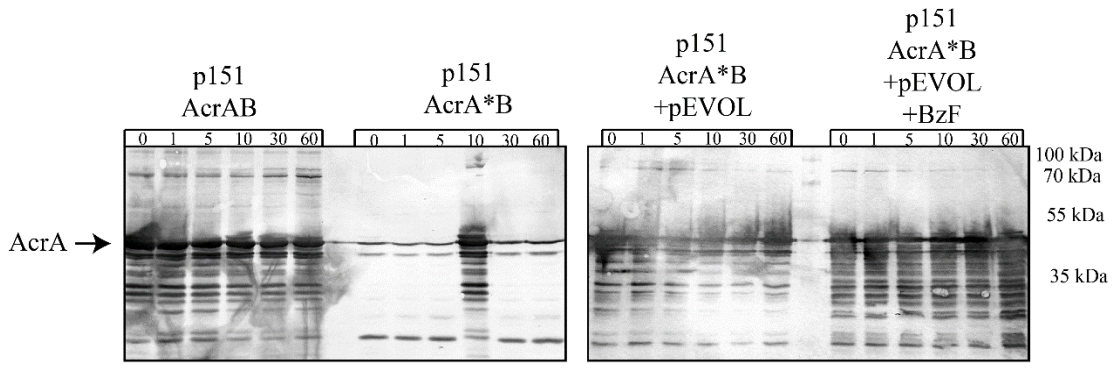

Figure 1.9 – AcrA*B contains significant incorporation of non-specific amino acids.

JWW2 cells carrying plasmid-expressed variants of AcrAB and +/- pEVOL were grown in media with or without BzF and were exposed to UV light for the indicated amount of time and then subjected to lysis. Membrane fractions were collected, protein amounts were quantified and membrane fractions were analyzed by immunoblotting with anti-AcrA antibody. The 10 minute p151AcrA*B time point is an identical sample to 10 minute wild-type p151AcrAB due to a loading error.

Results show that cells containing p151AcrAB encode full length AcrA, and the p151AcrA*B plasmid is unable to encode full-length AcrA as expected. However, contrary to expectations, cells containing AcrA*B and the pEVOL plasmid but grown in medium with no UAA added, full-length AcrA is seen running at the expected MW of ~45 kDa (Fig. 1.2). This indicates that a significant amount of background incorporation of other amino acids occurs, resulting in AcrA* containing a non-specific amino acid at position 225. This likely also occurs in cells grown with BzF, resulting in a very low amount of AcrA* containing BzF. While UAG codon should only encode

for the charged tRNA carrying BzF, which is produced via the pEVOL plasmid, non-specific incorporation of other natural amino acids, likely tyrosine, can result in the tRNA incorporating natural amino acids into the protein (Chin, Santoro et al. 2002).

To adapt, we investigated another UAA, p-azido-L-phenylalanine (AzF). AzF is a slightly smaller UAA than BzF with an MW of 206.2 g/mol as compared to 269.3 g/mol, and other experiments have shown better incorporation of AzF into other experiments utilizing this same technique, likely due to more efficient binding of AzF and the cognate tRNA. (Young, Ahmad et al. 2010)

1.3.7 – AcrA*B forms complexes upon exposure to UV light

In order to improve the fidelity of UAA incorporation into AcrA*B, we not only utilized the UAA AzF rather than BzF, we also grew cells in YT media, as described in previous publications (Farrell, Toroney et al. 2005). As previously described, proteins were produced by JWW2 cells and whole cells were exposed to UV light before cell lysis and membrane fractionation. Total membrane proteins were then quantified and loaded onto 12% SDS-PAGE gels for immunoblotting. For proteins visualized using anti-AcrA, 2 μg of total membrane extracts were loaded and anti-poly His proteins were detected in 20 μg of total membrane proteins loaded onto gels.

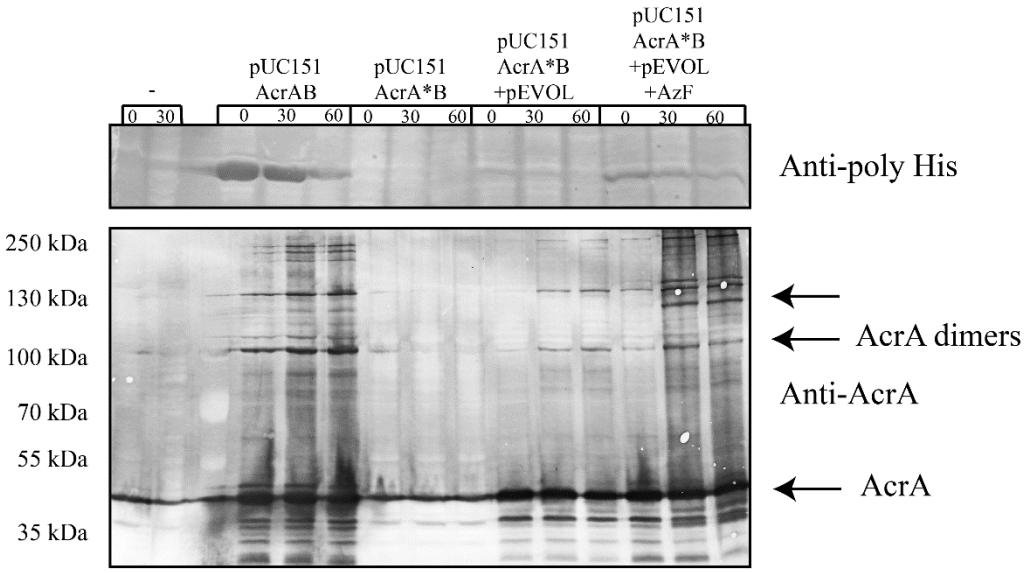

Figure 1.10 – AcrA*B forms specific complexes when expressed with AzF.

JWW2 cells carrying plasmid-expressed variants of AcrAB and +/- pEVOL were grown in media with or without AzF and were exposed to UV light for the indicated amount of time and then subjected to lysis. Membrane fractions were collected, protein amounts were quantified and membrane fractions were analyzed by immunoblotting with anti-AcrA and anti-poly His antibodies. An observed band between 100-130 kDa is indicated by an arrow.

While some background incorporation still remained, the overall level of AcrA* produced without AzF is lower than wild-type AcrA, indicating that a higher efficiency of UAA incorporation was occurring **(Figure 1.10)**. Additionally, when exposed to UV light, a new band between 100-130 kDa appeared in the samples isolated from cells also containing pEVOL and grown in the medium supplemented with AzF. A band of similar size is also observed in the WT AcrAB complex in lesser amounts, indicating that the crosslink may be stabilizing a biologically relevant complex.

In order to further characterize and establish this band, crosslinked protein was then purified from cells using His-bind resin charged with Cu^{2+}. Proteins were eluted with an imidazole gradient, and fractions eluted with 100 and 500 mM imidazole were separated on an 8% SDS-PAGE gel. After separation and immunoblotting, AcrA-containing bands were visualized using anti-AcrA antibody.

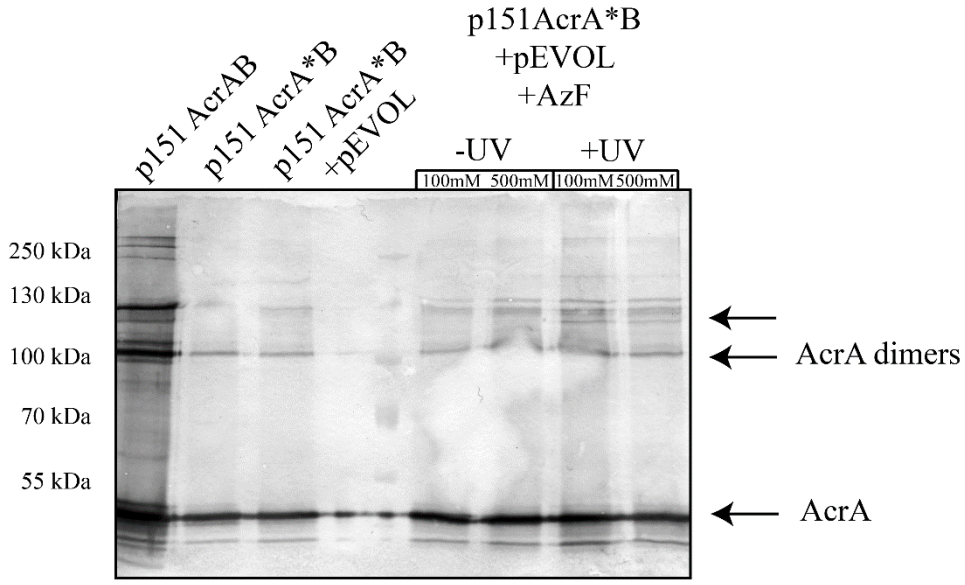

Figure 1.11 - AcrA* can be purified.

Membrane fractions containing AcrA variants, as well as AcrA* +/- UV exposure were solubilized in 5% Triton X-100. Insoluble fractions were removed by high-speed centrifugation and solubilized proteins were loaded onto a His-bind column. Bound proteins were eluted using 100 mM and 500 mM imidazole and quantified before analysis by SDS-PAGE and anti-AcrA immunoblotting. An indicated band between 100-130 kDa is highlighted by an arrow.

Again, a band reacting with anti-AcrA antibody is observed at a MW between 100-130 kDa in cells irradiated with UV light, but not in UV- cells. **(Figure 1.11)** The composition of this crosslinked band remains unknown as the observed size is difficult to reconcile, given the molecular weights of AcrA and AcrB, at approximately 45 kDa and 113 kDa, respectively. An AcrA crosslink-stabilized dimer would run below this observed band at ~90 kDa, and any AcrB-containing complexes with AcrA would be of a size greater than 150 kDa. There is the possibility of larger AcrB-containing complexes existing, but at amounts too low to detect with anti-AcrA or anti-poly His antibodies.

Thusly, we are able to observe some cross-linked complexes between AcrA and another component that closely interacts with residue R225. This indicates that photocrosslinking is possible using unnatural photoreactive amino acids and membrane-localized proteins. Additionally, the UAA AzF showed a greater efficiency of specific photocrosslinking and specific high molecular weight bands as compared to the UAA BzF. However, we are unable to confirm photocrosslinking AcrA residue R225 and AcrB. This could be because AcrA R225 does not directly contact AcrB, or it could be obscured by other protein structure within AcrA. Further studies of MFP-transporter interactions are needed to determine the MFP-transporter interface, but photoreactive amino acid crosslinking could serve to be a useful tool in linking membrane-associated proteins.

1.4 Discussion

MFPs are known to play an important role in the assembly and function of efflux systems, but the extent and specifics of this role remain uncertain. For example, MFPs are known to stimulate transporters as well as recruit OMFs in order to facilitate transport into extracellular space (Zgurskaya, Weeks et al. 2015). Additionally, very little is understood about how components of these transporters coordinate the efflux process. The MP and β-barrel domains are thought to primarily govern interactions between the MFP and the transporter component, whereas the lipoyl and α-helical domains principally interact with the OMF (Zgurskaya, Weeks et al. 2015). The study of these interfaces could provide a useful insight into the mechanism of these transporters as well as pave the way for future inhibitor and targeted drug design.

Here, we show that two distinct membrane fusion proteins, TriA and TriB function together as a heterodimer with unique binding sites and interfaces between the MP domain of the MFPs and transporter. We also show that a covalently linked heterodimer of TriAxB is functional with TriC. Thus, TriA and TriB function in a 1:1 ratio and their functional unit is a heterodimer that most likely trimerizes in the fully assembled complex. This result provides the strongest evidence yet that the functional unit of MFPs is a dimer, even in other efflux complexes. Previous studies focused on crystallographic structures of MFPs, such as the *P. aeruginosa* MexA, and the *E. coli* MFPs MacA and AcrA (Akama, Kanemaki et al. 2004) (Mikolosko, Bobyk et al. 2006) (Yum, Xu et al. 2009), which suggested the functional dimer unit, but did not provide strong evidence as early hydrodynamic studies and size-exclusion chromatography showed monomeric MFPs. (Zgurskaya and Nikaido 1999) (Tikhonova, Dastidar et al.

2009). The functionality of the AxB fusion protein combined with more recent kinetic data regarding the stability of MFPs (Tikhonova, Yamada et al. 2011) provide strong evidence that MFPs interact with one another as a dimer, and function as repeating dimer pairs within the assembled complex.

Additionally, we show that analogous deletions of conserved residues in the MP domain affect TriA and TriB differently. When deletion mutants are produced as separate polypeptides, only $TriB_{\Delta 9}$ is able to even partially rescue the susceptibility of JWW2. Additionally, deletion mutants in individual proteins do not affect interactions between the partner MFP and TriC. Thus, C-terminal deletions significantly weaken the association between MFPs and transporters, but binding to TriC is an independent event for each MFP. Taken into account with the data regarding TriAxB, this suggests that MFPs are able to bind the transporter independently of one another, and then interact in a dimeric fashion to form a functional efflux complex.

How the complete RND efflux complex assembles is a subject of intense investigation. Current crystal structures of the CusBA efflux complex place the individual protomers of the MFP CusB differently on the transporter CusA, primarily between the MP and the β-barrel domains. (Du, Wang et al. 2014). Additionally, the cryo-EM-based structure of the complete AcrAB-TolC complex (Su, Long et al. 2011) shows similar positioning of AcrA on the transporter AcrB. This difference in binding sites could suggest that the affinity of MFPs to transporters could be different depending on the protomer. Our experiments showed that all covalently linked TriAxB constructs were co-purified with TriC, but the amounts differed drastically depending on which MFP contained a deletion. Deletions in TriA of the fused protein had a larger

effect on interactions with TriC, whereas deletions in TriB were purified in near wild-type levels.

This result suggests that the affinity of the full-length MFP is enough to compensate for the deletion mutant, but since all mutants were essentially nonfunctional, this compensation is only enough to maintain interaction, and not enough to maintain activity of the pump. The discrepancy between the amount of co-purified TriAxB when comparing TriA and TriB deletions could stem from the specific contact interfaces formed between the MFPs and transporter, indicating that TriA interacts with the transporter more through the C-terminal end of the MP domain, and interactions between the transporter and TriB are not as dependent on this section of the MFP. This corresponds with MIC data, in which $TriB_{\Delta 9}$ was the only deletion mutant able to display even partial functionality. Additionally, since all MP domain mutants lost their ability to co-purify TolC from *E. coli*, we can conclude that the MP domain is important for assembly of the complete transport complex. While the MP domain is not thought to principally interact with the OMF, the MP domain could be important for translating conformational changes that recruit the OMF to the complex, and deletions therein abolish the ability of the complex to strongly interact with TolC.

In addition to deletion mutants, site-specific mutations in the MP domain affect TriA and TriB differently. Point mutations in TriA, produced either as a fused protein or separate polypeptides, were functional and able to provide resistance against SDS and triclosan. However, the analogous point mutation in TriB is unable to protect against SDS and triclosan, providing further evidence that the C-terminal domains of TriA and TriB interact with TriC differently. Interestingly, point mutations in either fused or

unfused TriB seem to not have any effect on interactions with TriC, but both fused and unfused TriA mutants co-purified in a lower amount than wild-type. This is correspondent to results from C-terminal deletions in which deletions within TriA co-purify in lower amounts than deletions in TriB. Thus, $TriB_{G339}$ is important for complex function but does not affect assembly of the MFP-transporter complex, whereas $TriA_{G350}$ is not essential for function, but affects overall stability of the complex. No point mutations were able to co-purify TolC, indicating that again, interactions between the MFP and TriC are important for recruitment of the OMF.

The model of MFP-dependent transport shows that the transporter and MFP exist in complex, awaiting stimulus for the MFP to recruit the OMF (Zgurskaya, Weeks et al. 2015). This stimulus could be binding of substrate to the transporter. Taking this into account, our results indicate that deletion of the C-terminal residues of the MFP abolish the ability of the MFP to recruit the OMF, possibly because the MFP is no longer able to respond to stimulus from the transporter, resulting in an inability to make the conformational changes necessary for TolC recruitment. Point mutations in TriB also yield a non-functional complex that is unable to recruit TolC, indicating this residue is required for assembly of a stable complex. Interestingly, the functionality of the analogous residue in TriA indicates that it is not required for complex assembly, but this complex is unable to co-purify TolC. This could indicate that mutation of this C-terminal residue in both TriA and TriB reduces stability of the overall complex, but in TriB it either abolishes the ability to recruit TolC entirely, or possibly results in a defect in different function of TriB, such as transporter stimulation.

Together, these results indicate that in the interface between MFPs and cognate transporters, TriA and TriB perform separate roles in the transport process. RND-type transporters relies on a functional rotation in which each protomer of the trimeric RND transporter cycles through three conformations in order to bind and extrude substrate (Pos 2009). Taking this into account, it is possible that as the individual protomers of the RND transporter transition between the open, loose and tight conformations, the individual protomers of the MFP may be responsible for translating these conformational changes to the OMF in such a way that one MFP is responsible for opening the OMF, and the other MFP responsible for stimulation of the transporter while the complex is assembled. Changes in the MP domain may abolish this ability to translate these conformational changes, rendering the complex nonfunctional. This has implications for other transporters, where instead of TriA and TriB performing separate roles, two different MFP molecules would be responsible, possibly for stimulation of the transporter and engagement of the OMF.

It is possible that since TriA and TriB are of different lengths, the larger deletions in TriA are the source of the more drastic assembly and function changes, but sequence homology shows that the C-terminal region of TriA and TriB share these common residues with many other MFPs, and likely have a very similar structure to common MFPs **(Figure I.3)** (Zgurskaya, Weeks et al. 2015). Additionally, in the fused protein it is possible that a C-terminal deletion in TriA changes the positioning and placement of TriB by way of shifting the second MFP, thereby changing and restricting how the fused protein is able to interact with the transporter.

We also utilized a method to link components of efflux transporters by the insertion of photoreactive amino acids into the genetic code. To establish the method, we used the well-studied AcrAB transporter from *E. coli*, and attempted to photocrosslink AcrA to its cognate transporter AcrB. We showed that AcrA* forms new high molecular weight complexes on exposure to UV light, running at approximately 120-130 kDa **(Figure 1.11)**. This band was also observed in the WT complexes at a much lower level, indicating that the formed complex may be of biological relevance. The identity of these complexes is unknown and difficult to reconcile, given the molecular weights of AcrA and AcrB at ~45 and ~115 kDa, respectively. Since samples were not boiled or run under reducing conditions, it is possible that the observed band is an AcrB-containing complex, but the discrepancy between observed and expected sizes makes it impossible to conclude that the observed complex contains AcrB.

The observed size could also correspond to an AcrA trimer, but the model of MFP oligomerization (Zgurskaya, Weeks et al. 2015) postulates that the functional unit of the MFP is a homodimer which then further trimerizes to form a hexameric functional MFP complex. Based on this current model, while possible, it is difficult to conclude that a ~135 kDa trimer of AcrA would form from photocrosslinking of R225. As an AcrAB complex has not been visualized with sufficient resolution to determine the exact interface between AcrA and AcrB, it is possible that residue R225 does not contact AcrB closely enough for UAA photocrosslinking to covalently link the proteins. While (Symmons, Bokma et al. 2009) reported that AcrA and AcrB crosslink at residue R225, this publication utilized bifunctional crosslinkers with spacer arms of 6.8 angstroms and 15.6 angstroms to link AcrA and AcrB. The photoreactive amino acids

used here have no spacer arms and impose a distance requirement of approximately 3.0 angstroms (Chin, Santoro et al. 2002). This could explain the discrepancy seen between the crosslinking results of previous publications and the experiments performed here. However, we can conclude that AcrA-containing complexes were formed, and that this method can be used to photocrosslink transporter components. However, due to the distance requirements imposed by the UAA crosslinking (Chin, Santoro et al. 2002), residues should be selected based on the closest possible interaction between complex components.

Future experiments with TriA and TriB could elucidate the MFP-transporter interface even further. While we have determined that TriA and TriB have different binding sites on TriC, still little is known about precise MFP placement on the fully assembled RND transporter. Modeling of the interfaces between TriA, TriB, and TriC can identify possible interaction points, which would provide a clearer picture of the interactions between complex components. To further characterize these interactions, site-specific crosslinking can be performed to elucidate the exact positioning of TriA and TriB on TriC. Residues predicted to contact the transporter can be identified both through using homologous residues from other MFP-transporter crosslinking experiments as well as molecular modeling. Using the method described here, TriA, TriB, and TriC with specific residues mutated to the amber codon can be exposed to UV light and photocrosslinked together in such a way that the specific contact interfaces between each MFP and the transporter can be characterized, allowing us to fully understand the placement of MFPs on the transporter.

Chapter 2. Interactions between OMFs and the MFPs TriA and TriB

2.1 Abstract

MFPs are known to play a role in the recruitment of outer membrane factors, and depending on a model, MFPs are believed to interact with OMFs anywhere from a full integration of the α-helical domains to a limited tip-to-tip interface. This study again focuses on the paired MFPs TriA and TriB and their interactions with other complex components. Here, I investigate their interactions with the non-cognate *E. coli* OMF TolC as well as the cognate *P. aeruginosa* OMF OpmH. As a paired MFP known to function as a heterodimer, TriA and TriB are expected to occupy different binding sites on the OMF. To gain insight into the interactions between the MFPs and the OMF, I created deletion mutants of the CC domain in TriA and TriB produced individually or as a fused polypeptide, and tested these mutants through functional MIC studies as well as co-purification steps that shed light on the assembly of the transporter. Results showed that deletions disrupt complex assembly with TolC in *E. coli*, but have no effect on interactions between the MFPs and TriC. Additionally, I created site-specific point mutants of conserved residues near the tip of the CC domain that have been identified as important for MFP-OMF interaction. I then tested the effects of these mutations on the native OMF, OpmH in *P. aeruginosa* and found similar results to TolC in *E. coli.* Results show that these point mutations affect TriA and TriB differently, and provide further evidence that TriA and TriB occupy two non-interchangeable binding sites within the fully assembled complex, and thus have different functions in the efflux process.

2.2 Introduction

While the MP domain of MFPs is thought to principally govern interactions between the IMF and MFP, OMFs are also known to closely interact with MFPs, except interactions seem to be governed mainly through the α-hairpin domain (Zgurskaya, Weeks et al. 2015). These interactions remain uncharacterized, and data published so far do not take into account a model in which each MFP protomer could have a different role and binding site. Current models of the resting state of the transporter place the MFP and transporter together, and upon substrate binding, the OMF is recruited by the MFP to allow efflux before dissociation of the OMF (Chuanchuen, Murata et al. 2005, Tikhonova, Yamada et al. 2011). The process in which the MFP recruits the OMF results in two distinct events occurring. Firstly, the MFP undergoes conformational changes when interacting with an OMF, and that those conformational changes are linked to the stimulatory activities of the MFP (Ge, Yamada et al. 2009, Modali and Zgurskaya 2011). Secondly, OMF binding to a MFP-transporter complex is proposed to lead to an opening of the OMF channel (Weeks, Celaya-Kolb et al. 2010, Janganan, Bavro et al. 2013). This overall model places the MFP in a crucial role of directing movement of substrate throughout the complex, but the specifics of this role are not well understood.

Kinetic experiments have shown that the affinity of the MFP to either the transporter or OMF changes as a function of pH (Tikhonova, Dastidar et al. 2009, Tikhonova, Yamada et al. 2011), indicating that changes in pH could trigger conformational changes in MFPs associated with the efflux process. As with MFP:transporter interactions, the ratio of MFP:OMF monomers is 6:3, resulting in two

MFP subunits contacting a single OMF protomer. This again indicates that the MFPs would have two separate binding sites to bind the OMF in the fully assembled complex. Existing crystal structures and models of MFP-OMF interactions place the two MFPs in the grooves of the OMF protein, specifically in the inter- and intra-protomer grooves of the OMF. This supports the idea of MFPs having two distinct binding sites as well as distinct functions between the individual MFPs.

The homotrimeric *E. coli* OMF TolC functions with various efflux pumps from multiple superfamilies, and we previously showed that it functions with the non-cognate *P. aeruginosa* TriABC transporter when expressed together in *E. coli*. **(Table 3).** TolC is a 12 β-strand barrel, which is 30 Å wide and contains six loops exposed to the surface, and extends into the periplasm as a 140 Å long α-barrel (Koronakis, Sharff et al. 2000). The periplasmic end of the α-barrel forms an aperture that is thought to change conformation upon binding the MFP that allows the movement of substrate through the OMF. This conformational change consists of a twist and dilation of the helicies on the periplasmic tip, thereby "opening" the channel on both ends (Bavro, Pietras et al. 2008, Pei, Hinchliffe et al. 2011). This transition between "open" and "closed" states of OMFs defines the transition between resting and active states, in which the periplasmic tip of the OMF changes conformation upon OMF-MFP interaction.

Models of interaction between OMFs and transporters are under debate, as some evidence shows that AcrB is able to directly contact TolC (Murakami, Nakashima et al. 2002) and other, recent structural evidence shows that there is no direct interaction between AcrB and TolC (Du, Wang et al. 2014). Additionally, transporters from ABC

and MF superfamilies lack a large periplasmic domain and would be unable to directly interact with the OMF (Lu and Zgurskaya 2013). The goal of this study is to characterize the specific interactions between MFPs and OMFs, as current models of MFP-dependent transport lack specific information on how MFPs interact with OMFs, and do not take into account the possibility of an unequal MFP dimer.

In this study, we focused on the triclosan efflux complex TriABC, introducing site-specific mutations as well as deletions within the coiled-coil region and analyzed the effects of mutations in TriA and TriB on functionality as well as complex assembly. Again, we utilized the *E. coli* model in which TriABC functions with the promiscuous OMF TolC in order to provide resistance against SDS and triclosan. Additionally, we investigate assembly of the complex in the native *P. aeruginosa* via co-purification of the native OMF, OpmH.

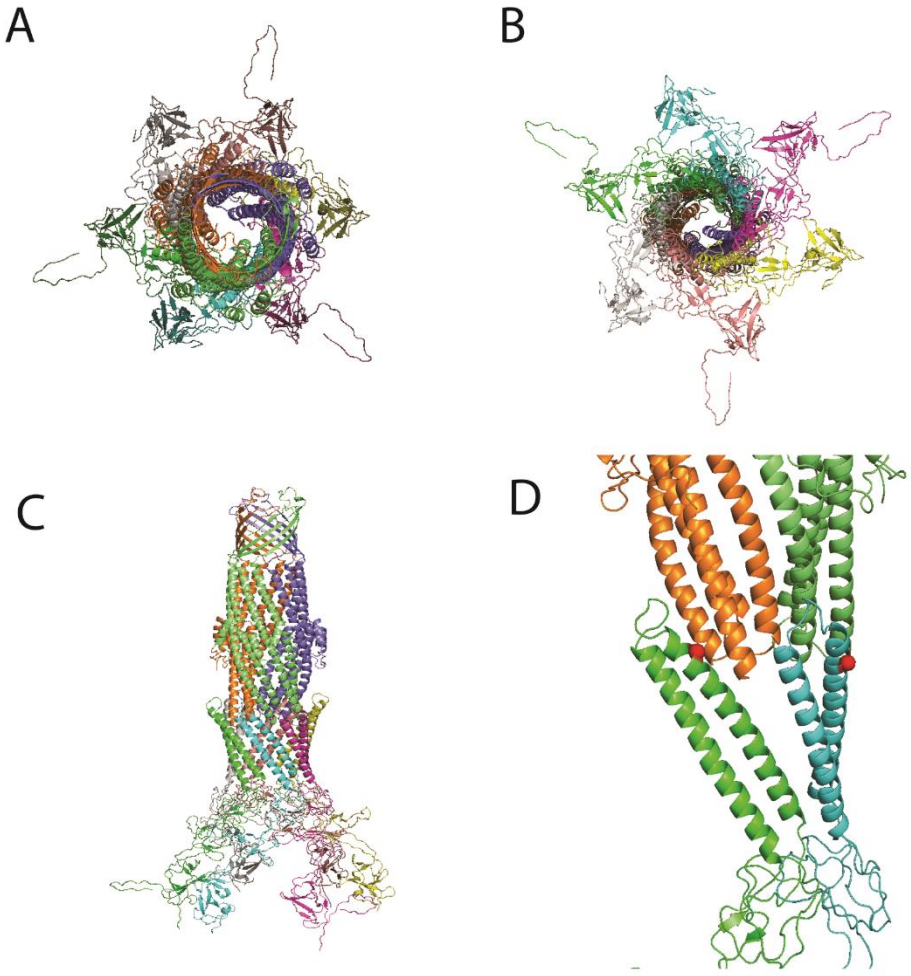

Figure 2.1 – Model of TriABC-OpmH interactions.

A. Top-down view of the complex. Individual protomers are distinctly colored. B. Bottom-up view of the complex. C. Side view of the complex. D. Interactions between single protomers of TriA, TriB, and OpmH. TriA is colored in green, TriB is colored in cyan, and OpmH protomers are colored in orange / dark green. Residues selected for point mutations in TriA and TriB are highlighted in red.

2.3 Results

2.3.1 – Mutations in the coiled-coil domains affect TriA and TriB function differently.

Previous studies implicate the α-helical hairpin domain in the recruitment of OMFs and assembly of a functional RND-MFP-OMF complex. (Chuanchuen, Murata et al. 2005, Lobedanz, Bokma et al. 2007, Tikhonova, Dastidar et al. 2009) However, some MFPs such as BesA and CusB (Greene, Hinchliffe et al. 2013) have unusual or even entirely missing α-helical domains. Despite this, both MFPs are able to function with an OMF in order to extrude substrate. To investigate the roles of the CC domain of TriA and TriB in the recruitment and function of the complex with TolC, the coiled-coil of each MFP was removed, leaving only the native CC turn linking the two halves of the lipoyl domain. This drastic change would allow characterization of the CC domains of TriA and TriB, determining if the domain is required in both MFPs.

Additionally, point mutations were made through site-directed mutagenesis, changing the highly conserved arginine residues of R130 in TriA and R118 in TriB near the tips of the α-helical hairpin to aspartic acid. Aspartic acid was chosen to contrast the basicity of the native arginine. These conserved arginine residues have been shown to be essential for function of efflux complexes and interaction of other MFPs with OMFs. Specifically, the MFPs MacA and AcrA both require this conserved arginine residue to bind TolC, despite their cognate transporters being in the ABC and RND families, respectively. (Kim, Xu et al. 2010, Xu, Sim et al. 2010) If TriA and TriB interact with TolC in the same way as these MFPs, this conserved arginine residue may be required for their interactions, but if TriA and TriB retain different interactions with the OMF,

this residue may only be required for one of the MFPs. As with MP domain mutations and deletions, these variants were produced in TriA and TriB proteins separately as well as a part of the covalently-linked TriAxB complex.

The newly created pBAD33-TriABC deletion mutants, pBAD33-TriA$_{\Delta cc}$BC, pBAD33-TriAB$_{\Delta cc}$C, as well as the point mutants pBAD33-TriA$_{R130D}$BC and pBAD33-TriAB$_{R119D}$C were transformed into *E. coli* JWW2 and tested for expression using 0.2% arabinose as an inducer. After membrane fractionation, extracts were analyzed using immunoblotting.

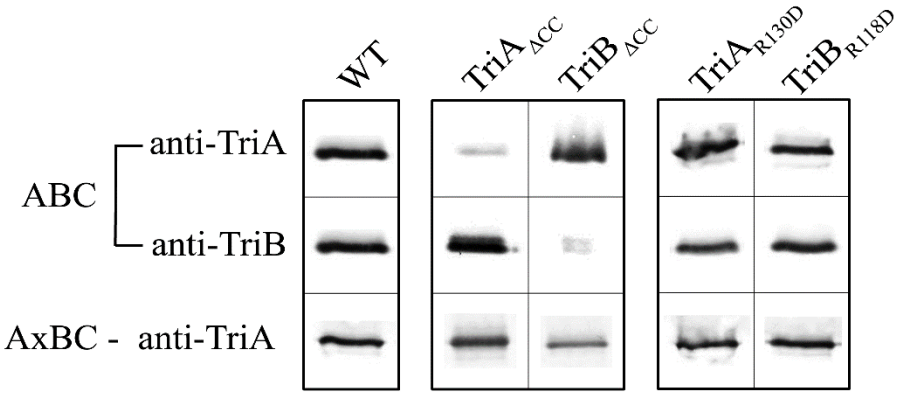

Figure 2.2 – Expression of TriA and TriB containing CC deletions and point mutations.

100 ng of membrane extracts of JWW2 cells expressing TriABC and TriAxBC variants were analyzed using SDS-PAGE followed by immunoblotting with antibodies specific for TriA and TriB in order to establish expression of the proteins.

Results indicate that all α-helical deletion mutants as well as point mutations are expressed in *E. coli*, although CC deletions in unfused TriA and TriB result in a noticeably reduced level of detectable protein. **(Figure 2.2)**

Having established that all variants are expressed in our model system, we tested functionality of these mutants using MICs with the previously established substrates of the TriABC efflux pump, triclosan and SDS.

	Variant	JWW2	
		SDS (μg ml^{-1})	Triclosan (ng ml^{-1})
1	-	39	0.25
2	TriABC	>2500	8
3	TriAxBC	>2500	4
4	$TriA_{R130D}BC$	39	<0.125
5	$TriAB_{R118D}C$	>2500	2
6	$TriA_{R130D}xBC$	39	<0.125
7	$TriAxB_{R118D}C$	>2500	1-2
8	$TriA_{\Delta CC}BC$	39	<0.125
9	$TriAB_{\Delta CC}C$	39	<0.125
10	$TriA_{\Delta CC}xBC$	39	4
11	$TriAxB_{\Delta CC}C$	39	4

Table 5 – Mutations and deletions in the coils of TriA and TriB affect complex function differently.

MIC measurements showed that both $TriA_{\Delta cc}$ as well as $TriB_{\Delta cc}$ were unable to complement the efflux-deficient JWW2 *E. coli* strain either as a fused or unfused complex. **(Table 5)** This result indicates that the α-helical domain is required for

complex function in both TriA and TriB. Of extreme interest, analogous point mutations in the CC domain of TriA and TriB affected each protein very differently. Complexes assembled with either $TriB_{R118D}$ or $TriAxB_{R118D}$ were fully functional. In contrast, complexes with $TriA_{R130D}$ and $TriA_{R130D}xB$ failed to provide resistance against either SDS or triclosan, indicating that this highly conserved residue is essential for the function of TriA but not TriB. This provides further evidence that these MFPs utilize different binding sites on the OMF, and have different functional roles in the efflux process.

2.3.2 – Mutations in the coiled-coil domain of TriA and TriB affect complex assembly differently.

Having established the lack of functionality of $TriA_{\Delta CC}$ and $TriB_{\Delta CC}$ mutants as well as the inequality of point mutations, we set out to establish how these changes affect the assembly of the efflux complex. The co-purification approach seen previously with MP domain mutations was utilized in which $TriC^{His}$ was expressed from pBAD-TriC in JWW2 *E. coli* alongside with pBAD33-based variants of TriABC and TriAxBC, and the histidine-tagged TriC was purified using affinity chromatography on His-bind resin charged with Cu^{2+}.

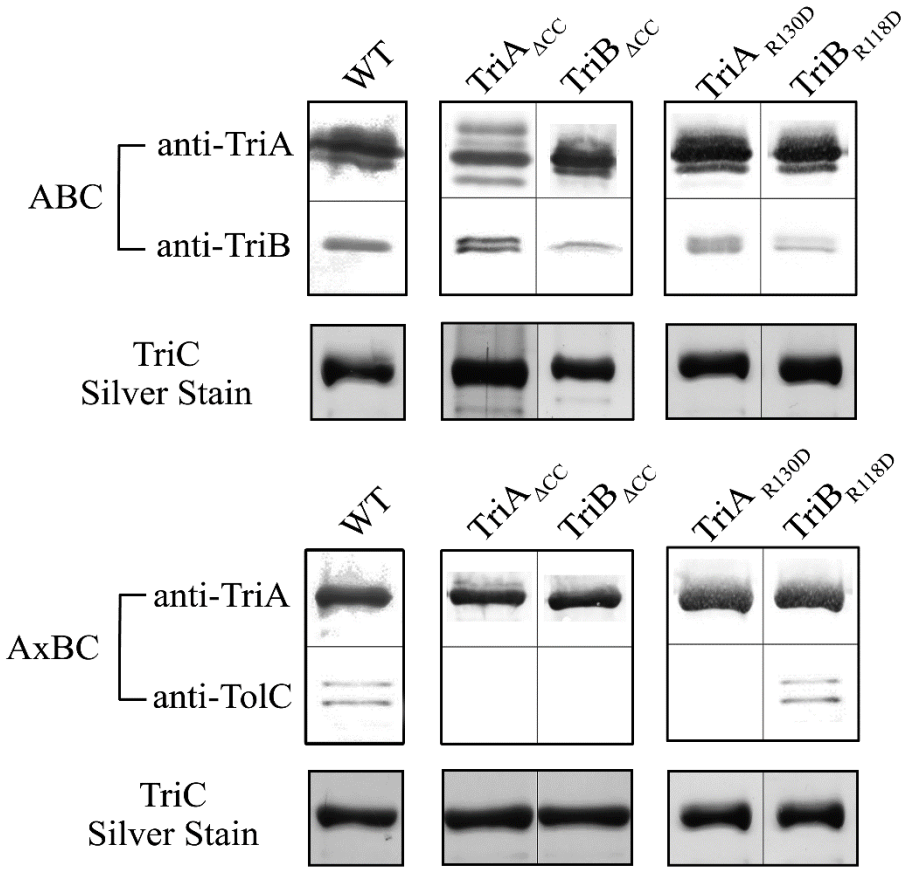

Figure 2.3 – Mutations in the CC domain of TriA and TriB do not affect co-purification with TriC.

Membrane fractions containing the indicated plasmid-expressed TriA, TriB, or TriAxB mutants with $TriC^{his}$ were solubilized and purified using affinity chromatography. Fractions were quantified and 0.1 μg of purified $TriC^{his}$ was separated by SDS-PAGE and proteins were analyzed via immunoblotting and silver staining.

Co-purification results show that neither substitutions nor deletions affect the ability of TriA or TriB to co-purify with TriC, either in a fused or unfused form. **(Figure 2.3)** Thus, as expected, mutations in the CC domain of MFPs do not affect

interactions with the transporter, even when the CC domain is removed entirely. We did find, however, that interactions with TolC were highly sensitive to deletions and substitutions in the CC domain. The only complex able to co-purify TolC was TriAxB$_{R118D}$, indicating that TriA$_{R130D}$ disrupts interactions between the MFP and OMF. This is consistent with both MIC data, as the TriA$_{R130D}$ mutant was shown to be non-functional, as well as data described in Chapter 1 showing that only the TriAxBC complex is able to stabilize interactions with TolC to a degree that can be shown with co-purification. Therefore, while TriB$_{R118}$ is not essential for complex formation and functionality, the analogous and highly conserved TriA$_{R130}$ is indeed required, and distinguishes the two MFPs in formation of a functional TriABC-OMF complex.

2.3.4 – Mutations in the coiled-coil domain of TriA and TriB affect interactions with OpmH differently

After investigating complex assembly in *E. coli*, we then set out to characterize interactions of the coil mutants with the native OMF, OpmH of *P. aeruginosa*. Previous experiments utilized the transporter as "bait," relying on continuous interactions between the MFP and transporter in order to obtain co-purified protein. It would be advantageous to purify the complex from the opposite direction, and utilize the OMF as "bait," thereby focusing on interactions between the MFP and OMF. Due to the difficulty of co-purifying TolC with unfused TriABC **(Figure 1.6)** we chose to utilize the native OMF, OpmH as "bait."

The pBAD33-based constructs were subcloned into pBSPII, and the resulting plasmids were transformed into *P. aeruginosa* JWW6, which expresses OpmH^{His} under

an arabinose-inducible promoter. **(Table 1)** $OpmH^{His}$ was induced using 1.0% L-arabinose, and the CC mutants were constitutively expressed from the pBSPII plasmid before cell lysis and affinity chromatography to purify $OpmH^{His}$. Difficulty subcloning pBSP-$TriA_{\Delta CC}$ resulted in an inability to test this mutant with OpmH.

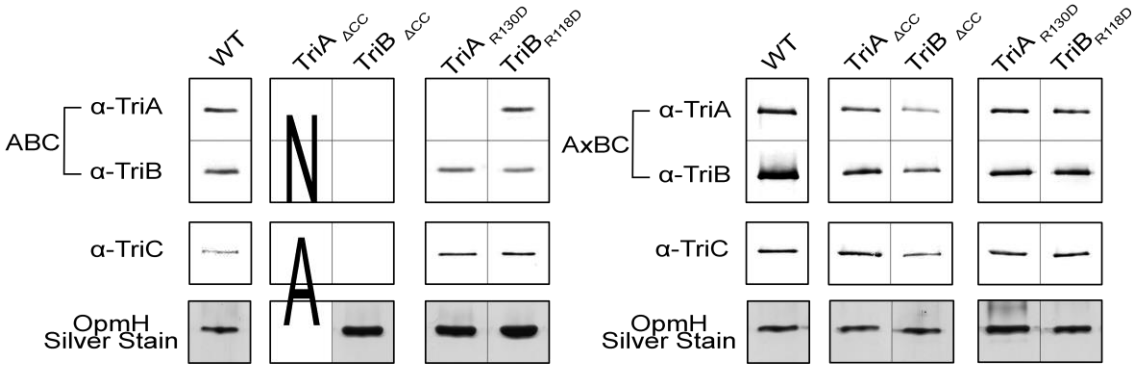

Figure 2.4 – Mutations in the CC domain of TriA and TriB affect interactions with OpmH differently

Membrane fractions of *P. aeruginosa* JWW6 carrying the indicated pBSP-expressed TriABC CC mutations were solubilized in 2% DDM overnight and subjected to affinity chromatography to purify $OpmH^{His}$. Fractions were quantified and 0.1 μg of purified OpmH was separated by SDS-PAGE and proteins were analyzed via immunoblotting and silver staining.

Results show that in *P. aeruginosa*, mutation of the conserved residue R130 in TriA results in an inability of TriA to co-purify with the rest of the complex, but the corresponding residue, R118 of TriB retains interactions with the complex during co-purification. Additionally, deletion of the coil domain of TriB results in an inability of any complex components to co-purify, but among fused protein constructs, all proteins

were able to co-purify in wild-type amounts. Interestingly, in the $TriA_{R130D}$ mutant, while TriA was unable to co-purify with OpmH, TriC co-purifies with TriB and OpmH. This indicates that with the native OMF, TriB is required to assemble the complex, but both MFPs are required for function. These mutants were also tested for functionality, and results showed non-functionality of all tested coil deletion mutants, but of the point mutants, only the unfused $TriA_{R130D}$ results in a nonfunctional protein (Abigail Ntreh, unpublished).

2.4 Discussion

The α-hairpin domain of MFPs has been shown to interact with OMFs, mainly through the minor and major grooves of the OMF (Misra and Bavro 2009, Zgurskaya, Weeks et al. 2015). The three-fold symmetry of the transporter complex indicates that one OMF protomer will contact MFPs through the inter- and intra-protomer grooves, for an overall stoichiometry of 2 MFP: 1 OMF. This indicates that there is more than one binding site between MFPs and OMFs, and in single MFP systems, different binding sites could impart different functions upon the MFP, allowing the same protein to fulfill multiple roles. Using TriABC, we show that a paired MFP transporter has unique binding sites for each MFP, and that each MFP may have a unique role in the transport process.

Deleting the CC domain from either fused or unfused TriB predictably eliminated transporter function, likely by preventing recruitment of the OMF by the MFP-IMF complex. This result is also seen in the fused TriA coli mutant. While we were unable to test the unfused TriA mutant due to difficulties in subcloning, we can

speculate that the same effect would be seen, as even the mutation of a single residue in the CC domain of TriA eliminated transporter function. This is supported by co-purification data in which the TriC transporter is able to co-purify all of the coiled-coil deletion and point mutants, whether expressed individually or as a single polypeptide, but unable to co-purify TolC. Thus, the CC domains of TriA and TriB are each required for complex function, but have no bearing on interaction with TriC, meaning that interaction of the MFP with the transporter is entirely independent of the CC domain.

Point mutants of a conserved arginine residue near the tip of the CC domain affected TriA and TriB differently both in terms of complex assembly as well as function. When TriA is expressed as $TriA_{R130D}$ in either the fused or unfused complex, we see an inability of the complex to provide resistance against triclosan and SDS, as well as a failure of TriC to purify with TolC, likely due to disruption of the functional linkage between the MFP and OMF. In contrast, $TriB_{R118D}$ retains all the ability and functionality of the wild-type protein, and is the only mutant in this study able to co-purify the OMF TolC. As the CC domains of TriA and TriB have the same length, either MFP could theoretically occupy either the inter- or intra-protomer grooves of the OMF TolC. Our results show here that when expressed separately, both CC domains are required for full interaction of the complex, but a point mutation in a conserved arginine residue on the tip of the TriA CC domain will inactivate the complex, but the analogous mutation in TriB does not affect complex function or assembly. Therefore, TriA and TriB interact very differently with TolC, and consistent with previous publications, the MFPs likely function as a dimeric unit that further trimerizes around the OMF in order to create a functional hexameric arrangement of MFPs.

Our results also indicate that interactions between TriABC and TolC are similar to that of TriABC and OpmH. When the same point and deletion mutants used with TolC were expressed and co-purified in *P. aeruginosa* using $OpmH^{His}$ as a bait, results showed that again, the point mutation $TriA_{R130D}$ was unable to maintain interactions with the OMF through the purification process, whereas $TriB_{R118D}$ showed no changes from wild-type protein. Interestingly, while the fused AxB-based mutants were unable to co-purify TolC in *E. coli* with the exception of $TriB_{R118D}$, all pBSP-based AxB mutants were able to co-purify with $OpmH^{His}$ in *P. aeruginosa*. This could be due to more specific interactions between TriAB and OpmH than TriAB and TolC. These more specific interactions would also explain the interesting result seen in the co-purification of $TriA_{R130D}$. Here, no TriA was seen in the purified sample, but TriB and TriC were co-purified with OpmH. This indicates that when utilizing the native OMF, TriB is able to assemble the complex and maintain interactions with TriC even in the absence of TriA. It is not known if TriA can provide the same effect in the absence of TriB.

Also of interest, no components of $TriAB_{\Delta CC}C$ were detected in purified OpmH fractions. This indicates that the coil domain of TriB is required to establish TriA-OMF interactions. This is in agreement with the *E. coli*-based TriC purifications, as any changes in the coil domain of either protein eliminate the ability of the OMF to co-purify with the transporter. Unfortunately, we were unsuccessful in obtaining a pBSP-based $TriA_{\Delta CC}BC$ mutant, and this construct could shed light on if full-length TriA is also required to establish TriB interactions. If so, then the paired MFPs must work in concert to recruit the OMF. Taken in light of our MP domain mutations, we have

established that MFPs are able to bind the transporter independently, but at least full-length TriB is required to assemble with the OMF, and studies of $TriA_{\Delta CC}BC$ can shed more light on the specifics of interaction between TriAB and OpmH.

Taking all CC domain results in tandem with studies regarding the MP domain, it appears that point mutations in conserved residues of TriA affect its engagement with the OMF more than with the IMF. Correspondingly, analogous mutations in TriB seem to have more adverse effects with the transporter than with the OMF. However, this would seem to be in contrast to some deletion mutant data, in which $TriB_{\Delta 9}$ is partially function, but $TriA_{\Delta 26}$ is not. It is more likely though that $TriA_{\Delta 26}$ is nonfunctional simply due to the lack of TriB expression in that specific mutant. Considering the roles of the MFP, it seems possible that both TriA and TriB are involved in complex assembly, as removal of the C-terminal domain of either protein results in an inability to recruit TolC. Considering the point mutants, it also appears that TriA is more involved with the OMF, although it is unclear if this involvement is specific to either recruiting or opening of the OMF. Additionally, it seems that TriB, while involved with assembly of the complex, is more engaged with the transporter.

What is clear, however, is that TriA and TriB occupy different binding sites on both TriC as well as TolC and OpmH, and that they retain unique roles in the transport process. We conclude here that TriA and TriB are unique membrane fusion proteins that occupy specific binding sites on the OMF. We can speculate that the primary role of TriB may be stimulation of the transporter, while TriA is primarily involved in recruitment of the OMF and therefore assembly of the full, functional complex.

Our approaches provide a way to further characterize interactions within the complex as a whole by purifying either the OMF or the transporter. The ability to purify either component allows for a more detailed understanding of how complex interactions are stabilized or destabilized by specific mutations. To better understand the interactions between TriAB and OMFs, site-specific crosslinking of residues identified through sequence homology and modeling could be performed, both with TolC as well as the native OMF, OpmH using techniques outlined in Chapter 1. This would provide the advantage of elucidating contact interfaces both with the cognate OMF, as well as a non-cognate OMF. These results could yield information critical to the assembly of these complexes, and provide evidence for a conserved model of MFP-dependent transport. Although previous attempts to clone and express OpmH in an *E. coli* background were unsuccessful (Jon Weeks, unpublished), working in the native organism *P. aeruginosa* could yield a more physiologically relevant background for experiments. By crosslinking specific identified residues, we can determine the exact placement of the MFPs on the OMF, and then by comparing models of RND-MFP transporters, determine which MFP interacts with the inter- or intra-protomer grooves of the OMF. This could yield further insight into the interfaces between MFPs and their transporters and pave the way for development of future inhibitors as well as drug design to disrupt the interactions between OMFs and MFPs.

Chapter 3. The Bacillus subtilis ABC Transporter YknWXYZ

3.1 Abstract

MFPs have been identified as required accessory proteins of transporters found in Gram-positive organisms. (Butcher and Helmann 2006) Gram-positive bacteria are known to have a single lipid bilayer, whereas Gram-negative bacteria have a dual-membrane cell envelope. This finding suggests that MFPs play a more defined role in the transport process than simply linking the inner and outer membrane components of efflux transporters. The ABC-type transporter YknWXYZ in *Bacillus subtilis* is a homolog of the *E. coli* macrolide efflux complex MacAB-TolC and is known to be responsible for resistance against an endogenously produced peptide, SdpC (Lamsa, Liu et al. 2012, Yamada, Tikhonova et al. 2012). The SdpC toxin is produced by *Bacillus* cells under starvation conditions in order to lyse surrounding cells and utilize nutrients for delay of sporulation, which is a costly and time-consuming process (Fujita, Gonzalez-Pastor et al. 2005). The individual components of the complex are YknW, a protein of unknown function, YknX, identified as a membrane fusion protein, and YknY and YknZ, which together form the ATPase and permease components of the transporter, respectively. In this study, I attempt to characterize the function of YknX through reconstitution of purified chimeric transporter complexes, in hopes of establishing that YknX retains conserved MFP functions associated with other ABC-type MFP-dependent transporters. I conclude that YknWXYZ is a unique, 4-component complex that warrants further investigation into the activities of Gram-positive MFPs.

3.2 Introduction

The cell envelopes of Gram-positive bacteria are not well understood. While Gram-negative and Gram-positive bacteria share some characteristics like the presence of phospholipids and peptidoglycan, Gram-positive envelopes are both chemically and compositionally distinct (Silhavy, Kahne et al. 2010).

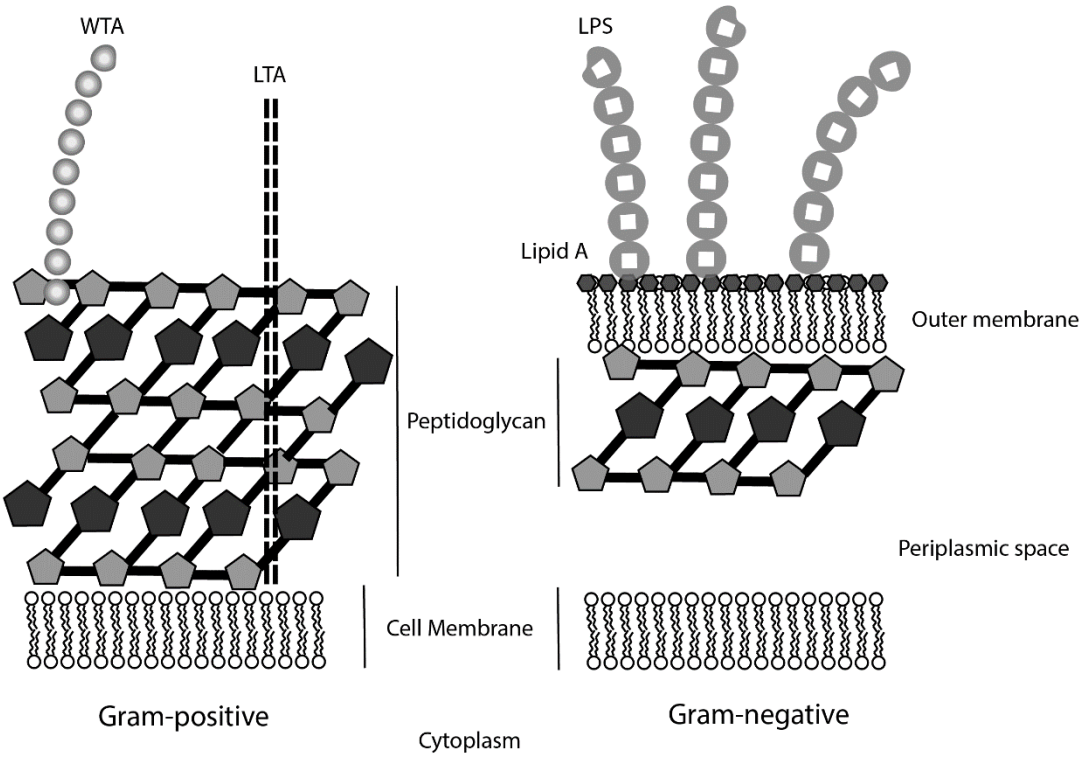

Figure 3.1 – Comparison of Gram-positive and Gram-negative cell envelopes. A graphical comparison of Gram-positive and Gram-negative membrane environments. Unique features are indicated. LPS – Lipopolysaccharide. LTA – Lipoteichoic acid. WTA – Wall teichoic acid.

Generally, Gram-positive envelopes are composed of a cytoplasmic membrane, consisting of a phospholipid bilayer which is coated on the outside by a thick layer of

peptidoglycan (Puech, Chami et al. 2001, Brennan 2003). Many transporters present in Gram-positive bacteria require MFPs for drug resistance, membrane biogenesis, and protein secretion, which is intriguing in the context of a single lipid bilayer (Butcher and Helmann 2006, Yamada, Tikhonova et al. 2012, Freudl 2013). As the primary roles of the MFP have been thought to provide a physical linker between the transporter and OMF, recruitment of an OMF, and translation of conformational changes within the complex, their requirement is puzzling in the absence of an OMF. Gram-positive MFPs are not well studied, but are believed to share the same general 4-domain architecture as Gram-negative MFPs based on both homology and secondary structure predictions (Zgurskaya, Yamada et al. 2009). The conservation of the coiled-coil domain in Gram-positive MFPs is also puzzling, as the domain is proposed to mediate interactions between the MFP and OMF. YknWXYZ contains YknX, which is the most studied Gram-positive MFP to date (Yamada, Tikhonova et al. 2012, Zgurskaya, Weeks et al. 2015), but still precious little is known about the function of the complex. Investigation of YknWXYZ could yield great insight into the function of MFPs, as well as the functional relationship between MFPs and their cognate transporters.

While MFPs are known to stimulate their cognate transporters, (Zgurskaya, Weeks et al. 2015) there are other proposed roles for MFPs, such as substrate binding that would make sense in a Gram-positive environment. The *E. coli* MFP MacA has been shown to bind a core LPS molecule, a putative substrate, and other MFPs involved in metal export such as ZneB and CusB have been shown to bind zinc and copper, respectively (Bagai, Liu et al. 2007, Mealman, Zhou et al. 2012, Lu and Zgurskaya 2013). Additionally, ZneB has been shown to exhibit structural changes upon zinc

binding (De Angelis, Lee et al. 2010). These MFP roles could be reconciled in a Gram-positive bacterium, and would suggest that like in Gram-negative organisms, MFPs have an active role in the transport process that is not yet clearly understood.

The *B. subtilis* protein complex YknWXYZ consists of four interacting components known to provide resistance against the endogenously produced toxin, SDP (Butcher and Helmann 2006). SDP is the processed form of the SdpC protein, which is produced under starvation conditions in *Bacillus* (Ellermeier, Hobbs et al. 2006). Starvation of the organism activates the Spo0A regulon which controls *Bacillus* entry into sporulation, and ultimately controls the *sdpABC* operon (Molle, Nakaura et al. 2003). After production, SdpC is then processed into the toxic form, SDP. While the details of processing SdpC into the toxin SDP are not known, SdpA and SdpB are both required to produce mature SdpC (Perez Morales, Ho et al. 2013). Upon processing and export, the extracellular SdpC induces the synthesis of SdpI, an immunity protein that protects cells from endogenously produced SdpC. SdpI is produced in the same operon as an autorepressor, SdpR. (Ellermeier, Hobbs et al. 2006)

YknWXYZ is under control of a separate system, the σ^{W} regulon, which is known to be activated as a response to antibiotic exposure (Butcher and Helmann 2006). Crosslinking experiments indicate that YknX is able to bind YknYZ, and YknW is able to interact with YknXYZ (Yamada, Tikhonova et al. 2012). This agrees with the current model of MFP-dependent efflux, wherein the MFP interacts directly with the transporter, and is involved in the assembly of a larger complex (Zgurskaya, Weeks et al. 2015). However, since the function of YknW remains unknown, it is difficult to pinpoint the role of YknW, especially as it relates to OMFs in Gram-negative bacteria.

Further complicating our understanding, when YknW is overproduced, it is able to provide partial protection against SdpC, but all four components are required for complete resistance (Yamada, Tikhonova et al. 2012).

To investigate this unique Gram-positive MFP-containing complex, we focused on finding the primary role of YknX in the complex. Since MFPs are known to stimulate their cognate transporters, we first attempted to purify the complex from the native organism, *B. subtilis* and then characterize the ATPase activity of YknY under different conditions. We then began chimeric analysis of components of this complex with another, more well-studied ABC-type transporter, MacB of *E. coli.* Such component-mixing experiments have been performed in RND-type transporters (Krishnamoorthy, Tikhonova et al. 2008), but none with ABC-type transporters from such a different background. We investigated interactions between transporters by creating fusion proteins, in which the ATPase domains and permease domains of YknYZ and MacB were switched, effectively creating hybrid proteins. This was done in such a manner that the ATPase domain of MacB would function with the permease domain YknZ, and the opposite construct was created as well. In addition, since MacB has a short linking peptide between the ATPase and permease domains that is not found in either YknY or YknZ, these constructs were created with and without the linking region.

We also cloned and expressed the fusion protein YknYLZ, in which the ATPase and permease domains of YknYZ are covalently linked together as a single polypeptide. ABC-type transporters extend the ATPase portion of the complex into the cytoplasm of the cell, and in MacB, this cytoplasmic domain is directly attached to the permease

domain embedded in the membrane. YknYZ, however, is expressed as two distinct polypeptides, and the stimulatory activity of YknX on YknY would depend on the stability of interactions between both YknX and YknZ, as well as YknZ and YknY, as the MFP is proposed to primarily interact with the periplasmic side of any membrane-bound transporter components. In order to stabilize this complex, YknY and YknZ were expressed as a covalently linked complex called YknYLZ wherein the two domains of the transporter were linked together via the same flexible linking region from MacB.

In order to determine if YknX could stimulate the ATPase activity of YknY, this fusion protein was purified and tested for ATPase stimulation in the absence and presence of complex components. Finally, we also investigated purification and analysis of unmodified YknY and YknZ through purification and ATPase assays.

3.3 Results

3.3.1 YknWXYZ and YknYZ show no intrinsic ATPase activity

To first establish YknWXYZ as a system to study MFPs in a Gram-positive organism, we used the native host, *B. subtilis* to purify the complex. This purification would allow us to obtain YknY, with which we could perform ATPase assays and establish the activity of the transporter, as well as establish which complex components co-purify with the membrane-bound YknZ permease. For this purpose, *B. subtilis* HB6127 cells were transformed with the shuttle vectors pHCMC04-YknWXYZ^{His} and pHCMC04-YknYZ^{His} (Yamada, 2012) and grown according to protocol (Methods). To optimize chances of co-purification of complex components, the YknWXYZ purification protocol was adopted from the MalFGK$_2$ transporter purification

(Landmesser, Stein et al. 2002), which also is an ABC-type transporter and has been utilized in similar ATPase assays. The purification protocol for YknYZ was adopted from (Yamada, Tikhonova et al. 2012) and solubilized proteins in the detergent Triton X-100, which has been used in ATPase assays with previous ABC-type transporters as well (Lu and Zgurskaya 2013). Both complexes YknWXYZ^{His} and YknYZ^{His} were purified using Ni-NTA resin charged with $NiSO_4$. **(Figure 3.2)**

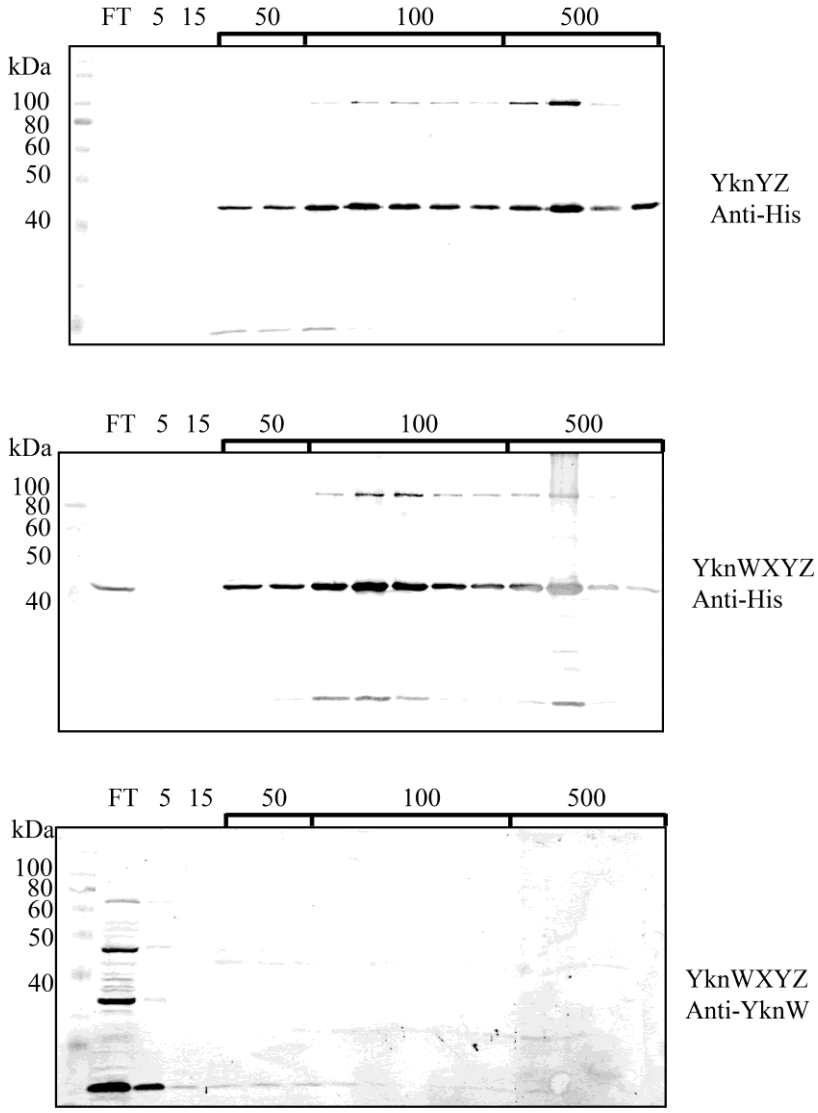

Figure 3.2 – Purification of Ykn complexes from *Bacillus subtilis*.

Membrane fractions of *B. subtilis* HB6127 cells expressing YknYZ or YknWXYZ induced with 0.5% L-xylose were solubilized in 5% Triton X-100 or 1% DDM, respectively, and his-tagged proteins were purified from the detergent-soluble fraction by Ni^{2+} affinity chromatography. The column was washed in 5 mM, 15 mM, and 50 mM steps before elution using 100 mM and 500 mM imidazole. Purified fractions were then visualized using immunoblotting with anti-poly His or anti-YknW antibodies.

Purification results indicate that YknZ (~42 kDa) can be purified from *B. subtilis* cells, but immunoblotting with anti-YknW antibodies indicated that YknW (24 kDa) does not co-purify with YknZ as a complex. Additionally, no YknY (25 kDa) was detected in purified YknZ^{His} fractions when visualized using CBB stain (data not shown). To establish if the purified proteins retain ATPase activity, purified fractions were quantified on 12% SDS-PAGE using a BSA standard and Imagequant analysis software before being subjected to an ATPase assay as described in the Methods. *E. coli*-based MacB was also purified according to the YknWXYZ or YknYZ protocols and used as a positive control for the ATPase assay. **(Figure 3.3)**

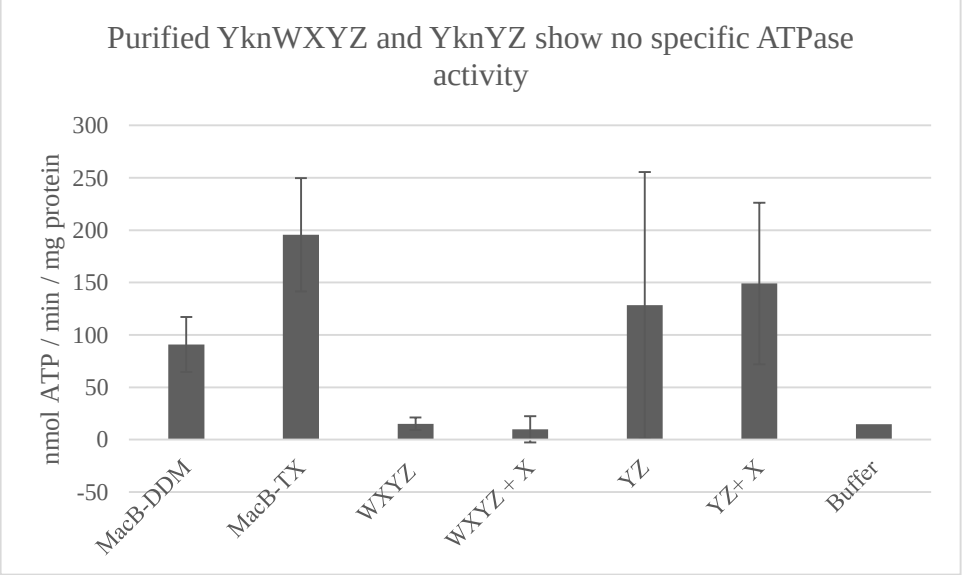

Figure 3.3 – Purified YknWXYZ and YknYZ show no ATPase activity. ATPase rates of MacB, and the purified YknWXYZ and YknYZ complexes.

Although results initially indicate ATPase activity for YknYZ, analysis of CBB-stained fractions showed a significant amount of non-specific proteins (Data not shown), and likely do not show ATPase activity intrinsically. Additionally, as purification of the whole complex showed no ATPase activity, it seems unlikely that YknYZ alone is able to support hydrolysis of ATP. In light of this, new approaches were needed to investigate the YknWXYZ complex.

Since purification of the complex from the native organism did not yield functional proteins, a recombinant system was used to purify the protein from *E. coli.* Several efflux transporters have been shown to have a degree of adaptability, and are able to function utilizing other transporter components (Krishnamoorthy, Tikhonova et al. 2008)(Chapter 2, Table 2). For instance, certain site-specific mutations allow AcrA to function with the non-cognate RND-type transporter MexB (Krishnamoorthy, Tikhonova et al. 2008). Additionally, Chapter 1 of this dissertation describes function of TriABC with the non-cognate OMF TolC **(Table 2)**. This indicates that efflux transporters have a very similar structure, and may be able to function utilizing components sourced from other efflux complexes.

In order to determine if YknWXYZ and ABC-type transporters share the same mechanism, we created chimeric proteins between MacB and YknYZ that combine the ATPase component of one transporter with the permease component of another **(Figure 3.4)**. Sequence alignments of an *in silico* fusion protein where YknY and YknZ are connected from the C-terminus of YknY to the N-terminus of YknZ show alignment with MacB, however, residues 228-243 within MacB, which lie between the permease and ATPase components, do not align with either YknY or YknZ. This is likely a

flexible region involved in allowing conformational changes between the two domains. In YknWXYZ, when the ATPase and permease regions are expressed separately, there would be much less restriction imposed on the interdomain flexibility of the proteins, as they are not covalently linked. To determine the requirement of the linker region we created our chimera both with and without the region, and attempted to express and purify these proteins to determine their ATPase activity.

Additionally, since co-purification of the entire complex made it difficult to determine if YknY co-purified with histidine-tagged YknZ, we also created a fusion protein between YknY and YknZ. This fusion protein covalently linked the N-terminus of YknY to the C-terminus of YknZ in order to both fix the stoichiometric ratio of the two proteins as well as impose a physical connection between the two proteins. Through these sets of fusion proteins, we establish a biochemical method to study YknWXYZ.

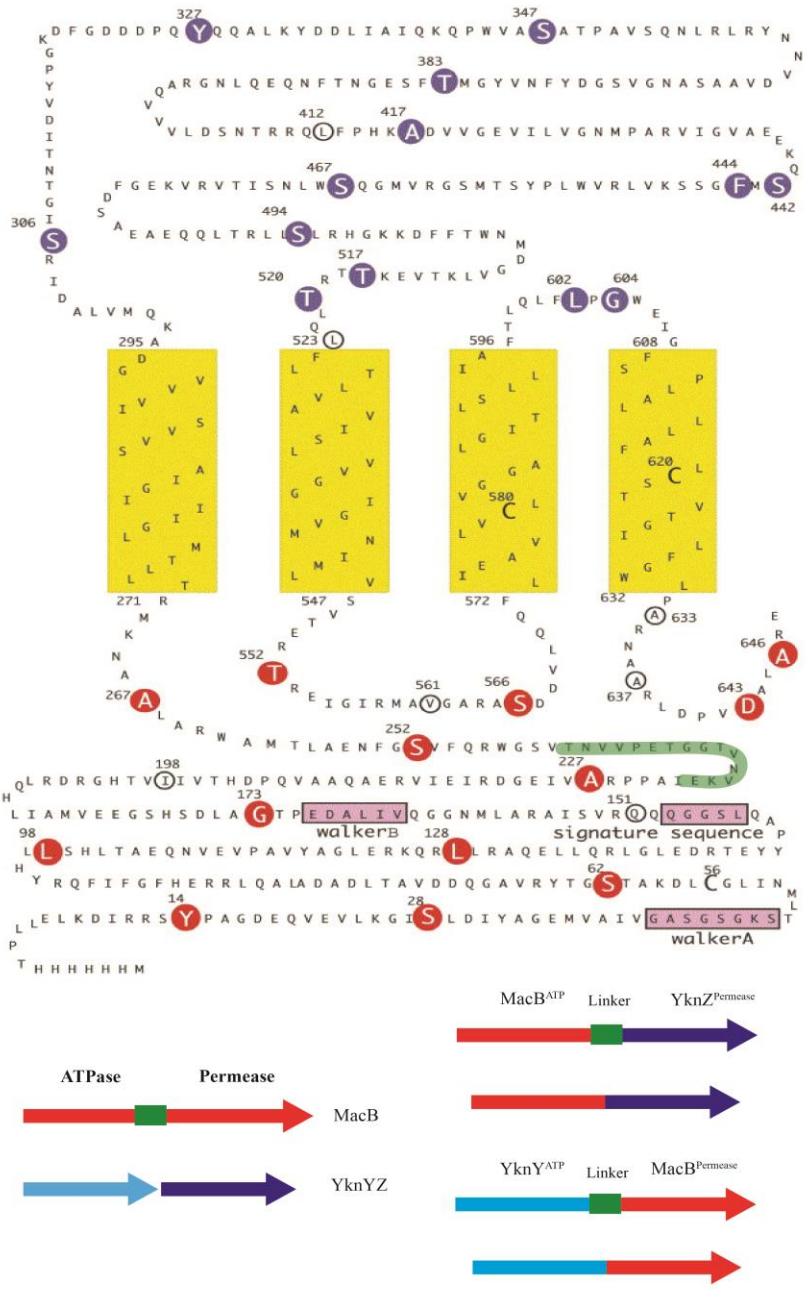

Figure 3.4 – Construction of YknYZ / MacB chimera.

Top: Topology diagram of MacB (Kobayashi, Nishino et al. 2003). The flexible linker region is highlighted in green. Bottom, Schematic of the assembled Ykn-MacB chimeric proteins.

Plasmids encoding chimeric proteins were constructed through PCR, in which the ATPase-encoding fragment from either pUC-MacB or pHCMCO4-YknWXYZ **(Table 1)** was amplified using an *EcoR*I restriction site in the forward primer and a *Kpn*I site in the reverse primer, and inserted into pUC18 digested with the same enzymes. After insertion, the permease fragment was amplified from either pUC-MacB or pHCMC04-YknWXYZ using a *Kpn*I forward primer and a *Sal*I reverse primer and inserted into the previously constructed plasmid. This insertion of a *Kpn*I site in between the ATPase and permease portions of the protein codes for glycine and threonine, two uncharged amino acids which are unlikely to affect protein structure. Constructs containing the linker region from MacB were created in the same way, except MacB primers were designed to amplify through the linker region either at the end of the ATPase fragment or starting at the beginning of the permease fragment, including the linking region.

The plasmid encoding the fusion protein linking the ATPase YknY and the permease YknZ was also created by PCR. The linking region between the ATPase and permease regions of MacB is thought to provide conformational flexibility between the two domains, allowing changes needed for function. This same linking region was incorporated in between the ATPase and permeases of YknY and YknZ in order to provide the same flexibility. pET-YknYLZ was constructed via PCR amplification of *yknY* from *B. subtilis 168* genomic DNA using an *Nco*I-containing forward primer and an *Xho*I-containing reverse primer. The linking region, taken from *macB* in the *E. coli* genome, was amplified by *Sal*I-containing forward primer and *Xho*I-containing reverse primer. Finally, the permease, *yknZ* was amplified in the same way as *yknY* except

utilizing *Sal*I-forward and *Xho*I-reverse primers. The individual fragments were ligated into pET21d(+) sequentially. This is possible as *Sal*I and *Xho*I create compatible restriction sites, which upon ligation, create a site which cannot be cleaved by either enzyme. This allowed sequential assembly of the plasmid without the utilization of multiple restriction sites.

3.3.2 Fusion proteins require a flexible linker for expression

The resulting plasmids, pUC-MZ^{His}, pUC-MLZ^{His}, pUC-YM^{His}, and pUC-YLM^{His} **(Table 1)** were transformed into *E. coli* BL21 (DE3) and cells were grown and induced with 1 mM IPTG according to protocol (Methods). The protein MZ^{His} contains the ATPase portion of MacB, but without the linking region, followed by the permease YknZ. **(Figure 3.4)** Correspondingly, the MLZ^{His} protein contains the ATPase portion of MacB linked to the permease YknZ along with the short linking peptide. YM^{His} and YLM^{His} follow the same convention, utilizing the ATPase YknY and the permease portion of MacB without and with the linking region, respectively. The fusion proteins pUC-MLZ^{His} and pUC-YLM^{His} were shown to express and localize to the membrane, however all other fusion proteins were undetectable with either anti-His or anti-MacB immunoblotting. **(Figure 3.5)** This indicates that a fused protein containing both the membrane-bound permease and the intracellular ATPase requires this flexible loop region in order to be processed and inserted correctly into the membrane. Interestingly, it appears that the fusion protein MLZ^{his} reacts strongly with anti-poly His antibody, but not anti-MacB antibody, and YLM^{his} reacts with anti-MacB but not anti-poly His. Reasons for this are unclear, as both proteins contain a poly-histidine tag and anti-MacB

antibodies are polyclonal, but MLZ^{His} concentrations could be below that of the anti-His detection limit, and anti-MacB antibodies could have a tendency to react more with the permease domain rather than the ATPase domain.

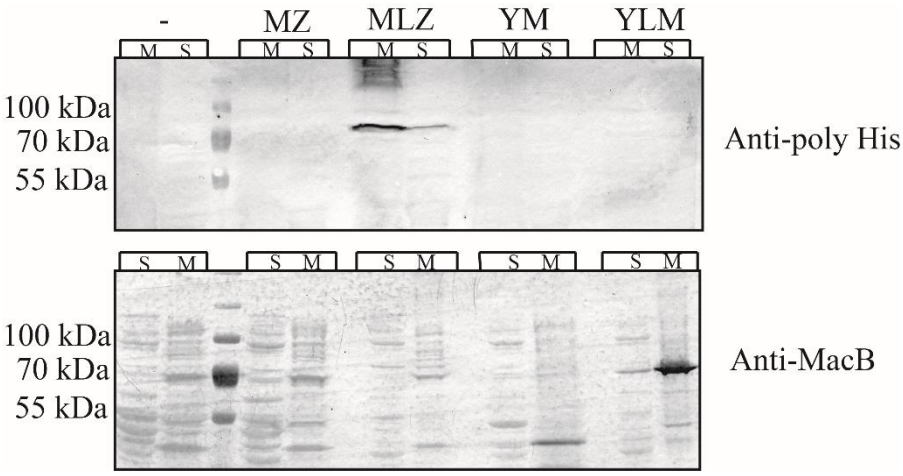

Figure 3.5 – Expression and localization of chimeric MacB-Ykn constructs. C43 cells carrying pUC-based chimeric constructs were grown and protein expressed using 1 mM IPTG. After cell lysis, membrane and soluble fractions were separated and 10 μg of total protein from either the membrane or soluble fraction was separated by 12% SDS-PAGE gels and visualized by immunoblotting with either anti-poly His or anti-MacB antibodies. S – Soluble fraction. M – Membrane fraction.

pET-YLZ^{His}, the construct linking the ATPase and permease regions of the Ykn complex was also transformed into *E. coli* C43 cells, with pET-X^{His} used as a positive control. Protein expression was induced using 1 mM IPTG, and membrane fractions were collected. To check YknYLZ localization and expression, both cytoplasmic and membrane fractions were resolved by 12% SDS-PAGE and subjected to immunoblotting with monoclonal anti-poly His antibody (Sigma). Histidine-tagged YknX was used as a positive control. Proteins reacting with monoclonal anti-poly His

were detected in both YknX and YknYLZ-expressing membrane fractions, indicating that the fusion protein YknYLZ folds correctly and is localized to the membrane of *E. coli*. **(Figure 3.6)**

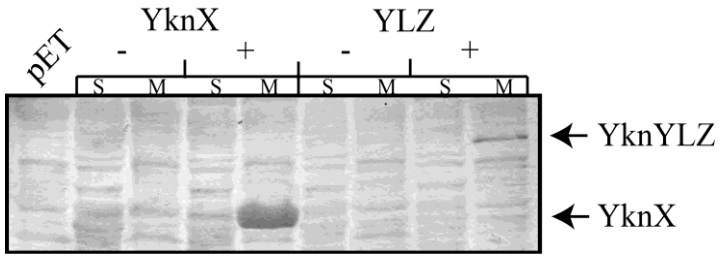

Figure 3.6 - YknYLZ expression and localization.

Anti-his immunoblot showing membrane and soluble fractions of cells carrying pET-based plasmids expressing proteins. C – Cytoplasmic (soluble) fraction. M – Membrane fraction. (-) – Culture not induced. (+) – Culture induced using 1 mM IPTG.

All fusion proteins, including chimeric proteins between MacB and Ykn were expressed only when containing the flexible linker region. Thus, the flexible linker is required when expressing the ATPase and permease as a single polypeptide.

Due to this result, we focused efforts solely on the fusion proteins YLZ, MLZ^{His} and YLM^{His}. In order to purify the proteins, we solubilized the membrane fractions of C43 cells expressing either MLZ^{His} or YLM^{His} in Triton X-100 and determined the localization and solubility of the fusion proteins. **(Figure 3.7)**

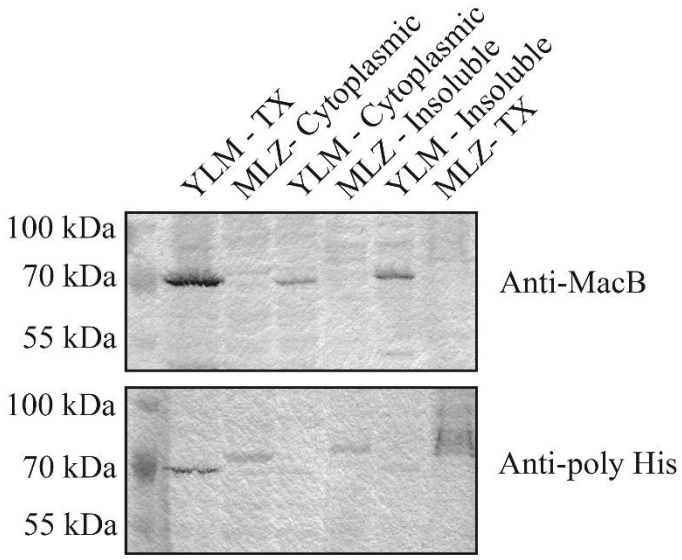

Figure 3.7 – Localization and solubility of the chimeric MLZ and YLM.

Membrane fractions of C43 cells expressing either MLZ^{His} or YLM^{His} proteins were solubilized in 5% Triton X-100 overnight, and then the insoluble fraction was pelleted by centrifugation. The detergent-solubilized, insoluble, and cytoplasmic fractions were all separated by 12% SDS-PAGE and visualized by immunoblotting with either anti-MacB or anti-poly His antibodies.

Immunoblotting revealed that both MLZ^{His} and YLM^{His} are soluble in Triton X-100, and that these proteins are localized to the membrane of *E. coli*. This indicates that the proteins have been processed correctly and inserted into the membrane, and may be suitable candidates for purification and ATPase assays.

To establish solubility of YLZ, YknYLZ was expressed in C43 cells at both 37° and 16° Celsius for 3 hours and overnight, respectively. By expressing at a lower temperature overnight, cells can be kept from reaching the stationary phase, and theoretically allowing for production of more protein. After cell growth, membrane

fractions were collected, and isolated membranes were incubated overnight in 20 mM Tris-HCl, 1 mM PMSF, 10 mM $MgCl_2$, 1 mM ATP-Mg^{2+}, and either 2% Triton X-100, 1% DDM, 40 mg/mL LPG, or 1% CHAPS.

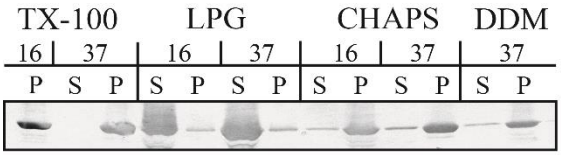

Figure 3.8 - Detergent screen of YknYLZ.

Anti-his immunoblot of membrane extracts containing expressed YknYLZ. Cells were grown at either 37 or 16 degrees Celsius, membranes were isolated, and the solubilized in the indicated detergent. P – Insoluble membrane pellet. S – Soluble membrane fraction.

After resolving on a 12% SDS-PAGE and subsequent immunoblotting with anti-poly His antibody, soluble fractions indicated that YknYLZ has a very low solubility in common detergents normally used in screening of membrane proteins, such as Triton X-100, CHAPS, and DDM. However, results indicate that YknYLZ is very soluble in the less commonly used detergent lysophosphatidylglycerol (LPG). **(Figure 3.8)** Thusly, LPG was chosen for solubilizing YknYLZ for future experiments. There was no observed difference in expression or solubility if the cells were grown at 37° or 16° Celsius, and thusly growth conditions were standardized at 37° Celsius with 3 hours of induction.

Having established the expression and solubility of all fusion protein constructs, a pilot purification was performed to determine the viability of utilizing the proteins in

further biochemical assays. Membrane fractions were collected from cells expressing either MLZ^{His} or YLM^{His}, and solubilized as previously described. After ultracentrifugation to pellet the insoluble fraction, proteins were purified from the detergent-soluble fraction by Ni^{2+} affinity chromatography. Fractions were then analyzed for protein presence using immunoblotting. **(Figure 3.9)**

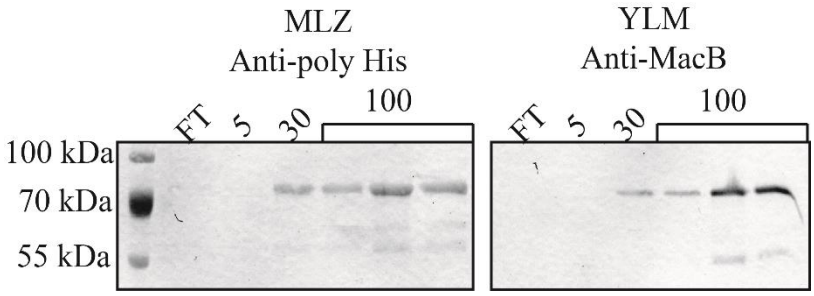

Figure 3.9 – Purification of MLZ^{his} and YLM^{his}.
Detergent-solubilized membranes were loaded onto a 1 mL Ni-NTA column charged with Ni^{2+}. After collecting the flowthrough (FT), the column was washed with binding buffer containing 5 mM (5) and 30 mM (30) imidazole. Protein was then eluted using 100 mM (100) imidazole. After collection, fractions were analyzed using immunoblotting for anti-poly His and anti-MacB antibodies.

Analysis of the immunoblots revealed that MLZ^{His} and YLM^{His} are both able to be purified from the membranes of *E. coli*. However, protein yield and purity were too low to be considered for an ATPase assay when fractions were analyzed by staining with CBB (Data not shown).

To increase protein yield, pUC-MLZ^{his} and pUC-YLM^{his} were subcloned into the high-copy plasmid pET-21a (+) which uses a T7 phage promoter rather than the *lac*-

based promoter of the pUC plasmids. This was selected to increase protein production, which would allow for stronger washing steps, and better overall purification of YLM^{His} and MLZ^{His}. After subcloning, the newly constructed pET-MLZ^{His} and pET-YLM^{His} were transformed into *E. coli* C43 cells and after protein expression, subjected to the same membrane fractionation and solubility assay to determine the localization and expression of the proteins. **(Figure 3.10)**

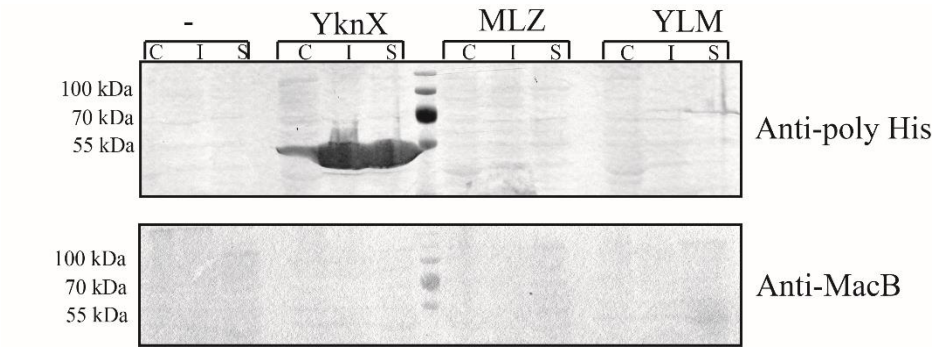

Figure 3.10 – MLZ and YLM from pET21d are not expressed.

Plasmids encoding the proteins MLZ^{His}, YLM^{His} and $YknX^{His}$, which was used as a positive control were transformed into C43 cells. Cells were induced for 3 hours using 1 mM IPTG. After cell lysis and membrane fractionation, the membrane fraction was solubilized in Triton X-100. Soluble and insoluble fractions were analyzed via SDS-PAGE and anti-poly His and anti-MacB immunoblotting. C – cytoplasmic fraction. I – detergent-insoluble membrane fraction. S – detergent-soluble membrane fraction.

Unfortunately, no expression from pET-based plasmids was seen for the chimeric Mac-Ykn proteins, using either anti-MacB or anti-poly His immunoblotting. Hence, pUC-based constructs of MLZ and YLM can be used to obtain protein.

Having established a method to express chimeric proteins between MacB and Ykn, we set out to purify YknYLZ. As a positive control we also purified MacB, which has been previously used in experiments to characterize ATPase activity (Lu and Zgurskaya 2012). For this purpose, the plasmids pET-X, pET-YLZ, and the positive control pET-MacB **(Table 1)** were transformed into *E. coli* C43 cells. After growth and protein expression, membrane fractions from the cells were collected. YknYLZ was solubilized in LPG, whereas YknX and MacB were solubilized in Triton X-100. Next,

solubilized membranes were loaded onto a Ni-NTA column charged with Ni^{2+}, and proteins were purified according to the established protocol. **(Figure 3.11)**

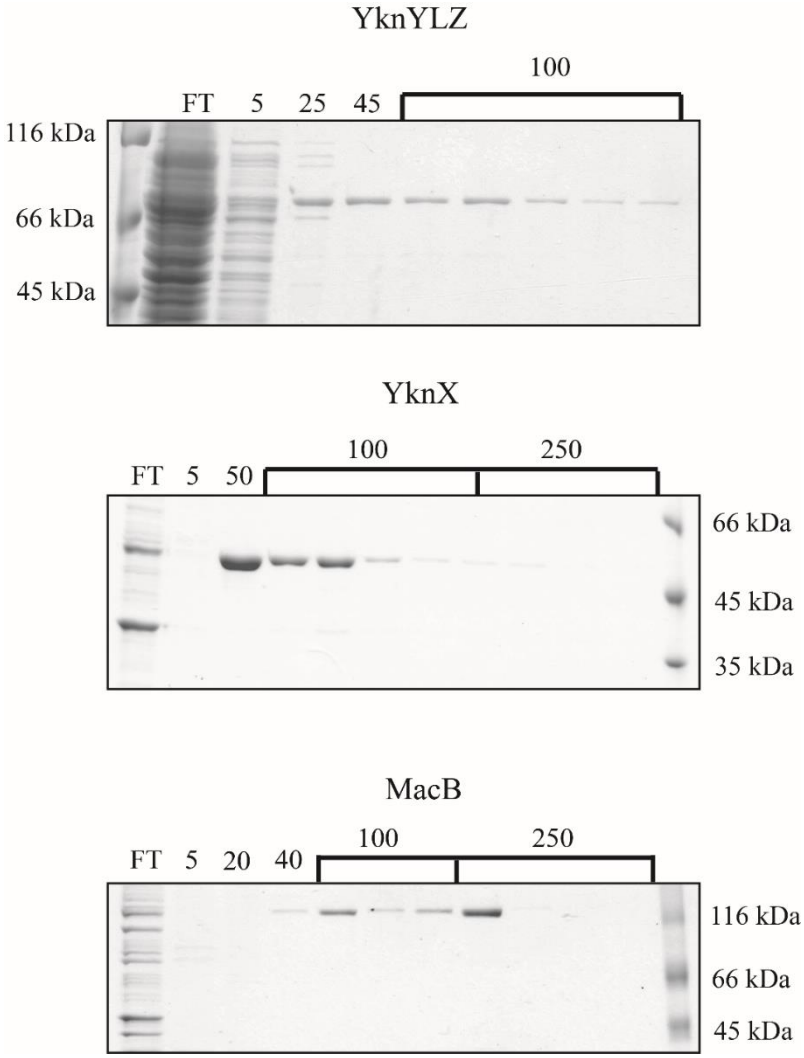

Figure 3.11 – Purification profiles of YknYLZ, YknX, and MacB.

Total membranes of C43 cells expressing various constructs were solubilized in either 5% Triton X-100 or 20 mg/mL LPG. The detergent-soluble fraction was loaded onto Ni^{2+} charged NTA column and bound proteins were eluted with the indicated imidazole concentrations. Fractions were resolved by 12% SDS-PAGE and visualized with CBB. A. Purification profile of YknYLZ. B. Purification profile of YknX. C. Purification profile of MacB. FT - Flowthrough

After purification, fractions were checked for the presence of purified protein using standard SDS-PAGE, and then fractions containing purified protein were combined and dialyzed to remove contaminating buffer components. As a control, a portion of purified MacB and YknX were then transferred into LPG as described in the Methods section.

Having purified and established concentrations of purified proteins, we then performed an ATPase assay to determine the ability of YknYLZ to bind and hydrolyze ATP, as well as the ability of YknX to have an effect on ATP hydrolysis rates. In the assay, purified proteins were mixed according to protocol with reaction buffer, and incubated at 37° Celcius (Tikhonova, Devroy et al. 2007). At 4 minute intervals, aliquots of 1 μL were removed from the reaction mixture and placed into stop solution. In addition to previously mentioned proteins and detergent mixtures, a previously purified MacB stored in glycerol was used as a positive control for technique, in both LPG and TX-containing buffers. Once the time course was completed, aliquots were spotted on a TLC plate and amounts of hydrolyzed ATP were quantified using a Phosphoimager and ImageQuant. ATPase activity was recorded as a function of nmol ATP / min / mg protein. We found that the ATPase activity of MacB is severely inhibited by the presence of the detergent LPG. **(Figure 3.12)** This is likely due to the ionic nature of LPG, as compared to Triton X-100, which is a non-ionic detergent.

Experiments to exchange LPG for Triton X-100 were performed by binding YknYLZ to an affinity column and running large volumes of Triton-containing wash buffer over the protein before elution were unsuccessful. (Data not shown)

Additionally, no stimulation of ATPase activity was observed upon addition of YknX to either MacB or YknYLZ, regardless of detergent conditions. (Data not shown)

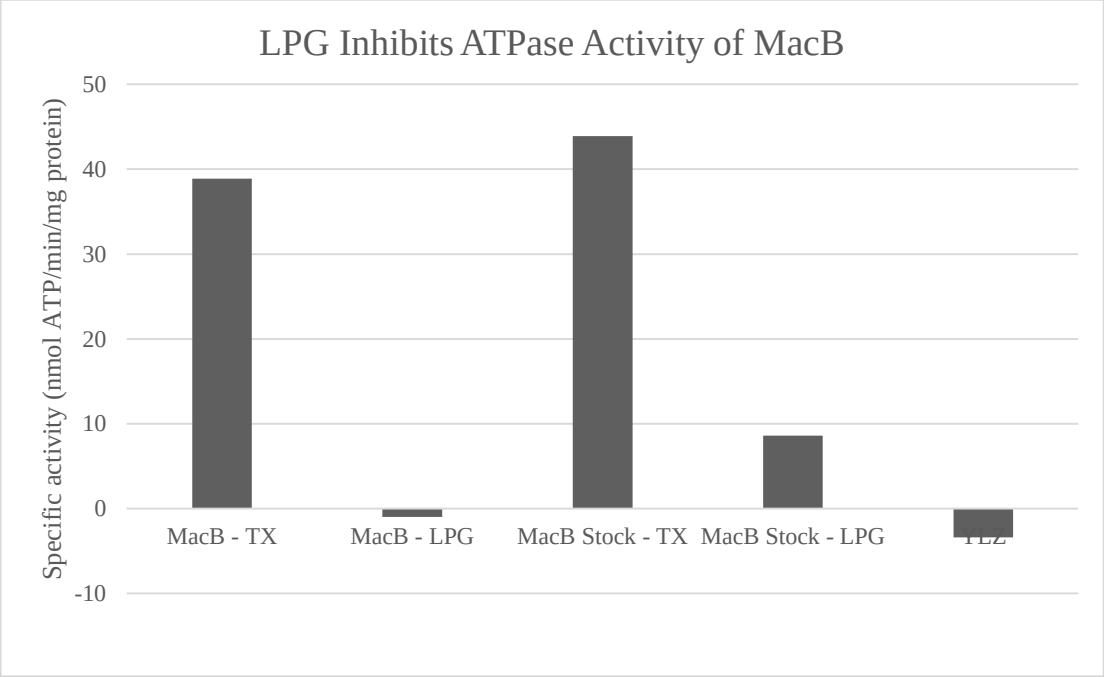

Figure 3.12 - LPG inhibits ATPase activity of purified MacB.

ATPase rates of MacB and YknYLZ purified from *E. coli*. Proteins with the suffix "TX" are solubilized in Triton X-100, and proteins with the suffix "LPG" are solubilized in the anionic detergent LPG.

Since YknYLZ is insoluble in most common detergents, and the only found detergent that solubilizes the protein is shown to inhibit ATPase activity, further investigation into ATPase activity of YknY was warranted.

3.3.3 – YknY localizes to the membrane fraction.

Previous results in this and other publications (Yamada, Tikhonova et al. 2012) made it difficult to determine if YknY co-purified with his-tagged YknZ in either YknWXYZ or YknYZ purifications. In previous studies, a ~50 kDa band was observed in purifications with YknZ co-expressing YknY (Yamada, Tikhonova et al. 2012). This could correspond to a dimeric YknY, which had a predicted monomeric size of 25.3 kDa. However, our efforts yielded no positive confirmation of YknY being purified with other complex components, likely due to being below the detection limit. Adding a tag and then purifying YknY would facilitate both the ability to detect the protein using immunoblotting as well as the ability to pull on the complex from another component. By purifying YknY, we can determine if YknY alone is sufficient for ATPase activity, or we can determine if a complex of YknYZ is required. To facilitate this, a strep-tag was cloned onto the N-terminus of YknY in the shuttle vector pHCMC04-YknYZ^{HIs}. The N-terminus of the protein was chosen for the tag due to the structure of the ATPase, in which the active regions of the protein are localized to the C-terminal region. By placing the tag on the opposite side of the protein, chances of the tag interfering with functionality were minimized. After construction of the plasmid, cells were transformed with the newly constructed plasmid, and expression and localization of the protein was confirmed by membrane isolation and immunoblotting. **(Figure. 3.13)**

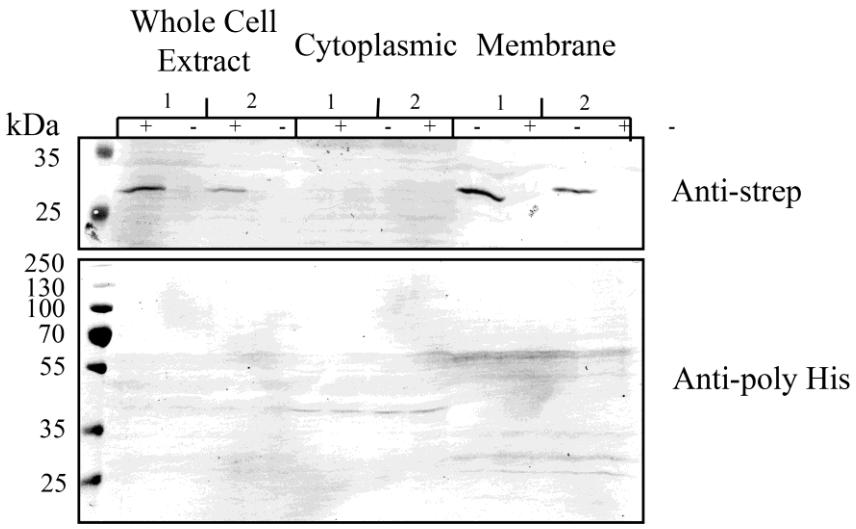

Figure 3.13 – Ykn^{Strep}YZ^{His} expresses YknY but not YknZ.

B. subtilis HB6127 cells carrying two different clones of ^{Strep}YZ^{His} were induced using 0.5% L-xylose, lysed and subjected to membrane fractionation. 50 μg of protein was loaded onto 12% SDS-PAGE and subjected to anti-strep and anti-poly His immunoblotting.

Immunoblotting results show a clear band running just above the predicted monomeric MW of 25 kDa for YknY, however no bands appear on an anti-poly His immunoblot despite an overwhelmingly large amount of total protein loaded. The absence of expression of YknZ is puzzling, as the PCR product for cloning was amplified from the YknZ-expressing pHCMC04-YknYZ^{His} and no changes were made near the overlapping YknY-YknZ stop / start codon. One explanation is that expression has been disrupted by downstream effects of the introduction of the strep-tag.

To take a different approach in the purification of YknY, we chose to utilize the plasmid pET-YknY^{His} and purify YknY alone and utilize it in ATPase assays with other complex components. As YknY is not predicted to have any transmembrane segments,

we first needed to check the localization and expression of the protein encoded by the pET-YknY^{His} plasmid. Since it is possible that YknY could exist in either the soluble or membrane fractions, as well as form inclusion bodies, after cell lysis, we pelleted unbroken cells via low-speed centrifugation, and then before pelleting membrane fractions at >100,000 xg, we pelleted inclusion bodies via centrifugation at 25,000 xg for 1 hour. (DeLisa, Lee et al. 2004) After isolation, fractions were analyzed by immunoblotting. **(Figure. 3.14)**

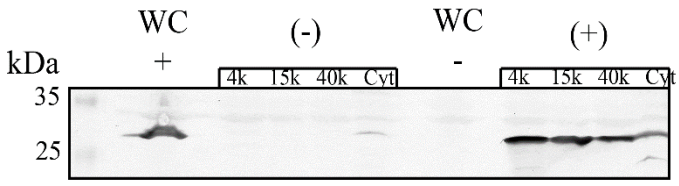

Figure 3.14 – Localization and expression of pET-YknY^{His}.

E. coli cells carrying pET-based YknY constructs were induced using 1 mM IPTG and expressed empty vector (-) or YknY^{His} (+). Cells were lysed and subjected to low-speed centrifugation, then increasing speeds to pellet inclusion bodies and membrane fractions before fraction analysis with anti-poly His immunoblotting. WC – whole cell lysate.

Results indicate that YknY^{His} is expressed from pET21-d plasmid, and localizes broadly, with roughly equal amounts detected in inclusion bodies as well as membrane fractions. Slightly less YknY was observed in the soluble fraction of the cell.

Due to the complications of purifying protein from inclusion bodies, including the requirements of unfolding and refolding the protein (Palmer and Wingfield 2004), we chose to purify YknY^{His} from the membrane fraction of *E. coli*. Cells were grown

and protein expressed according to protocol (Methods), and the membranes solubilized with 5% Triton X-100. Protein was purified using Ni^{2+} affinity chromatography. Fractions were analyzed by SDS-PAGE and staining with CBB. **(Figure. 3.15)**

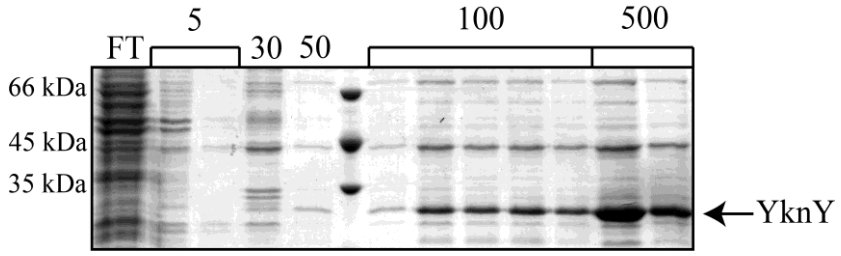

Figure 3.15 – Purification of $YknY^{His}$.

E. coli cells carrying pET-$YknY^{His}$ were induced using 1 mM IPTG, subjected to lysis and membrane fractionation, and His-tagged proteins purified using Ni^{2+} affinity chromatography with increasing amounts of imidazole. YknY can be seen purified, running at an expected MW of ~25 kDa.

Purification results were mixed, as YknY was readily purified from the detergent-soluble membrane fraction, but fractions contained a significant amount of contamination. Additionally, a strong band of approximately ~45 kDa can be seen in most fractions, and very strongly in elution fractions. This could be a YknY dimer, which has an expected MW of ~50 kDa. The stability of the YknY dimer seems to be strongest in purified protein, as these bands were not observed in previous experiments utilizing whole membrane fractions. From this, we can conclude that YknY is expressed and can be purified.

3.4 Discussion

MFPs have been implicated in Gram-positive transport systems, indicating that they have an active role in the transport process that extends beyond simply linking two membrane transport components (Harley, Djordjevic et al. 2000). While we know that they are involved in recruitment of OMFs and that they display a range of conformational flexibility, neither of these facts reconciles their presence in a Gram-positive environment. The only currently defined role for MFPs applicable in a Gram-positive organism would be to stimulate a cognate transporter. In order to further identify how MFPs stimulate the ATPase component of transporters, we chose to express, purify, and reconstitute the YknWXYZ transporter in various ways that would determine if YknX is able to stimulate its cognate ATPase, YknY.

Initially, purification of the transporter from the native organism, *B. subtilis* was attempted. YknWXYZ and YknYZ were purified, each with a histidine tag on YknZ, relying on co-purification of other complex components. Purification of YknWXYZ showed that YknZ is readily purified from the native organism, but in contrast to published results, YknW does not co-purify with YknZ. Previous data showed that YknW will co-purify only in the presence of YknXYZ, but immunoblotting analysis of the purification profile shows YknW largely in the flow-through fraction. This discrepancy can be explained in that purification conditions described here differ from published methods (Yamada, Tikhonova et al. 2012) in a few specific ways. Firstly, the oligomerization profile of YknW can change based on if the column was charged with Cu^{2+}, indicating that a column used here, charged with Ni^{2} could alter the oligomeric state, and thus functionality of YknW. Additionally, membrane fractions were

solubilized in DDM rather than Triton X-100 which could potentially affect interactions between complex components. Either of these changes individually have the potential to negatively affect complex affinity, and together, are likely the source of discrepancies between published results and the results seen here. Further investigation of purifying the YknWXYZ complex from *B. subtilis* would require optimization of purification procedures.

Purification of YknYZ also yielded YknZ in relatively large amounts, but no YknY could be detected using CBB or silver staining. When YknZ-containing fractions from purification were collected, concentrated, and subjected to ATPase assays, YknYZ showed ATPase activity, but the purification was not of sufficient purity to conclude that the observed ATPase activity was a result of YknY. Any contaminating non-specific ATPases could drastically skew results, and the lack of activity in the YknWXYZ purification indicates that the activity seen in YknYZ was non-specific, as it seems unlikely that purifying YknYZ in the presence of YknW and YknX would render the complex inactive. Purifications could be investigated further to obtain pure YknY, and could include further purification steps such as gel-filtration chromatography. The lack of ATPase activity in the purified YknWXYZ fractions could be due YknY not co-purifying with $YknZ^{His}$, or a more complex explanation, such as YknYZ being a very slow ATPase, an intrinsic instability of the complex, or other component requirements for ATPase activity of the transporter.

In order to establish a system in which to study YknX, we created chimeric proteins that combine the ATPase of either MacB or YknYZ with the permease of the opposite protein. Chimeric proteins would also offer insight into the mechanism of

ATPase stimulation by MFPs, as chimeric proteins may be stimulated by one, both, or neither cognate MFP.

Chimeric proteins were constructed between *E. coli* MacB and *B. subtilis* YknYZ, with and without a flexible linker region contained between the ATPase and permease regions of MacB. A fusion protein consisting of YknY covalently linked to YknZ was also created, also with a flexible linker region. Upon expression analysis, proteins containing the flexible loop region were expressed in *E. coli* and found to localize to the membrane, including MLZ, YLM, and MLZ. Thus, when the ATPase and permease of these chimeric transporters are covalently linked together, a flexible linker region is required for proper expression and localization to the membrane. This linker region likely imparts structural flexibility to the protein, and allows conformational changes needed for transport. This is consistent with MacB, which contains this linking region, and suggests that when the ATPase and permease components of efflux transporters are expressed as a single polypeptide, the linking region is required to allow movement of the domains relative to one another.

After expression analysis, these proteins were purified from solubilized membrane extracts and analyzed for contaminating proteins. Upon analysis, it was determined that the purity of samples coming from membranes expressing YLM and MLZ were not sufficient to use in ATPase assay. Purification protocols were optimized, however protein was still unable to be collected in a sufficient quantity and purity for assays.

In order to improve expression of protein, YLM and MLZ were sub-cloned into a high-copy plasmid, however both YLM and MLZ were found to not express from

pET-based plasmids. These plasmids were sequenced, and contained no mutations or unexpected sequences, so their lack of expression is confusing. It is possible that by changing the restriction site upstream of the start codon, expression was limited by inductive effects. While YLM and MLZ purifications expressed from pUC-based plasmids could be optimized with larger culture volumes and more stringent purification steps such as gel-filtration chromatography, it was determined that the most effective method to determine the conserved features of YknX would be to investigate it alongside YLZ. In the future, YLM and MLZ could both be investigated further, and purified from a pUC-based expression vector.

After creation of the YknYLZ fusion protein, expression analysis and membrane fractionation showed that YknYLZ is expressed and localized to the membrane of *E. coli*. Unfortunately, upon solubility tests, it was shown that YknYLZ is largely insoluble in the common non-ionic detergent Triton X-100. To solubilize and purify YknYLZ, an exotic detergent LPG was used. However, upon analysis, it was shown that a control sample of MacB solubilized and purified in Triton X-100 showed an ATPase rate of 38.9 nmol ATP / min / mg protein, but the same sample of MacB solubilized and purified in LPG was unable to support ATPase activity. Thus, it seems likely that ionic interactions between the detergent LPG and the protein prevent active hydrolysis of ATP for both MacB and YknYLZ. Harsher detergents can interfere with protein structure, rendering some inactive. Non-ionic detergents are typically less likely to modify and denature proteins, making them more favorable for the solubilization of proteins.

Pursuant to our goal of obtaining pure YknY to study through ATPase assays, we chose to place a tag on YknY and purify the ATPase component of the transporter directly. A strep-tag was placed on the N-terminus of YknY in order to facilitate this purification. The N-terminus of the protein was chosen because the ATP-hydrolyzing domains of the protein are located at the C-terminal end of YknY, and placing a tag on the opposite end of the protein reduces chances that the tag would interfere with protein function. The strep-tagged YknY was expressed alongside his-tagged YknZ, but only YknY was detectable through immunoblotting. The loss of expression of YknZ is puzzling, as the only changes made on the construct were on the 5'-end of YknY, and no changes were made near YknZ-encoding regions of the plasmid. One possible explanation is downstream inductive effects from changes on YknY.

The *E. coli*-based pET-YknY plasmid was used to express the protein and determine if YknY could be purified in sufficient quantity and purity for ATPase assays. Localization checks indicated that YknY is present in roughly equal amounts in the membrane fraction and in inclusion bodies, and a lower amount of the protein is localized to the cytoplasmic fraction of the cell. Since YknY is predicted to associate with the membrane, it was decided to purify YknY from the membrane fraction of the cell, especially because ATPase assays would require the mixing of YknY with detergent-solubilized membrane proteins also purified from the membrane fraction. Unfortunately, while YknY purification yielded a large amount of the protein, seen both in monomeric and dimeric forms, fractions contained a large amount of contaminants, and further efforts are needed to optimize purifications.

YknX is the only characterized Gram-positive MFP to date, but no conserved MFP functions have been associated with it or YknWXYZ. In order to characterize the identity of YknX as a conserved, functional MFP in a Gram-positive organism, we took approaches to establish that YknX can stimulate the ATPase activity of YknY, just as MacA can stimulate the ATPase activity of its cognate transporter, MacB. Unfortunately, the YknWXYZ complex presented many difficulties in terms of purifying and isolating proteins for further study. The chimeric fusion proteins YLM and MLZ both expressed when cloned into pUC-based vectors, but not in pET-based plasmid backgrounds. Further investigation into purification of both these chimeric proteins could be continued in pUC-based vectors, rather than the non-expressing pET-based constructs, and more stringent purification procedures could yield protein in sufficient purity and quantity for ATPase assays. While other complex components would be based in a different plasmid background, purified proteins could still be mixed together and studied to determine if these chimeric proteins are able to be stimulated by other complex components such as YknX, MacA, and YknW. Additionally, the fusion protein YknYLZ could be re-investigated utilizing a broader detergent screen, possibly providing conditions under which the protein can be solubilized and tested. Detergents should be selected based on their overall charge, with a preference for non-ionic detergents that would likely not interfere with ATPase assays.

Purifications of proteins from the native organism could also be re-visited, utilizing optimized purification protocols, as well as adding additional purification steps such as gel-filtration chromatography. It would be useful to develop anti-YknY antibodies to determine if the ATPase component of the transporter is definitively able

to co-purify with other transporter components. If indeed YknY is able to co-purify with YknZ, and samples can be purified in sufficient quantity and purity, then it would be feasible to combine complex components in ATPase assays and determine the ATPase activity and stimulation of YknY, purified either from YknWXYZ or YknYZ. Additionally, YknY purifications could yield this same result, and YknY purifications could be attempted from other fractions of the cell, such as inclusion bodies or the cytoplasmic fraction.

While there is no clear evidence that SdpC is the substrate of the YknWXYZ complex, (Yamada, Tikhonova et al. 2012) it is also possible that addition of SdpC to ATPase assays could have an effect on the ATP hydrolysis rate of the transporter. This would be a difficult proposal due to the small size of SdpC, (42 amino acids) but plasmid constructs exist that express SdpC in *B. subtilis* and it can be isolated using TCA precipitation (Yamada, Tikhonova et al. 2012). Further investigation into the viability of utilizing SdpC in reaction buffers would be required to determine if it has any possible effect on the transporter.

While the YknWXYZ transporter presented significant difficulties in characterizing conserved MFP functions, as well as determining ATPase activity of the proposed transporter, there is still much to be learned about Gram-positive MFP-dependent transporters. The further investigation of an ABC-type transporter from such a unique background would provide insight into the conserved functions of MFP-dependent transporters, as a large amount of the research done today concerns Gram-negative, RND-type transporters. Furthering our knowledge of how these transporters assemble and function across multiple families and species will allow for more

intelligent drug design in the future, as well as pave the way for inhibitors that could disrupt the function of these transporters that present a constant threat to public health.

References

Akama, H., M. Kanemaki, M. Yoshimura, T. Tsukihara, T. Kashiwagi, H. Yoneyama, S. Narita, A. Nakagawa and T. Nakae (2004). "Crystal structure of the drug discharge outer membrane protein, OprM, of Pseudomonas aeruginosa: dual modes of membrane anchoring and occluded cavity end." J Biol Chem **279**(51): 52816-52819.

Akama, H., T. Matsuura, S. Kashiwagi, H. Yoneyama, S. Narita, T. Tsukihara, A. Nakagawa and T. Nakae (2004). "Crystal structure of the membrane fusion protein, MexA, of the multidrug transporter in Pseudomonas aeruginosa." J Biol Chem **279**(25): 25939-25942.

Andersen, C., E. Koronakis, E. Bokma, J. Eswaran, D. Humphreys, C. Hughes and V. Koronakis (2002). "Transition to the open state of the TolC periplasmic tunnel entrance." Proc Natl Acad Sci U S A **99**(17): 11103-11108.

Bagai, I., W. Liu, C. Rensing, N. J. Blackburn and M. M. McEvoy (2007). "Substrate-linked Conformational Change in the Periplasmic Component of a Cu(I)/Ag(I) Efflux System." J Biol Chem **282**(49): 35695-35702.

Bavro, V. N., R. L. Marshall and M. F. Symmons (2015). "Architecture and roles of periplasmic adaptor proteins in tripartite efflux assemblies." Frontiers in Microbiology **6**.

Bavro, V. N., Z. Pietras, N. Furnham, L. Perez-Cano, J. Fernandez-Recio, X. Y. Pei, R. Misra and B. Luisi (2008). "Assembly and channel opening in a bacterial drug efflux machine." Mol Cell **30**(1): 114-121.

Bayley, H. and J. V. Staros (1984). 9 - Photoaffinity Labeling and Related Techniques. Azides and Nitrenes. E. F. V. Scriven, Academic Press**:** 433-490.

Brennan, P. J. (2003). "Structure, function, and biogenesis of the cell wall of Mycobacterium tuberculosis." Tuberculosis (Edinb) **83**(1-3): 91-97.

Butcher, B. G. and J. D. Helmann (2006). "Identification of Bacillus subtilis sigma-dependent genes that provide intrinsic resistance to antimicrobial compounds produced by Bacilli." Mol Microbiol **60**(3): 765-782.

Butcher, B. G. and J. D. Helmann (2006). "Identification of Bacillus subtilissigma-dependent genes that provide intrinsic resistance to antimicrobial compounds produced by Bacilli." Mol Microbiol **60**(3): 765-782.

Chin, J. W., S. W. Santoro, A. B. Martin, D. S. King, L. Wang and P. G. Schultz (2002). "Addition of p-azido-L-phenylalanine to the genetic code of Escherichia coli." J Am Chem Soc **124**(31): 9026-9027.

Chuanchuen, R., T. Murata, N. Gotoh and H. P. Schweizer (2005). "Substrate-dependent utilization of OprM or OpmH by the Pseudomonas aeruginosa MexJK efflux pump." Antimicrob Agents Chemother **49**(5): 2133-2136.

Chung, Y. J. and M. H. Saier, Jr. (2001). "SMR-type multidrug resistance pumps." Curr Opin Drug Discov Devel **4**(2): 237-245.

Damron, F. H., E. S. McKenney, H. P. Schweizer and J. B. Goldberg (2013). "Construction of a Broad-Host-Range Tn7-Based Vector for Single-Copy PBAD-Controlled Gene Expression in Gram-Negative Bacteria." Applied and Environmental Microbiology **79**(2): 718-721.

Datsenko, K. A. and B. L. Wanner (2000). "One-step inactivation of chromosomal genes in Escherichia coli K-12 using PCR products." Proc Natl Acad Sci U S A **97**(12): 6640-6645.

Davidson, A. L., E. Dassa, C. Orelle and J. Chen (2008). "Structure, Function, and Evolution of Bacterial ATP-Binding Cassette Systems." Microbiol. Mol. Biol. Rev. **72**(2): 317-364.

De Angelis, F., J. K. Lee, J. D. O'Connell, L. J. W. Miercke, K. H. Verschueren, V. Srinivasan, C. Bauvois, C. Govaerts, R. A. Robbins, J.-M. Ruysschaert, R. M. Stroud and G. Vandenbussche (2010). "Metal-induced conformational changes in ZneB suggest an active role of membrane fusion proteins in efflux resistance systems." Proceedings of the National Academy of Sciences **107**(24): 11038-11043.

de Lorenzo, V. and K. N. Timmis (1994). "Analysis and construction of stable phenotypes in gram-negative bacteria with Tn5- and Tn10-derived minitransposons." Methods Enzymol **235**: 386-405.

DeLisa, M. P., P. Lee, T. Palmer and G. Georgiou (2004). "Phage shock protein PspA of Escherichia coli relieves saturation of protein export via the Tat pathway." J Bacteriol **186**(2): 366-373.

Delmar, J. A., C. C. Su and E. W. Yu (2013). "Structural mechanisms of heavy-metal extrusion by the Cus efflux system." Biometals **26**(4): 593-607.

Dorman, G. and G. D. Prestwich (1994). "Benzophenone Photophores in Biochemistry." Biochemistry **33**(19): 5661-5673.

Du, D., Z. Wang, N. R. James, J. E. Voss, E. Klimont, T. Ohene-Agyei, H. Venter, W. Chiu and B. F. Luisi (2014). "Structure of the AcrAB-TolC multidrug efflux pump." Nature **509**(7501): 512-515.

Eicher, T., M. A. Seeger, C. Anselmi, W. Zhou, L. Brandstatter, F. Verrey, K. Diederichs, J. D. Faraldo-Gomez and K. M. Pos (2014). "Coupling of remote alternating-access transport mechanisms for protons and substrates in the multidrug efflux pump AcrB." Elife **3**.

Elkins, C. A. and H. Nikaido (2002). "Substrate Specificity of the RND-Type Multidrug Efflux Pumps AcrB and AcrD of Escherichia coli Is Determined Predominately by Two Large Periplasmic Loops." J Bacteriol **184**(23): 6490-6498.

Ellermeier, C. D., E. C. Hobbs, J. E. Gonzalez-Pastor and R. Losick (2006). "A three-protein signaling pathway governing immunity to a bacterial cannibalism toxin." Cell **124**(3): 549-559.

Farrell, I. S., R. Toroney, J. L. Hazen, R. A. Mehl and J. W. Chin (2005). "Photo-cross-linking interacting proteins with a genetically encoded benzophenone." Nature methods **2**(5): 377-384.

Freudl, R. (2013). "Leaving home ain't easy: protein export systems in Gram-positive bacteria." Research in Microbiology **164**(6): 664-674.

Fujita, M., J. E. Gonzalez-Pastor and R. Losick (2005). "High- and low-threshold genes in the Spo0A regulon of Bacillus subtilis." J Bacteriol **187**(4): 1357-1368.

Ge, Q., Y. Yamada and H. Zgurskaya (2009). "The C-terminal domain of AcrA is essential for the assembly and function of the multidrug efflux pump AcrAB-TolC." J Bacteriol **191**(13): 4365-4371.

Greene, N. P., P. Hinchliffe, A. Crow, A. Ababou, C. Hughes and V. Koronakis (2013). "Structure of an atypical periplasmic adaptor from a multidrug efflux pump of the spirochete Borrelia burgdorferi." FEBS Letters **587**(18): 2984-2988.

Harley, K. T., G. M. Djordjevic, T. T. Tseng and M. H. Saier (2000). "Membrane-fusion protein homologues in gram-positive bacteria." Mol Microbiol **36**(2): 516-517.

Higgins, C. F. (2007). "Multiple molecular mechanisms for multidrug resistance transporters." Nature **446**(7137): 749-757.

Higgins, C. F. and K. J. Linton (2004). "The ATP switch model for ABC transporters." Nat Struct Mol Biol **11**(10): 918-926.

Hinchliffe, P., N. P. Greene, N. G. Paterson, A. Crow, C. Hughes and V. Koronakis (2014). "Structure of the periplasmic adaptor protein from a major facilitator superfamily (MFS) multidrug efflux pump." FEBS Lett **588**(17): 3147-3153.

Hvorup, R. N., B. Winnen, A. B. Chang, Y. Jiang, X. F. Zhou and M. H. Saier, Jr. (2003). "The multidrug/oligosaccharidyl-lipid/polysaccharide (MOP) exporter superfamily." Eur J Biochem **270**(5): 799-813.

Jack, D. L., N. M. Yang and M. H. Saier (2001). "The drug/metabolite transporter superfamily." European Journal of Biochemistry **268**(13): 3620-3639.

Janganan, T. K., V. N. Bavro, L. Zhang, M. I. Borges-Walmsley and A. R. Walmsley (2013). "Tripartite efflux pumps: energy is required for dissociation, but not assembly or opening of the outer membrane channel of the pump." Molecular Microbiology **88**(3): 590-602.

Jones, P. M. and A. M. George (2014). "A reciprocating twin-channel model for ABC transporters." Q Rev Biophys **47**(3): 189-220.

Kauer, J. C., S. Erickson-Viitanen, H. R. Wolfe, Jr. and W. F. DeGrado (1986). "p-Benzoyl-L-phenylalanine, a new photoreactive amino acid. Photolabeling of calmodulin with a synthetic calmodulin-binding peptide." J Biol Chem **261**(23): 10695-10700.

Kim, H. M., Y. Xu, M. Lee, S. Piao, S. H. Sim, N. C. Ha and K. Lee (2010). "Functional relationships between the AcrA hairpin tip region and the TolC aperture tip

region for the formation of the bacterial tripartite efflux pump AcrAB-TolC." J Bacteriol **192**(17): 4498-4503.

Kobayashi, N., K. Nishino, T. Hirata and A. Yamaguchi (2003). "Membrane topology of ABC-type macrolide antibiotic exporter MacB in Escherichia coli." FEBS Lett **546**(2-3): 241-246.

Koronakis, V. (2003). "TolC--the bacterial exit duct for proteins and drugs." FEBS Lett **555**(1): 66-71.

Koronakis, V., J. Eswaran and C. Hughes (2004). "Structure and function of TolC: the bacterial exit duct for proteins and drugs." Annu Rev Biochem **73**: 467-489.

Koronakis, V., A. Sharff, E. Koronakis, B. Luisi and C. Hughes (2000). "Crystal structure of the bacterial membrane protein TolC central to multidrug efflux and protein export." Nature **405**(6789): 914-919.

Krishnamoorthy, G., E. B. Tikhonova and H. I. Zgurskaya (2008). "Fitting periplasmic membrane fusion proteins to inner membrane transporters: mutations that enable Escherichia coli AcrA to function with Pseudomonas aeruginosa MexB." J Bacteriol **190**(2): 691-698.

Lamsa, A., W. T. Liu, P. C. Dorrestein and K. Pogliano (2012). "The Bacillus subtilis cannibalism toxin SDP collapses the proton motive force and induces autolysis." Mol Microbiol **84**(3): 486-500.

Landmesser, H., A. Stein, B. Bluschke, M. Brinkmann, S. Hunke and E. Schneider (2002). "Large-scale purification, dissociation and functional reassembly of the maltose ATP-binding cassette transporter (MalFGK(2)) of Salmonella typhimurium." Biochim Biophys Acta **1565**(1): 64-72.

Levy, S. B. and B. Marshall (2004). "Antibacterial resistance worldwide: causes, challenges and responses." Nat Med **10**(12 Suppl): S122-129.

Li, X. Z. and H. Nikaido (2004). "Efflux-mediated drug resistance in bacteria." Drugs **64**(2): 159-204.

Lobedanz, S., E. Bokma, M. F. Symmons, E. Koronakis, C. Hughes and V. Koronakis (2007). "A periplasmic coiled-coil interface underlying TolC recruitment and the assembly of bacterial drug efflux pumps." Proc Natl Acad Sci U S A **104**(11): 4612-4617.

Locher, K. P. (2009). "Review. Structure and mechanism of ATP-binding cassette transporters." Philos Trans R Soc Lond B Biol Sci **364**(1514): 239-245.

Lorca, G. L., R. D. Barabote, V. Zlotopolski, C. Tran, B. Winnen, R. N. Hvorup, A. J. Stonestrom, E. Nguyen, L. W. Huang, D. S. Kim and M. H. Saier, Jr. (2007). "Transport capabilities of eleven gram-positive bacteria: comparative genomic analyses." Biochim Biophys Acta **1768**(6): 1342-1366.

Lu, S. and H. I. Zgurskaya (2012). "Role of ATP binding and hydrolysis in assembly of MacAB-TolC macrolide transporter." Mol Microbiol **86**(5): 1132-1143.

Lu, S. and H. I. Zgurskaya (2013). "MacA, a Periplasmic Membrane Fusion Protein of the Macrolide Transporter MacAB-TolC, Binds Lipopolysaccharide Core Specifically and with High Affinity." J Bacteriol **195**(21): 4865-4872.

Ma, D., D. N. Cook, M. Alberti, N. G. Pon, H. Nikaido and J. E. Hearst (1993). "Molecular cloning and characterization of acrA and acrE genes of Escherichia coli." J Bacteriol **175**(19): 6299-6313.

Mealman, T. D., M. Zhou, T. Affandi, K. N. Chacon, M. E. Aranguren, N. J. Blackburn, V. H. Wysocki and M. M. McEvoy (2012). "N-terminal region of CusB is sufficient for metal binding and metal transfer with the metallochaperone CusF." Biochemistry **51**(34): 6767-6775.

Mikolosko, J., K. Bobyk, H. I. Zgurskaya and P. Ghosh (2006). "Conformational Flexibility in the Multidrug Efflux System Protein AcrA." Structure **14**(3): 577-587.

Mima, T., S. Joshi, M. Gomez-Escalada and H. P. Schweizer (2007). "Identification and characterization of TriABC-OpmH, a triclosan efflux pump of Pseudomonas aeruginosa requiring two membrane fusion proteins." J Bacteriol **189**(21): 7600-7609.

Misra, R. and V. N. Bavro (2009). "Assembly and transport mechanism of tripartite drug efflux systems." Biochim Biophys Acta **1794**(5): 817-825.

Modali, S. D. and H. I. Zgurskaya (2011). "The periplasmic membrane proximal domain of MacA acts as a switch in stimulation of ATP hydrolysis by MacB transporter." Mol Microbiol **81**(4): 937-951.

Molle, V., Y. Nakaura, R. P. Shivers, H. Yamaguchi, R. Losick, Y. Fujita and A. L. Sonenshein (2003). "Additional Targets of the Bacillus subtilis Global Regulator CodY Identified by Chromatin Immunoprecipitation and Genome-Wide Transcript Analysis." Journal of Bacteriology **185**(6): 1911-1922.

Murakami, S., R. Nakashima, E. Yamashita, T. Matsumoto and A. Yamaguchi (2006). "Crystal structures of a multidrug transporter reveal a functionally rotating mechanism." Nature **443**(7108): 173-179.

Murakami, S., R. Nakashima, E. Yamashita and A. Yamaguchi (2002). "Crystal structure of bacterial multidrug efflux transporter AcrB." Nature **419**(6907): 587-593.

Nikaido, H. (2009). "Multidrug resistance in bacteria." Annu Rev Biochem **78**: 119-146.

Nikaido, H. and J. M. Pages (2012). "Broad-specificity efflux pumps and their role in multidrug resistance of Gram-negative bacteria." FEMS Microbiol Rev **36**(2): 340-363.

Palmer, I. and P. T. Wingfield (2004). "Preparation and Extraction of Insoluble (Inclusion-Body) Proteins from Escherichia coli." Current protocols in protein science / editorial board, John E. Coligan ... [et al.] **CHAPTER**: Unit-6.3.

Pei, X. Y., P. Hinchliffe, M. F. Symmons, E. Koronakis, R. Benz, C. Hughes and V. Koronakis (2011). "Structures of sequential open states in a symmetrical opening transition of the TolC exit duct." Proc Natl Acad Sci U S A **108**(5): 2112-2117.

Perez Morales, T. G., T. D. Ho, W. T. Liu, P. C. Dorrestein and C. D. Ellermeier (2013). "Production of the cannibalism toxin SDP is a multistep process that requires SdpA and SdpB." J Bacteriol **195**(14): 3244-3251.

Piddock, L. J. (2006). "Multidrug-resistance efflux pumps - not just for resistance." Nat Rev Microbiol **4**(8): 629-636.

Pos, K. M. (2009). "Drug transport mechanism of the AcrB efflux pump." Biochim Biophys Acta **1794**(5): 782-793.

Puech, V., M. Chami, A. Lemassu, M. A. Laneelle, B. Schiffler, P. Gounon, N. Bayan, R. Benz and M. Daffe (2001). "Structure of the cell envelope of corynebacteria: importance of the non-covalently bound lipids in the formation of the cell wall permeability barrier and fracture plane." Microbiology **147**(Pt 5): 1365-1382.

Rath, A., M. Glibowicka, V. G. Nadeau, G. Chen and C. M. Deber (2009). "Detergent binding explains anomalous SDS-PAGE migration of membrane proteins." Proceedings of the National Academy of Sciences **106**(6): 1760-1765.

Rosenblatt-Farrell, N. (2009). "The Landscape of Antibiotic Resistance." Environmental Health Perspectives **117**(6): A244-A250.

Saier, M. H., Jr. and I. T. Paulsen (2001). "Phylogeny of multidrug transporters." Semin Cell Dev Biol **12**(3): 205-213.

Saier, M. H., Jr., I. T. Paulsen, M. K. Sliwinski, S. S. Pao, R. A. Skurray and H. Nikaido (1998). "Evolutionary origins of multidrug and drug-specific efflux pumps in bacteria." FASEB Journal **12**(3): 265-274.

Seeger, M. A., A. Schiefner, T. Eicher, F. Verrey, K. Diederichs and K. M. Pos (2006). "Structural asymmetry of AcrB trimer suggests a peristaltic pump mechanism." Science **313**(5791): 1295-1298.

Senior, A. E., M. K. al-Shawi and I. L. Urbatsch (1995). "The catalytic cycle of P-glycoprotein." FEBS Lett **377**(3): 285-289.

Sennhauser, G., P. Amstutz, C. Briand, O. Storchenegger and M. G. Grutter (2007). "Drug export pathway of multidrug exporter AcrB revealed by DARPin inhibitors." PLoS Biol **5**(1): e7.

Siarheyeva, A., R. Liu and F. J. Sharom (2010). "Characterization of an asymmetric occluded state of P-glycoprotein with two bound nucleotides: implications for catalysis." J Biol Chem **285**(10): 7575-7586.

Silhavy, T. J., D. Kahne and S. Walker (2010). "The Bacterial Cell Envelope." Cold Spring Harbor Perspectives in Biology **2**(5).

Su, C.-C., F. Long, M. T. Zimmermann, K. R. Rajashankar, R. L. Jernigan and E. W. Yu (2011). "Crystal structure of the CusBA heavy-metal efflux complex of Escherichia coli." Nature **470**(7335): 558-562.

Su, C. C., F. Yang, F. Long, D. Reyon, M. D. Routh, D. W. Kuo, A. K. Mokhtari, J. D. Van Ornam, K. L. Rabe, J. A. Hoy, Y. J. Lee, K. R. Rajashankar and E. W. Yu (2009). "Crystal structure of the membrane fusion protein CusB from Escherichia coli." J Mol Biol **393**(2): 342-355.

Symmons, M. F., E. Bokma, E. Koronakis, C. Hughes and V. Koronakis (2009). "The assembled structure of a complete tripartite bacterial multidrug efflux pump." Proc Natl Acad Sci U S A **106**(17): 7173-7178.

Takatsuka, Y. and H. Nikaido (2007). "Site-directed disulfide cross-linking shows that cleft flexibility in the periplasmic domain is needed for the multidrug efflux pump AcrB of Escherichia coli." J Bacteriol **189**(23): 8677-8684.

Takatsuka, Y. and H. Nikaido (2009). "Covalently linked trimer of the AcrB multidrug efflux pump provides support for the functional rotating mechanism." J Bacteriol **191**(6): 1729-1737.

Tikhonova, E. B., V. Dastidar, V. V. Rybenkov and H. I. Zgurskaya (2009). "Kinetic control of TolC recruitment by multidrug efflux complexes." Proc Natl Acad Sci U S A **106**: 16416-16421.

Tikhonova, E. B., V. K. Devroy, S. Y. Lau and H. I. Zgurskaya (2007). "Reconstitution of the Escherichia coli macrolide transporter: the periplasmic membrane fusion protein MacA stimulates the ATPase activity of MacB." Mol Microbiol **63**(3): 895-910.

Tikhonova, E. B., Q. Wang and H. I. Zgurskaya (2002). "Chimeric Analysis of the Multicomponent Multidrug Efflux Transporters from Gram-Negative Bacteria." J Bacteriol **184**(23): 6499-6507.

Tikhonova, E. B., Y. Yamada and H. I. Zgurskaya (2011). "Sequential Mechanism of Assembly of Multidrug Efflux Pump AcrAB-TolC." Chem Biol **18**(4): 454-463.

Tseng, T. T., K. S. Gratwick, J. Kollman, D. Park, D. H. Nies, A. Goffeau and M. H. Saier, Jr. (1999). "The RND permease superfamily: an ancient, ubiquitous and diverse family that includes human disease and development proteins." J Mol Microbiol Biotechnol **1**(1): 107-125.

Vakharia, H., G. J. German and R. Misra (2001). "Isolation and characterization of Escherichia coli tolC mutants defective in secreting enzymatically active alpha-hemolysin." J Bacteriol **183**(23): 6908-6916.

Vogel, H. J. and D. M. Bonner (1956). "Acetylornithinase of Escherichia coli: partial purification and some properties." J Biol Chem **218**(1): 97-106.

Weeks, J. W., V. N. Bavro and R. Misra (2014). "Genetic assessment of the role of AcrB beta-hairpins in the assembly of the TolC-AcrAB multidrug efflux pump of Escherichia coli." Mol Microbiol **91**(5): 965-975.

Weeks, J. W., T. Celaya-Kolb, S. Pecora and R. Misra (2010). "AcrA suppressor alterations reverse the drug hypersensitivity phenotype of a TolC mutant by inducing TolC aperture opening." Mol Microbiol **75**(6): 1468-1483.

Weeks, J. W., L. M. Nickels, A. T. Ntreh and H. I. Zgurskaya (2015). "Non-equivalent roles of two periplasmic subunits in the function and assembly of triclosan pump TriABC from Pseudomonas aeruginosa." Molecular Microbiology: n/a-n/a.

WHO (2014). Antimicrobial resistance: global report on surveillance, World Health Organization.

Wilkens, S. (2015). "Structure and mechanism of ABC transporters." F1000Prime Reports **7**: 14.

Xu, Y., M. Lee, A. Moeller, S. Song, B.-Y. Yoon, H.-M. Kim, S.-Y. Jun, K. Lee and N.-C. Ha (2011). "Funnel-like Hexameric Assembly of the Periplasmic Adapter Protein in the Tripartite Multidrug Efflux Pump in Gram-negative Bacteria." Journal of Biological Chemistry **286**(20): 17910-17920.

Xu, Y., S. H. Sim, S. Song, S. Piao, H. M. Kim, X. L. Jin, K. Lee and N. C. Ha (2010). "The tip region of the MacA alpha-hairpin is important for the binding to TolC to the Escherichia coli MacAB-TolC pump." Biochem Biophys Res Commun **394**(4): 962-965.

Yamada, Y., E. B. Tikhonova and H. I. Zgurskaya (2012). "YknWXYZ is an unusual four-component transporter with a role in protection against sporulation-delaying-protein-induced killing of Bacillus subtilis." J Bacteriol **194**(16): 4386-4394.

Yamaguchi, A., R. Nakashima and K. Sakurai (2015). "Structural basis of RND-type multidrug exporters." Frontiers in Microbiology **6**: 327.

Young, T. S., I. Ahmad, J. A. Yin and P. G. Schultz (2010). "An enhanced system for unnatural amino acid mutagenesis in E. coli." J Mol Biol **395**(2): 361-374.

Yu, E. W., G. McDermott, H. I. Zgurskaya, H. Nikaido and D. E. Koshland, Jr. (2003). "Structural basis of multiple drug-binding capacity of the AcrB multidrug efflux pump." Science **300**(5621): 976-980.

Yum, S., Y. Xu, S. Piao, S. H. Sim, H. M. Kim, W. S. Jo, K. J. Kim, H. S. Kweon, M. H. Jeong, H. Jeon, K. Lee and N. C. Ha (2009). "Crystal structure of the periplasmic component of a tripartite macrolide-specific efflux pump." J Mol Biol **387**(5): 1286-1297.

Zgurskaya, H. I., G. Krishnamoorthy, A. Ntreh and S. Lu (2011). "Mechanism and function of the outer membrane channel TolC in multidrug resistance and physiology of enterobacteria." Frontiers in Microbiology **2**.

Zgurskaya, H. I. and H. Nikaido (1999). "AcrA is a highly asymmetric protein capable of spanning the periplasm." J. Mol. Biol. **285**: 409-420.

Zgurskaya, H. I. and H. Nikaido (1999). "Bypassing the periplasm: reconstitution of the AcrAB multidrug efflux pump of Escherichia coli." Proc Natl Acad Sci USA **96**(13): 7190-7195.

Zgurskaya, H. I. and H. Nikaido (2000). "Multidrug resistance mechanisms: drug efflux across two membranes." Molecular Microbiology **37**(2): 219-225.

Zgurskaya, H. I., J. W. Weeks, A. T. Ntreh, L. M. Nickels and D. Wolloscheck (2015). "Mechanism of coupling drug transport reactions located in two different membranes." Front Microbiol **6**: 100.

Zgurskaya, H. I., Y. Yamada, E. B. Tikhonova, Q. Ge and G. Krishnamoorthy (2009). "Structural and functional diversity of bacterial membrane fusion proteins." Biochim Biophys Acta **1794**(5): 794-807.

Appendix A: List of primers

Primer Name	Primer Sequence (5'-3')
Ystrepfwd	ATTAACTAGTATGTGGTCGCATCCTCAATTTGAA AAGATTCAGCTTTCTAATGTGCG
Zhisrev	TAATGGATCCCTAGTGGTGGTGGTGGTGGTGCTC ATAACGCAGCGC
YfwdNdeI	CTAGCATATGATTCAGCTTTCTAATGTGCG
ZrevXhoI	CTAGCTCGAGCTCATAACGCAGCGC
MacBfwdNdei	CTAGCATATGACGCCTTTGCTCG
MacBATPfwd	ATAGCGCTTAAGATGACGCCTTTGC
YknYATPfwd	ATAGCGCTTAAGATGATTCAGCTTTCTAATGTGC G
MacBpermrev	ATAGCGCAGCTGTTAGTGGTGGTGGTGGTGGTGC TCTCGTGCCAG
YknZpermrev	ATAGCGCAGCTGCTAGTGGTGGTGGTGGTGGTGC TCATAACGCAGCGC
ZfwdMacrev	GGACAGAGCTTAGAGCCATGGTACCGGCGGGAG GATTG
ZfwdMaclinkrev	GGACAGAGCTTAGAGCCATGGTACCCGTCAGCGC CTC
MacfwdYrev	CGCCATGCCATGGTACCTTCTCCCACACTCCTTTG TCC
MaclinkfwdYrev	CAATGGCGGGGGTACCAACAATGTTTCCGTCACG C
fyknYZNcoI	GACTCCATGGCCATTCAGCTTTC
ryknYXhoI	GAATTCTCGAGTTCTCCCACACTCC
fLinkerSalI	GTATTATGTCGACCGCAATCCTCCCGCCATTG
rLinkerXhoI	GGCGGCTCGAGGTTAAAACCGCTGACAAAC
fyknZSalI	GACGGCGTCGACTTGGAAAACATCAG
ryknYZXhoI	GCATCTCGAGCTCATAACGCAG
AcrA*fwd	CCAGTCCAGCAACGACTTCTTATAGCTGAAACAG GAACTGGCGAATGGCACG
AcrA*rev	CGTGCCATTCGCCAGTTCCTGTTTCAGCTATAAGA AGTCGTTGCTGGACTGG
A26rev	CGATCATATGTGGCCCGGATGGAGC
A47rev	CGATCATATGATGACCACCTTCTCGCTGGC
Actermfwd	ACTGCATATGAAGCCGTTTTCCCTCGCC
B9rev	CGATCATATGCCGGGCTTGAGGC
B30rev	CGATCATATGATCACCACCTGGCGTTCG
Bctermfwd	ACTGCATATGAAGGGCGGTTTCAACC
Axctermfwd	ACTGACTAGTGGCAACTCTAGAGGAGGCGACG
Ax26rev	CAGTACTAGTCTGGCCCGGATGGAGC

Ax47rev	CAGTACTAGTGATGACCACCTTCTCGCTGGC
TriA NcoI FWD	AATTCCATGGCATCAGACGCCAGAGGCGCT
TriA-His XhoI REV	AATACTCGAGTCAATGATGATGATGATGATGTGG CTGGCCTCCGCCCAC
TriB NcoI FWD	ATTACCATGGCAAAGCCGTTTTCCCTCGCC
TriB-His XhoI REV	GCCGCTCGAGTCAATGATGATGATGATGATGTCG CGCATCCTCGTCGAG
TriC PciI FWD	GACCACATGTACAAGGGCGGTTTCGGCCTG
TriC-His HindIII Rev	CGTGCTAAGCTTCAATGATGATGATGATGATGGC GTCCCGGTTCCGGAATC
TriA SacI FWD	TTAGGAGCTCAGGAGGAATTCACCATGTCAGACG CCAGAGGCGC
TriAxB XbaI Fusion FWD	CGGAGGCCAGCCAGGCAACTCTAGAGGAGGCGA CGAGCCGC
TriAxB XbaI Fusion REV	GCGGCTCGTCGCCTCCTCTAGAGTTGCCTGGCTG GCCTCCG
TriA-R131D FWD	CCGACCTCAACTACCAGGACCAGAAGGCGCTGCT GCC
TriA-R131D REV	GGCAGCAGCGCCTTCTGGTCCTGGTAGTTGAGGT CGG
TriA-G351C FWD	GGTGGTCACGGTGTGCGGCCAACTGCTCC
TriA-G351C REV	GGAGCAGTTGGCCGCACACCGTGACCACC
TriA Del Coiled-coil FWD	GGTGCTGGCGCGGCTCGACCCTCTGCTGCCCAAA GGATACACCAGCCAGACCGAGCTGCGTGCCTCC
TriA Del Coiled-coil REV	GGAGGCACGCAGCTCGGTCTGGCTGGTGTATCCT TTGGGCAGCAGAGGGTCGAGCCGCGCCAGCACC
TriB-R119D FWD	GCCCAGGCCAATGCCGACCGCCAGGAAGAACTG
TriB-R119D REV	CAGTTCTTCCTGGCGGTCGGCATTGGCCTGGGC
TriB-G340C FWD	GGTGGTCCGCGCCTGCGTCAACAGCCTCAAGCC
TriB-G340C REV	GGCTTGAGGCTGTTGACGCAGGCGCGGACCACC
TriB Del Coiled-coil FWD	CGCGCTGCTGGCGACCCTCGACCCTCTGTTTGCCC GAAGTGTGACCGCCCAGACGCGCCTGGTGACCG
TriB Del Coiled-coil REV	CGGTCACCAGGCGCGTCTGGGCGGTCACACTTCG GGCAAACAGAGGGTCGAGGGTCGCCAGCAGCGC G
OpmH NcoI FWD	AATTCCATGGCCCTGCGCAGACTCTCCCTGGC
OpmH-His PstI REV	TTAGCTGCAGCTAATGGTGATGGTGATGGTGGTA CTGCTGGCGCGGCTTGCTCTG

TolC NcoI FWD	AATTCCATGGCCAAGAAATTGCTCCCCATTCTTATCGG
TolC-His HindIII	GCTCTAGAAGCTTAGTGATGGTGATGGTGATGGTTACGGAAAGGGTTATGACC
PA glmS Up	GCACATCGGCGACGTGCTCTC
PA glmS Down	CTGTGCGACTGCTGGAGCTGA